The World Bank

Climate Change and Impacts in Central Asia – An Overview

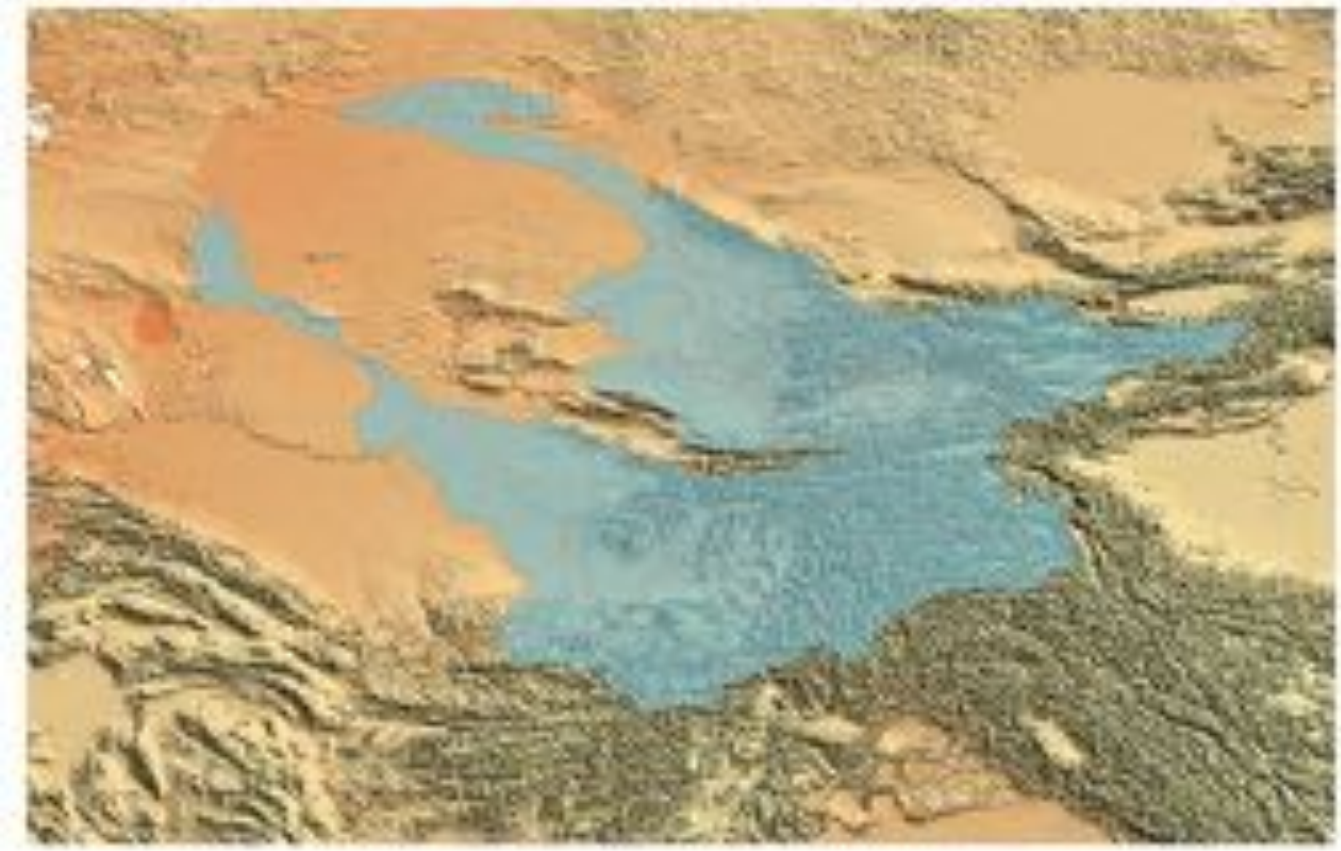

Final Draft Paper

Version: Monday, June 03, 2013

Authors

Tobias Siegfried, Andrey Yakovlev, Sebastian Stoll
hydrosolutions ltd.
Technoparkstrasse 1
CH-8005 Zurich, Switzerland
Telephone: +41 44 632 73 28
hs@hydrosolutions.ch and www.hydrosolutions.ch

Revision: 6/3/2013, Title Picture: Amu Darya & Syr Darya Basins are shown on top of a digital terrain model (ASTER DEM).

Contents

List of Figures

List of Tables

Acronyms & Abbreviations

ADB	Asian Development Bank
CMIP3	Coupled Model Intercomparison Project Phase 3
CMIP5	Coupled Model Intercomparison Project Phase 5
CORDEX	Coordinated Regional Climate Downscaling Experiment
CV	Coefficient of Variation
CV	Coefficient of Variation
DJF	December, January, February season
ENSO	El Niño Southern Oscillation
FAO	Food and Agricultural Organization
GCM	Global Circulation Model
GDP	Gross Domestic Product
GLIMS	Global Land Ice Measurements from Space
GLOF	Glacial Lake Outburst Flows
GPCC	Global Precipitation Climatology Centre
JJA	June, July, August season
KAZ	Kazakhstan
KYG	Kyrgyzstan
MAM	March, April, May season
masl	meters above sea level
SON	September, October, November season
SRES A2	Special Report on Emission Scenarios – Scenario A2
SRTM	Shuttle Radar Topography Mission
SSA	Singular Spectrum Analysis
TAJ	Tajikistan
TUR	Turkmenistan
UZB	Uzbekistan
WCRP	World Climate Research Programme
WGI	World Glacier Inventory

Acknowledgments

We acknowledge helpful commentaries and suggestions by the World Bank / COWI teams and by Dr. Lee Addams.

Executive Summary

Central Asia is an extraordinarily complex region from the hydroclimatological perspective. Large topographical gradients and variations in precipitation and temperature are found between the high mountain regions in the upstream of the Amu and Syr Darya and the steppes in the downstream.

Most of the region has an arid climate, with strong seasonal and interannual precipitation and temperature variations. These large-amplitude year-to-year variations and associated implications for runoff and water availability in the region were one of the main reasons for the construction of a large number of surface reservoirs to help regulate flows of the Amu and Syr Darya. Low-frequency climate modulations influence the region at decadal, centennial and millennial scales.

Because of the combined effects of snowmelt and glacial runoff, about 80 percent of runoff in the Aral Sea basin occurs between March and September. The onset of the snowmelt period shifts from early spring to early summer with increasing elevation, distributing snowmelt-driven runoff over a period of several months. In the summer months, glacial ablation peaks and prolongs the period of peak runoff.

Warm season river flows in central Asia are closely related to the regional-scale climate variability of the preceding cold season. The peak river flows occur in the warm season (April–August) and are highly correlated with the regional patterns of precipitation, moisture transport, and jet-level winds of the preceding cold season (November–March) that are the key determinants of the synoptic situation over the region.

Climate change has the potential to impact the hydrological regimes of the rivers in a significant way. This can translate into societal hardship and conflict if these impacts are not adequately understood and managed. The urgency to better understand climate change and impacts in the region is exacerbated by increasing population pressure.

The analysis of 20th century temperature, precipitation and runoff in Central Asia reveals interesting insight of past climate and its influence on the hydrology of the Amu and Syr Darya. Using gridded GPCC climatology data (1901 – 2006), it can be shown that winter precipitation has increased slightly in the winter season DJF along parts of the northern Tien Shan range. Statistically robust precipitation trends are otherwise absent in the region.

Converse to that, most of Central Asia experienced a significant warming over the 20th century (1.5 – 4 degree Celsius range derived from Univ. of Delaware Air Temperature gridded dataset, 1900 - 2010). Trends of annual warming are high in the eastern Kazakh Alatau and in the Alay

range as well as the Pamirs. Except for the Aral Sea region, most of the lowlands in the river basins experienced only moderate warming. Analyses of selected time series data of high mountain stations in the Syr Darya catchment confirm the above assessment.

The complete set of station-based in-situ measured actual evapotranspiration (ET) data in Central Asia was used for analysis. The latter reveals that negative long-term trends persist, despite the regional warming and that actual ET has on average actually been declining over the region over the last 60 years.

Interesting robust high warming trends can be observed in the vicinity of the large cities Tashkent in Uzbekistan and Almaty in Kazakhstan. The signals there might in fact be non-climatic and effectively be related to a heat island effect where a growing population in an expanding urban environment has led to local ambient heating that is picked up by the city-based meteorological stations.

Long-term runoff time series from 10 stations of tributaries to the Syr Darya and Amu Darya were utilized to analyze the variability in water supplies in the basins. For most rivers of these rivers, approximately 90 years of monthly data was available. Filtered time series and spectral analyses reveal an interesting multi-decadal 50 years cycle in the Syr Darya tributaries which led to near consistent increases in mean runoff from the 1990ies onwards after a 20 year period of decline in the previous decades (see Figure below). The same low-frequency modulation is visible in the Vaksh River which is one of the large tributaries to the Amu Darya. Apart from the Sokh River, these modulations dominate trends by far in all catchments which is very important to acknowledge.

Sokh River and Surkhandarya show long-term positive trends in their hydrographs starting around mid-20th century. There, additional runoff might be generated from the loss of land ice due to warming. Unlike the other tributaries, Zerafshan River runoff exhibits a periodicity of 8 – 10 years which is also visible in some of the Syr Darya tributaries, though to a lesser extent.

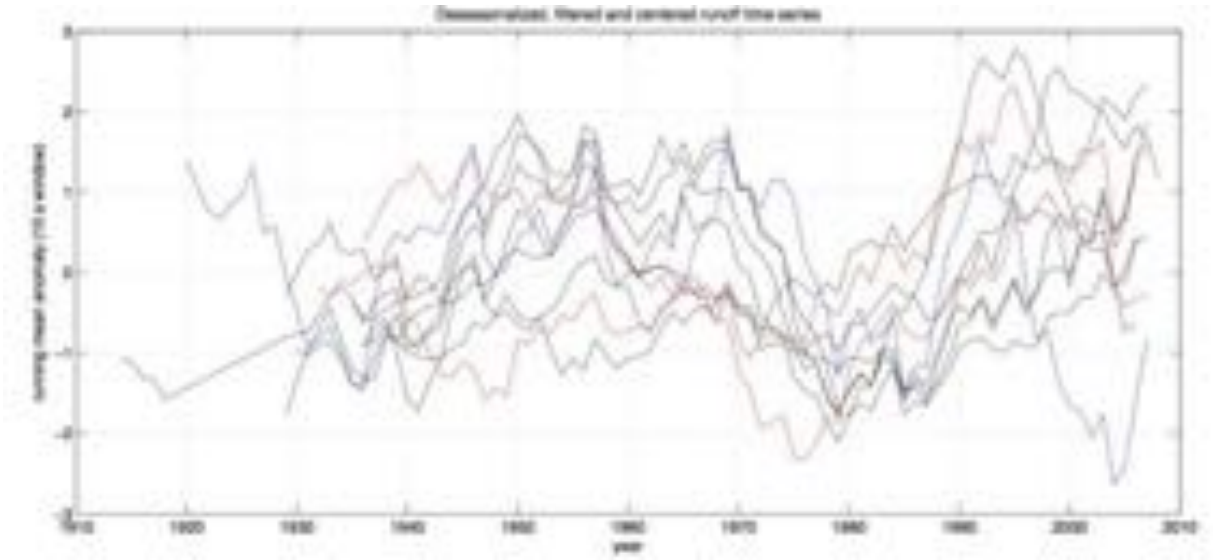

Figure shows the low-frequency variability in runoff of selected tributaries to the Amu and Syr Darya. Syr Darya tributaries' data are shown in black, Amu Darya tributaries are shown in red and Zerafshan running mean runoff data is shown in blue colors.

The relative water abundance in the Syr Darya from 1980 onwards is confirmed when looking at naturalized flows in the main stem of the river (see Table below). If the half-centennial cycle is confirmed, we would expect to see declining mean river flows over the next decades in the tributaries of the Syr Darya. This might be masked by additional runoff contributions for the years to come due to land ice loss in glaciated catchments. However, more research is required to establish linkages to the underlying drivers of these modulations in the region.

For the analysis of historic extremes in the runoff of the two rivers, naturalized runoff time-series were utilized to mask the effect of the upstream damming. Results are shown in the two tables below.

The analysis of the Naryn - Syr Darya naturalized runoff confirms the analysis from above on long-term runoff and its modulation in selected tributaries to the river. Whereas the second half of the 20th century until 1990 was marked by recurring dry and extremely dry years, flows were normal to above normal from there onwards with the exception of the year 2008, a year where there was severe water stress and conflict in the basin, also due to the fact that water deficits could not be compensated by releases from Toktogul since the latter was near to empty at the beginning of the irrigation season. Thus, in a lucky turn, the conflict-laden years in the last decade of the 20th century until nowadays were marked by good hydrological conditions that certainly helped muting the transboundary water allocation disputes in the region to a certain extent.

Syr Darya												
	1900										2000	
Year	I	II	III	IV	V	VI	VII	VIII	IX	X	I	II
0							37%	15%	52%	43%	54%	4%
1							89%	41%	57%	67%	65%	
2							94%	61%	76%	35%	9%	
3							72%	30%	83%	19%	6%	
4							48%	96%	81%	7%	26%	
5							85%	98%	70%	59%	13%	
6							46%	93%	87%	33%	28%	
7							80%	91%	22%	63%	39%	
8						50%	69%	56%	17%	11%	78%	
9						44%	2%	24%	74%	20%	31%	

Table shows assessment of hydrological years in the Syr Darya (1958 - 2011) . Calculations of exceedance probabilities are based on the Kritkyi-Menkel formula and use a normalized series of average annual flows in m^3/s. Columns are decades, rows are years. The numbers are the p-values in percentages as reported above. Color coding is - extreme dry year, - dry year, - normal year, - wet year, - extremely wet year, - no data. Normalized runoff data was obtained from the Uzbek Hydrometeorological Service.

Table 7 shows the assessment for the Amu Darya.

Amu Darya												
	1900										2000	
Year	I	II	III	IV	V	VI	VII	VIII	IX	X	I	II
0							36%	43%	47%	39%	90%	15%
1				54%			74%	81%	71%	32%		17%
2		42%		25%			82%	79%	92%	3%	56%	26%
3		49%				10%	85%	11%	60%	19%	22%	
4		6%				7%	51%	96%	38%	8%	61%	
5		24%				67%	86%	76%	33%	63%	13%	
6		64%	65%	46%		29%	21%	57%	94%	40%	69%	
7		89%	72%			83%	50%	78%	44%	68%	88%	
8			18%				53%	28%	14%	4%	99%	
9			31%				1%	58%	93%	35%	75%	

Assessment of hydrological years in the Amu Darya (1959 - 2011) . Calculations of exceedance probabilities are based on the Kritkyi-Menkel formula and use a normalized series of average annual flows in m^3/s. Columns are decades, rows are years. The numbers are the p-values in percentages as reported above. Color coding is - extreme dry year, - dry year, - normal year, - wet year, - extremely wet year, - no data. Normalized runoff data was obtained from the Uzbek Hydrometeorological Service.

Similarly to the situation in the Syr Darya, 2008 was a critical extremely dry year in the Amu Darya basin.

Global climate model output from the World Climate Research Programme's (WCRP's) Coupled Model Intercomparison Project phase 3 (CMIP3) multi-model dataset were used for the analysis of the future climate in the region. Data from 16 models were analyzed over the period 2000 - 2050.

The results of the assessment of the future precipitation climate confirm findings in other regions. Namely, future precipitation trends are highly uncertain and vary greatly from one model to another. Model inconsistences are shown in the Figure below. In the zones of recharge formation of the two rivers, i.e. the Tien Shan mountains and the Pamirs, only very few models show a statistically significant trend over the 50 year period of the assessment.

This finding has important repercussions for any impact and mitigation study with regard to the estimation of future runoff and its changes in the two basins. Care should be taken to properly quantify uncertainties in such undertakings as otherwise, false conclusions are likely to be drawn.

The lack of a good understanding of future water availability in the basins should also guide decision-makers in the region to prepare flexible, yet effective mitigation measures, including sound management strategies. The current water sector reforms in the upstream republics Kyrgyzstan and Tajikistan should also be reviewed in light of these findings.

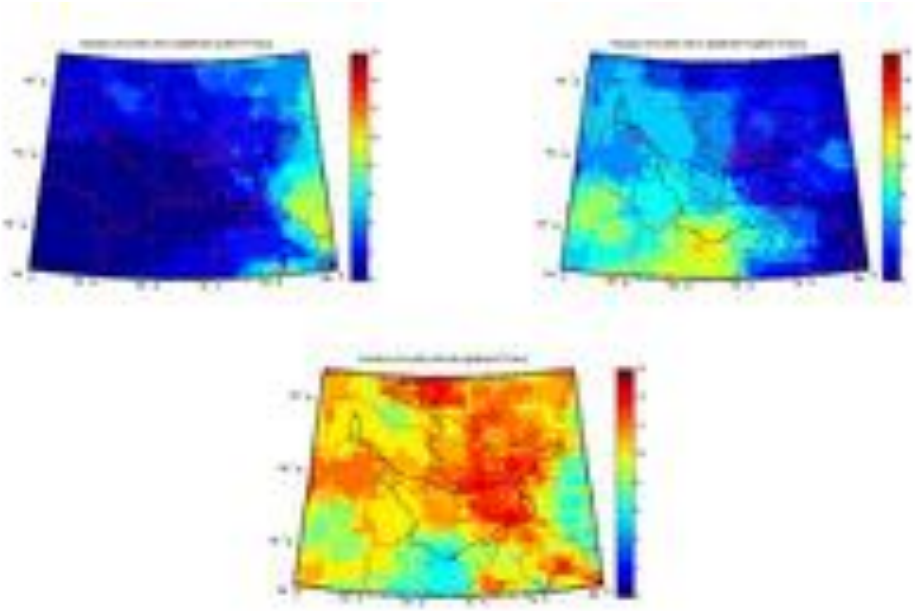

Number of multi-model ensemble members with a significant positive trend in precipitation at the level of individual grid cells (upper left plate). Number of multi-model ensemble members with a significant negative precipitation trend (upper right plate) and number of models (out of 16 ensemble members) without significant annual future precipitation trends (lower center plate). Note: direction of significant trends is not shown.

Conversely to precipitation, future temperature trends show consistent and strong positive signals across all multi-model members (see Figure below which shows seasonal robust trends). Over Central Asia, multi-model mean climate model output suggests a warming between 2 – 2.75 degrees Celsius from 2000 – 2050. For both river catchments, the warming trends are higher in the uplands as compared to the lowlands. The south-western region, including the Pamirs is more strongly affected by warming than the other regions. An interesting transition zone exists between the two large consistent regions with lower and higher temperature trends.

Due to the fact that runoff formation processes are mainly from snow- and glacier-melt in the two basins, the future warming will impact the rivers' hydrographs through the corresponding temperature effects on ice and snow.

Land ice will continue to melt in the high mountain areas of both catchments. Recent research shows that under the SRES A2 emissions scenario, approximately one third of present total land-ice volume will melt over this period in the basin, with an expected volumetric loss of 31 ± 4 percent relative to the current volume (200 km^3, approximately). As a result, the mean annual runoff contribution from ice is expected to be in the order of 50 m^3/s under this scenario. This corresponds to roughly 2.7 ± 2 percent of total natural basin runoff, or around one third of present average inflow into the Aral Sea after all upstream consumptive water use has been accounted for in the Syr Darya. Therefore, basin-wide glacier-melt contributions to river flow are and will likely remain small in the Syr Darya when compared with the natural runoff regime.

In the Amu Darya catchment, the two main glaciated catchments are the Pianj (170 - 200 km^3 land ice) and the Vaksh (200 - 240 km^3 land ice). This corresponds to an overall ice volume in both catchment areas of around 370 - 440 km^3 (with an uncertainty range of ± 25 – 30 percent) or roughly double the one in the entire Syr Darya. Under the assumption of an average temperature increase of 2 degree C until 2050 and no change in precipitation, research has shown that the ice reserves in the two catchments will decline at an accelerated rate, compared to the past with an expected total average volume reduction of 75.5 percent for the Pianj basin and of 53 percent for the Vakhsh basin

Using a simple back of the envelope approach and assuming uniform melting of the total volume from 2003 - 2050, it can be shown that this volumetric loss will translate into annual additional runoff contributions in the order of 4.8 km^3 – 5.8 km^3 or an additional 6.5 percent – 7.8 percent of runoff over the long-term mean. The relative contribution of glaciers in the Amu Darya to overall runoff under an A2 scenario is thus roughly three times larger as compared to the Syr Darya.

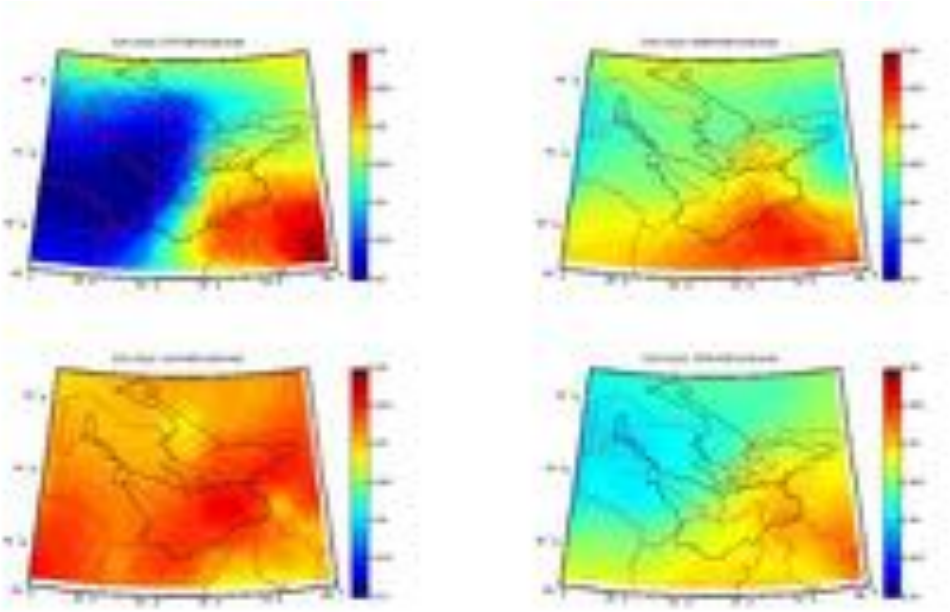

Robust linear regression (Sen's slope) for the climate change SRES A2 multi-model mean seasonal temperature data. Slope values are in derees C per season. Only cells with statistically significant trends are shown, i.e. white cells are non-significant trend cells. River basins outlined in black color, country borders are shown in red.

Temperature-induced impacts on hydrographs were studied with a coupled climate-hydrology model. Only impacts on the Syr Darya tributaries were studied since no similar model for the Amu Darya was available.

For the investigation, the SRES A2 scenario was used for the time period 2040 – 2050 which was compared with the long-term average runoff situations over the course of the 20th century until the year 2012. Emphasis was put here on investigating changes in runoff seasonality due to the above-mentioned warming trend while assuming in the first place that total annual runoff will not change. This is warranted since we really do not know much about the future precipitation climate in the region. Lower (dry year) and upper (wet year) boundary scenarios for runoff in the main tributaries to the Syr Darya River are also reported.

The methods utilized for the investigation of climate impacts on the Syr Darya consist of coupling a physically-based rainfall runoff modeling to different realization of future climate under the SRES A2 forcing. With the model, a monthly runoff correction factor is calculated. If the factor exceeds 1 for a particular month, it means that runoff is increasing relative to long-term mean runoff values for the particular catchment under consideration. Conversely, if the climate change correction factor is smaller 1, this suggests that flows will be expected to decrease under the SRES A2 scenario in the corresponding month in the 2040 – 2049 decade.

The table below shows the climate change correction factors for the main tributaries of the Syr Darya. They were computed by taking the ratio of the mid-21st century monthly runoff versus the corresponding mean 20th monthly runoff values. Red colors in the Table indicate a relative decrease and blue colors an increase of mean monthly flows correspondingly. The decrease of summer runoff and increases in the cold season runoffs are clearly visible, especially for the South Fergana Valley tributaries. Similar computations can be carried out for corresponding wet and dry year scenarios.

#	River Name	J	F	M	A	M	J	J	A	S	O	N	D
1	Naryn	1.45	1.11	1.24	1.52	1.89	1.14	0.58	0.51	0.68	1.05	1.67	1.89
2	Yassy	1.37	1.76	1.86	1.07	0.64	0.62	0.90	1.45	2.24	2.64	1.96	1.38
3	Akbura	1.25	0.94	0.91	1.03	1.23	0.85	0.58	0.74	1.01	1.40	2.02	1.94
4	Aravansay	0.89	0.85	0.98	1.16	0.80	0.55	0.70	0.96	1.32	1.92	1.83	1.18
5	Isfaramsai	1.17	0.90	0.86	0.99	1.22	0.90	0.59	0.74	1.00	1.36	1.97	1.86
6	Shakimardan	1.20	0.89	0.85	0.98	1.17	0.80	0.56	0.70	0.97	1.33	1.91	1.85
7	Sokh	1.37	1.04	0.99	1.13	1.35	0.93	0.64	0.81	1.11	1.54	2.21	2.13
8	Isfara	1.59	1.23	1.36	1.66	2.09	1.26	0.64	0.56	0.75	1.15	1.83	2.08
9	Khodjabakirgan	1.25	0.92	0.88	1.02	1.22	0.84	0.58	0.74	1.01	1.39	1.99	1.92
10	Aksu	1.28	0.95	0.90	1.00	1.23	0.84	0.59	0.74	1.02	1.41	1.97	1.96
11	Arys	NA	NA	NA	NA	NA	NA	NA	NA	NA	NA	NA	NA
12	Keles	1.42	1.74	1.05	0.54	0.47	0.61	0.88	1.60	1.75	1.33	1.02	1.14
13	Chirchik	1.17	1.20	1.47	1.62	1.01	0.59	0.53	0.73	1.19	1.88	2.15	1.63
14	Chadaksai	2.20	1.73	1.22	1.38	1.88	2.15	1.32	0.68	0.59	0.80	1.25	1.91
15	Gavasi	2.14	1.40	1.06	1.00	1.23	1.40	0.97	0.67	0.84	1.15	1.58	2.27
16	Koksareksai	1.00	0.75	1.00	1.29	0.84	0.64	0.76	1.00	1.38	2.00	1.75	1.25
17	Sumsarsa	0.80	1.00	1.14	0.92	0.61	0.77	1.07	1.44	1.83	1.80	1.25	1.00
18	Kasansai	0.97	1.08	1.32	0.91	0.63	0.79	1.08	1.51	2.13	2.08	1.31	1.00
19	Padshata	1.78	2.04	1.60	1.17	1.29	1.60	1.85	1.10	0.59	0.51	0.70	1.11

Monthly climate change coefficients for the Syr Darya tributaries. Ratio of normal mid-21st century versus mean 20th century runoff is shown. Colors indicate directions of change with red colors indicating a decrease of monthly average flows and blue colors indicating an increase accordingly. Coefficients for wet and dry years (not shown) can be computed accordingly.

Several recent studies report climate impacts on water supplies in the Amu Darya basin. However, some of these studies suffer from significant shortcomings which render their results regarding future projections very dubious at best. The recent, scientifically robust and honest FAO study about 'Climate Impact on Stream Flow in the Amu Darya Basin' however is a welcome exception. For this reason, it is recommended to draw on the study's main findings when discussing climate change impacts in the Amu Darya. While the FAO report only investigates 2 small subcatchments in the Amu Darya, the authors argue in a very plausible way that the quantified impacts at the small subcatchment scale will very likely also be visi-

ble at the scale of the larger tributaries, i.e. the Vaksh River and Pinaj River. The reported main impacts for hydrological mean years are

- a 10 – 50 percent increase in annual runoff;
- a significant increase of runoff in May and June due to earlier and more intense snow melt; and
- a 10 – 30 percent reduction of runoff in August.

The development of future supply versus demand ratios will be determined by combined effects of supply-side variability, i.e. at intra-annual, seasonal, interannual and longer time-scales as well as the development of the water demand where agriculture will continue to be the main driver with highest probability in the region.

Increasing minimum, mean and maximum daily temperatures increases will be the main driver of increasing evapotranspiration over irrigated lands via increases in crop water requirements. It is likely that maximum demand coverage deficits during the summer months are expected to occur in the early growing stages which are the most sensitive periods for plant growth regarding water stress (see also the Table above). Careful management interventions, most likely coupled with additional manmade storage in unregulated catchments together with corresponding conveyance will be required to cover this deficit

However, as mentioned above and as the analysis of 20th century data shows, a better understanding of the future development of actual and potential evapotranspiration and their climate linkages is required at this point so as to further substantiate this point.

Climate change will likely increase risks and hazards in the region. As glaciers retreat, large volumes of melt water can get trapped behind unstable terminal moraines. If these moraines collapse, glacier lake outbursts can occur. Such outbursts can potentially cause catastrophic flooding downstream. The Fergana Valley region and parts of Tajikistan are particularly exposed to these geohazards. Furthermore, the tributaries of the two larger rivers frequently experience mudflow events. These threaten population and infrastructure, esp. in the spring and summer seasons. Due to global warming, mudflow frequency might be rising under increasing precipitation extremes and decreasing slope stability due to the loss of permafrost. The management of those risks is a major challenge as there are no effective early warning systems in place.

In summary, climate change will affect the Central Asian region mainly through temperature effects on the snow and ice cover in the mountain ranges where runoff is formed. Drastic changes in annual water availability in absolute terms, relative to current conditions, are unlikely as impacts from climate change are likely to unfold gradually over the next 40 years.

Neo-Malthusian scenarios of acute water scarcity and conflict over the water resources of the Amu and Syr Darya are unrealistic. However, the expected impacts from environmental change call for preparedness.

BELOW, SUGGESTIONS & DIRECTIONS FOR FURTHER ANALYSIS ARE PROVIDED IN TEXT BOXES.

1 Introduction

The Syr Darya and Amu Darya are located in the Central Asian republics of Kyrgyzstan, Uzbekistan, Tajikistan, and Kazakhstan and are the principal tributaries to the Aral Sea. An estimated 22 percent of total average runoff in the Amu Darya stems from the Afghan side of the basin. Figure 1 shows a map of the region.

About 22 million people in the region depend on irrigated agriculture for their livelihoods, and 20 percent to 40 percent of GDP in the riparian countries is derived from agriculture, most of which is irrigated. Much of the region has an arid climate, with strongly seasonal precipitation and temperature patterns and large interannual variability. These large amplitude year-to-year variations and associated implications for runoff and water availability in the region were one of the main reasons for the construction of a large number of surface reservoirs that help to regulate flows. The extensive development of irrigation in the basin is associated with a number of environmental problems including desiccation of the Aral Sea, which has lost up to 90 percent of its pre-1960 volume and has received international attention as an environmental disaster area (Pereira-Cardenal et al., 2011 and references therein).

The bulk of the Syr Darya and Amu Darya runoff comes from melting snow and glaciers in the Tien Shan Mountains of Kyrgyzstan and the Pamirs in Tajikistan respectively. Table 1 and Table 2 show detailed long-term average water balances of the rivers. On average, Syr Darya runoff is half that of the Amu Darya. A unique feature of the Syr Darya is that return flows from irrigation constitute a large fraction of downstream available water (approx. 70 percent, see CAWaterInfo for more information).

River basin	The state, where it is formed								Total	
	Kyrgyzstan		Kazakhstan		Tajikistan		Uzbekistan		Syr Darya Basin	
	Total	Transb.	Total	Transb.	Total	Transb.	Total	Transb.	Total	Transb.
Naryn	14.544	12.831	—	—	—	—	—	—	14.544	12.831
Karadarya	3.921	2.06	—	—	—	—	—	—	3.921	2.06
Rivers of Fergana Valley	6.04	5.4	—	—	0.855	0.7	0.91	0.8	7.805	6.9
Midstream Rivers	—	—	—	—	0.15	—	0.145	—	0.295	—
Chirchik	3.1	3.1	0.749	0.749	—	—	4.1	3	7.949	5.849
Akhangaran	—	—	—	—	—	—	0.659	—	0.659	—
Keles	—	—	0.247	—	—	—	—	—	0.247	—
Arys	—	—	1.183	—	—	—	—	—	1.183	—
Downstream Rivers	—	—	0.6	—	—	—	—	—	0.6	—
Total runoff (km^3/a)	**27.605**	**23.991**	**2.426**	**0.749**	**1.005**	**0.7**	**5.167**	**2.8**	**37.203**	**27.64**
(%)	100	84.7	100	30.9	100	69.7	100	45.4	100	74.3
Share (%)	74.2	84.6	6.5	2.7	2.7	2.6	16.6	10.1	100	100

Table 1: Detailed supply-side average water balance of the Syr Darya. Source: CAWaterinfo.

Because of the combined effects of snowmelt and glacial runoff, about 80 percent of runoff in the Aral Sea basin occurs between March and September. The onset of the snowmelt period shifts from early spring to early summer with increasing elevation, distributing snow-

melt-driven runoff over a period of several months. In the summer months, glacial ablation peaks and prolongs the period of peak runoff (Pereira-Cardenal et al., 2011).

River basin	River flow generated within the countries					Total Amu Darya Basin
	Kyrgyzstan	Tajikistan	Uzbekistan	Turkmenistan	Afghanistan and Iran	
Pyandj	—	30.081	—	—	3.3	33.381
Vakhsh	1.654	18.4	—	—	—	20.054
Kafirnigan	—	5.535	—	—	—	5.535
Surkhandarya	—	—	4.841	—	—	4.841
Sherabad	—	—	0.228	—	—	0.228
Kashkadarya	—	—	1.222	—	—	1.222
Murgab	—	—	—	0.771	0.771	1.542
Tedjan	—	—	—	0.488	0.489	0.977
Atrek	—	—	—	0.136	0.137	0.273
Rivers of Afghanistan	—	—	—	—	6.167	6.167
Total runoff (km^3/a)	**1.654**	**54.056**	**6.291**	**1.405**	**10.814**	**74.22**
Share (%)	2.2	72.8	8.5	1.9	14.6	100

Table 2: Detailed average water balance of the Amu Darya. Source: CAWaterinfo. It should be noted that the numbers reported here for the Afghan and Iranian contributions are only measured flows and not total volumes. A simple area-based volumetric runoff assessment shows that likely Afghan contributions to the Pyanj are in the order of 16.3 km^3/a (47 % of total Pyanj flow above Nizh Pyanj station). For more information on Pyanj runoff formation, see (Borovikova, Agaltseva, Ivanov, Novikov, & Borovikova, 2003).

Warm season river flows in central Asia are closely related to the regional-scale climate variability of the preceding cold season. The peak river flows occur in the warm season (April–August) and are highly correlated with the regional patterns of precipitation, moisture transport, and jet-level winds of the preceding cold season (November–March). The importance of regional-scale variability in determining the snowpack that eventually drives the rivers in subsequent summer months has been demonstrated in many instances (M. a. Barlow & Tippett, 2008).

In the National Hydrometeorological Agencies in the Central Asian republics, this relationship is used for flow forecasting at seasonal scales (see e.g. Siegfried, 2012). The agencies forecast all major tributaries to the Amu and Syr Darya. In the latter case, for example, the Kyrgyz Hydrometeorological Agency provides monthly forecasts for the April to September period for the Naryn, i.e. the inflow into Toktogul reservoir. A the same time, the Uzbek Hydrometeorological Agency provides forecasts for the Kara Darya River (inflow into Andijan reservoir) and the Chirchik River (inflow into Charvak reservoir). The Uzbek agency also complies all this information for informing ICWC on their bi-annual meetings where transboundary water allocations are being discussed and decided upon. Table 3 provides a sample forecast for the 2013 growing season as was compiled by the Uzbek Hydrometeorological Service.

River	Item	Expected runoff April – Sept.		Previous year value	Long-term statistics [m^3/s]		
		[m^3/s]	[mio. m^3]	[m^3/a]	Mean	Min	Max
Syr Darya	Lateral inflow to the reservoir Kairakkum	180-220	2850-3480	264	212	70.3	305
Syr Darya	Lateral flow of water between the Kairakkum and Chardarya reservoir	120-220	1930-3480	168	200	46.8	696
Kara Darya	The inflow of water in the Andijan reservoir	140-200	2210-3160	172	193	61.4	407
Kara Darya	Lateral flow of water from the reservoir to the mouth of Andijan	120-170	1900-2690	167	163	97.9	264
Chirchik	The inflow of water into Lake Charvak + Ugham River	270-370	4270-5850	393	365	214	721
Chirchik	Lateral flow of water from the deep lake to the mouth	70-90	1110-1420	96.1	93.3	29.5	138
Total Naryn-Syrdarya cascade		900-1'270	14'550-20'550	1330	1300	783	2330

Table 3: Sample forecast for the 2013 growing season. Source: UZB Hydrometeorological Service, Tashkent.

Recent research shows that hydrological regimes of snow- and glacier-melt driven rivers will be impacted by a warming climate. Avoiding major water allocation conflicts within and between countries will require improved water management and planning, and the latter is contingent on advances in our understanding of how impacts from climatic changes are likely to unfold in affected basins (Siegfried et al., 2011, and refereneces therein).

Population pressure in the Central Asian region will greatly increase over the course of the 21st century. Figure 2 shows expected developments. An average increase of one third over current numbers is expected in the region. The relative increase will be largest in Tajikistan whereas the absolute growth most pronounced in Uzbekistan where the Fergana Valley will experience the bulk of the growth. This will put great burden on a country where already nowadays an estimated one third of the population is affected by inadequate food calories intake on a recurrent base.

Thus, even under a no climate change assumption, per capita water availability will be reduced on average by more than 33% by 2050 over today's availability, all else being equal. In conjunction with ongoing soil salinization and the erosion of the rural income base, this pos-

es threat, mostly for the rural population, especially in densely populated places such as the Fergana valley.

Figure 1: Map of the Aral Sea basin. Typical runoff and allocation flows are indicated. Source: (United Nations, 2010).

Increasing population pressure and climate change will both be important in the Central Asian region, a region where complex allocation tradeoffs exist. The energy-poor yet water-rich upstream countries (Kyrgyzstan and Tajikistan) use water for hydropower production in the winter. Conversely, the downstream states (Uzbekistan, Turkmenistan and Kazakhstan) consumptively utilize water in the summer irrigation season. Allocation conflicts are exacerbated by the fact that effective international institutions for mitigating these types of disputes are absent in the region. The appeasement and likely development of the Afghan part of the Amu Darya basin will further complicate allocation there in the future.

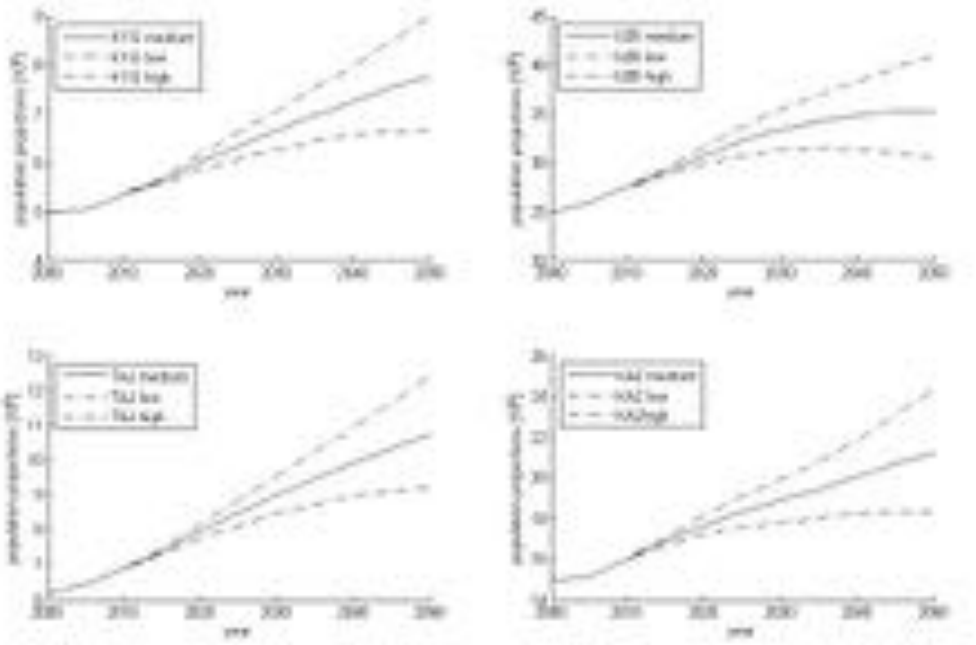

Figure 2: Population development in the individual republics. Medium, low and high projection variants are shown for Kyrgyzstan (KYG), Uzbekistan (UZB), Tajikistan (TAJ) and Kazakhstan (KAZ).Source: (Dept. of Economic and Social Affairs, United Nations Secretariat, 2010). Percentage levels of population increases for the medium variants and relative to the year 2010 are: KYG = 45.6 percent, UZB = 29.1 percent, TAJ = 56.2 percent and KAZ = 32.3 percent.[1]

[1] Note, the current Turkmen population is estimated to be 5 million, approx. (2010 figures). According to the medium growth variant, the population there is expected to grow by 1.5 by 2050. Source: (Dept. of Economic and Social Affairs, United Nations Secretariat, 2010)

2 Hydroclimatology of Central Asia

The Central Asian region is located between temperate and subtropical climate zones. Extreme continentality and large topography gradients are unique features of the region. Throughout the year, the western and north-western plains of Central Asia are open to cold northerly and north-westerly inflows as well as to moist westerly Atlantic air masses. To the south and east, the Himalayan, Pamir, Hindukush and Tien Shan mountains almost completely isolate Central Asia from moist air masses that have their origin in the Indian Ocean. Nevertheless, given the contemporaneous monsoonal amplitude, approximately 10 percent of runoff variability in the Amu Darya and Zerafshan river can be attributed to the Indian Summer Monsoon features (Schiemann & Lüthi, 2008).

The location of the jet stream determines the synoptic situations over the region. Four typical configurations can be distinguished (see Schiemann & Lüthi, 2008, and references therein for more information)

- Cyclonic intrusions across the south of Central Asia from Iran and Afghanistan with large-scale inflow of warm air. Processes of this group entail warm winter weather and above-normal precipitation in Central Asia.
- Cooler summer and cold winter weather associated with cold northerly and north-westerly intrusions. The main part of winter time snow accumulation is due to these processes. In summer, they cause thunderstorms and showers in the mountains.
- Anticyclonic weather without precipitation, e.g. when Central Asia is located at the periphery of the Siberian High. Figure 3 below shows an Anticyclonic blocking pattern over Central Asia which caused one of the coldest winters on record with little precipitation and severe water shortages in the 2008 irrigation season.
- Mid-latitude cyclonic activity to the north of Central Asia. In summer, these situations are characterized by a small cooling, strong winds, and dust storms. The winter cooling is also small, but normally accompanied by precipitation.

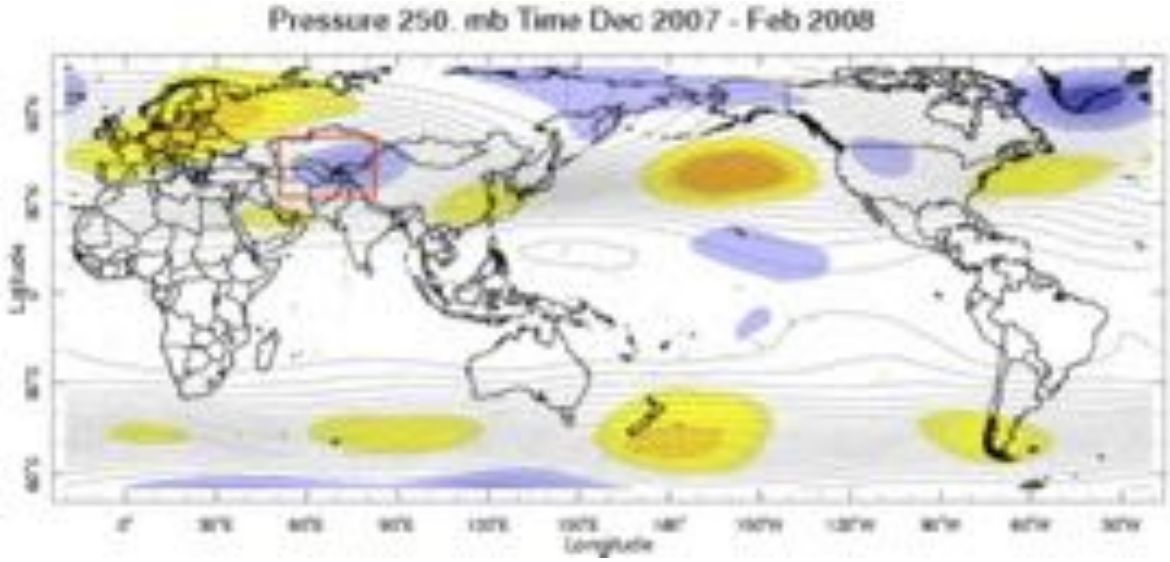

Figure 3: This map shows the seasonal (3-month average) geopotential height climatology and anomalies at the 250 hPa pressure level in the atmosphere from December 2007 through February 2008 using the 1981-2010 base period for the season shown. The 2007-08 winter was one of the coldest on record in Central Asia (red box, blue colors indicate negative height anomalies). Source: iridl.ldeo.columbia.edu/maproom/Global/Atm_Circulation/Seasonal_Height_250hPa.html

It is a general feature of the mountainous regions in Central Asia that climatic conditions can change considerably within a small area. At the Fedchenko glacier station (38.8 deg N, 72.2 deg E, 4169 masl) in Tajikistan, for instance, 87 percent of the annual precipitation falls during winter while at the Murgab station (38.2 deg N, 74.0 deg E, 3580 masl), the winter season accounts only for 27 percent of the precipitation. The distance between these two stations is less than 150 km (Khromova, Osipova, Tsvetkov, Dyurgerov, & Barry, 2006).

Through temperature and moisture controls, these mid- and high-latitude driven atmospheric large-scale features also control snow-cover extent. The most relevant factors for the snow-cover extent in Central Asia are temperature distributions over western Eurasia and the boreal Atlantic region. A negative temperature anomaly over Scandinavia, the North Atlantic/Arctic and Greenland and a positive temperature anomaly over Eastern Europe and NW Siberia result in much-reduced snow cover over Central Asia. Conversely, lowered temperatures over Eastern Europe and north-western Siberia, but warmer temperatures over Scandinavia and the northern-most realm of the North Atlantic, trigger more extensive snow cover (Clark, Serreze, & Robinson, 1999).

Lowered net snow accumulation and more restricted snow extent (possibly in combination with decreased glacial extent) resulted historically in lowered runoff in the Amu Darya and Syr Darya. Ice core analysis has revealed that prolonged periods of reduced runoff have persisted during AD 1150–1250, AD 1380–1450, AD 1580–1680 and during several low frequency events between AD 100–300 and after AD 1800. Glacier advances in different regions of

Tien Shan occurred from 100 BC–AD 300, AD 1400–1500, AD 1700–1750 and AD 1800–1850. The latest advance was observed at the beginning of the 20th century. Historically, the timing of increased runoff in the Aral Sea basin is related to higher snow accumulation and generally matches glacier advances (Oberhänsli et al., 2011, and references therein).

The regional-scale climate variability in the Central Asian region is strongly linked to large-scale climate variability and tropical sea surface temperatures, with the circulation anomalies influencing precipitation through changes in moisture transport (M. a. Barlow & Tippett, 2008). For example, linkages to El Niño Southern Oscillation (ENSO) events have been demonstrated. Enhanced precipitation in Central Asia during warm ENSO events results from an anomalous southwesterly moisture flux coming from the Arabian Sea and tropical Africa, which is generated along the northwestern flank of the high pressure anomaly over the Indian and western Pacific Oceans. The ENSO impact on Central Asia precipitation is found to be greatest in the transition seasons of autumn and spring, but the dynamical impact on pressure and circulation persists throughout the year (M. Barlow, Cullen, & Lyon, 2002; Mariotti, 2007).

3 20th Century Trends & Variability

In this Chapter, we report 20th century climate developments over Central Asia. We use both, in-situ station data on precipitation, temperature and selected runoff stations and gridded data from the GPCC Precipitation Climatology from 1901 – 2000 Version 6 as well as temperature data from the University of Delaware Air Temperature dataset V3.01 (see Appendix for more information).

For the analysis of trends, we use the non-parametric Mann-Kendall test. The Mann-Kendall test is a statistical test widely used for the analysis of trend in climatologic and in hydrologic time series (Mavromatis & Stathis, 2010; Yue & Wang, 2004). The test was run at 5% significance level on the gridded precipitation and temperature time series data for each grid cell.

For the estimation of the trend, a robust linear estimation method was used, i.e. the Sen's slope estimator. The method chooses the median slope among all lines through pairs of two-dimensional sample points. It can be computed efficiently, and is insensitive to outliers. It can be significantly more accurate than simple linear regression for skewed and heteroskedastic data, and competes well against simple least squares even for normally distributed data (see http://en.wikipedia.org/wiki/Theil–Sen_estimator and references therein). The Sen's slope is calculated over the respective times for each cell independently.

For the assessment of runoff variability, we report general considerations of river flows and present the methodology with which the Hydrometeorological services do flow assessments on an annual base. Using these types of methods for the determination of average, dry and wet years ensures a sound quantitative assessment of situations of extremes for the Amu and Syr Darya.

Long-term time-series analysis of flows is drawing on standard methods for the identification of trends and variability, also at decadal scales and beyond.

3.1 Climate

3.1.1 Analysis of In-Situ Temperature, Evapotranspiration & Precipitation Data

Available data from meteorological stations in the Tien Shan is shown in Figure 4. Data from 6 stations are shown. Data ranges are 1933 – 2006 for precipitation data and 1917-2006 for temperature. For precipitation, no significant trend can be identified and the data are characterized by high interannual variability. For temperature, all stations exhibit a significant positive trend between 0.10 to 0.24 deg. C. per decade (mean trend over the complete peri-

od of time is 0.15 deg. C. per decade). From 1990 onwards, the mean trend over all stations was 0.3 deg. C. per decade which is a bit more than half of the ensemble mean temperature trend per decade as derived from the GCM SRES A2 runs (see Chapter 4, Section 4.2 below). Figure 5 shows that these developments can be mainly attributed to a winter warming in the Tien Shan mountain ranges. This corresponds well to the results from the spatio-temporal analysis of gridded data (see Section 0 below).

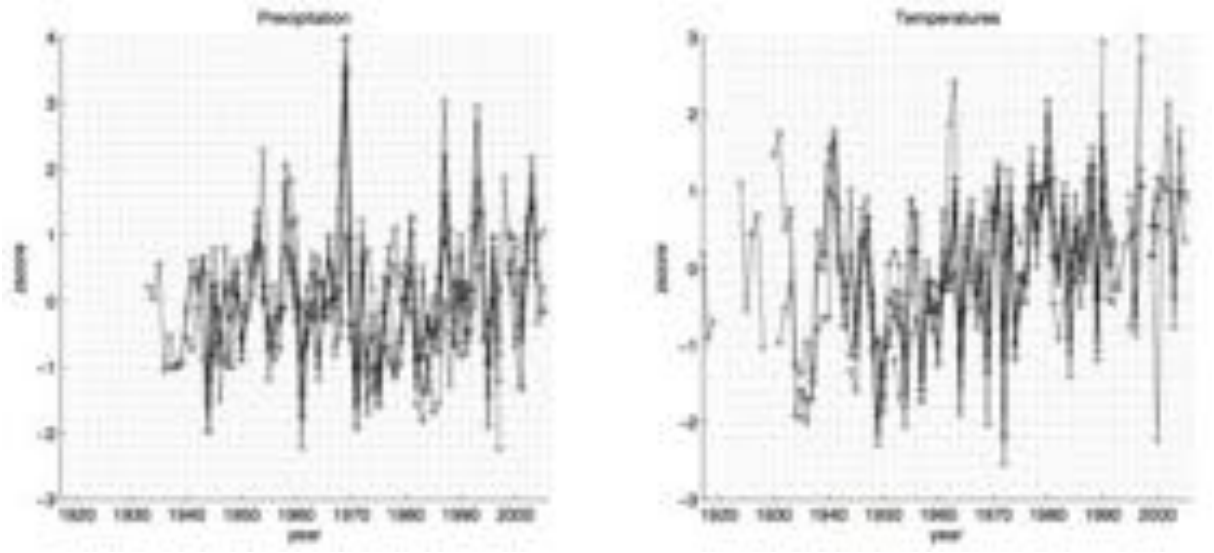

Figure 4: Annual centered and normalized precipitation and mean temperatures for 6 stations in the Tien Shan mountains. Stations are: Naryn (41 deg 26' N, 75 deg 59' E), Tian Shan (41 deg 26' N, 75deg 59' E), Pskem (41 deg 54' N, 70 deg 20' E), Chatkal (41 deg 55' N, 71deg 20' E), Padsha-Ata (41 deg 35' N, 71 deg 40' E), Ak-Terek-Gava (41 deg 20' N, 72 deg 42' E). The extremely wet year in 1969 is clearly visible. See (Siegfried et al., 2011)

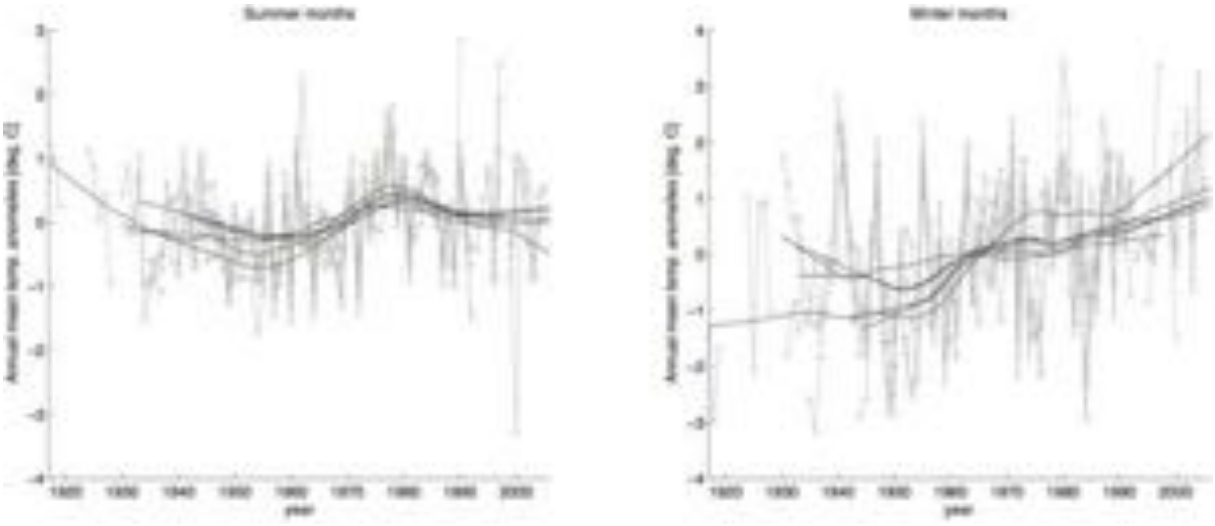

Figure 5: The left plate shows summer (April through September) anomalies, the right plate shows winter anomalies for the months October through March. A pronounced warming trend in the winter months over the second half of the 20th century is discernible. Gray lines: Actual data, black lines: 25 year robust local regression filtered time series.

Figure 6 shows time series from in-situ station based measurements on land evapotranspiration. Data are available for the second half of the 20th century. As is visible, actual evapotranspiration has been declining until the year 2000. This is in line with the global observations made by (Jung et al., 2010) who hypothesized that this is due to increasing limitation from soil moisture supply to the atmosphere. The filtered data show an interesting 10-11 year cycle which might be linked to solar activity.

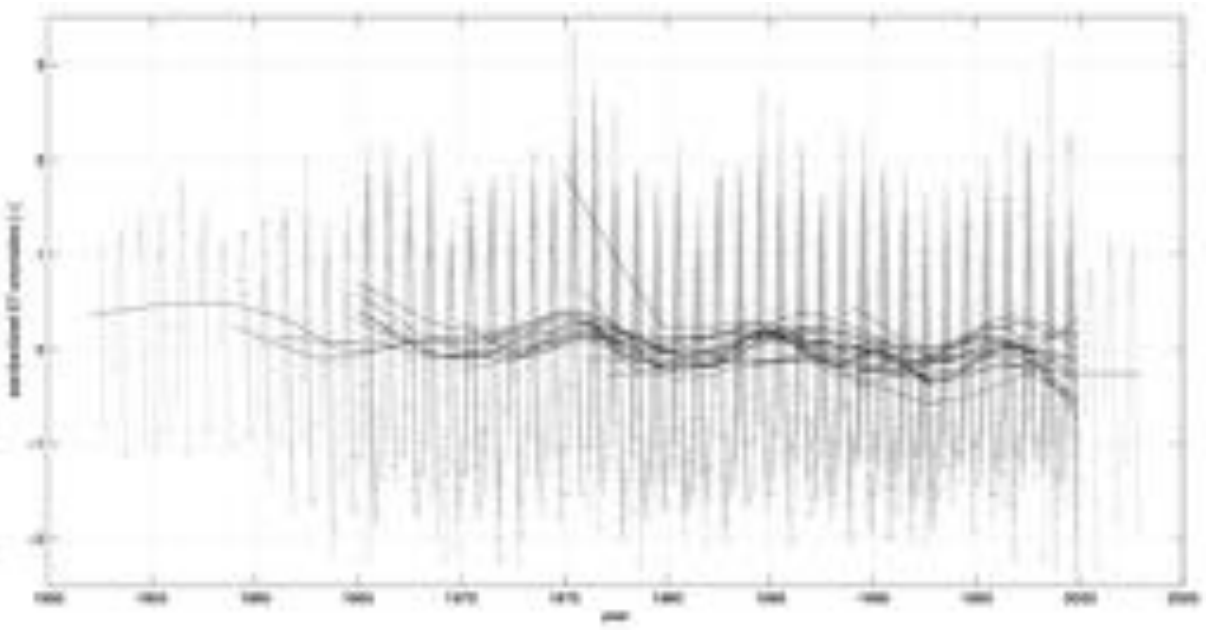

Figure 6: ET has been declining with a marked multi-year cycle that might be solar cycle induced. Gray lines: Actual data, black lines: 10 year robust local regression filtered time series.

It should be however noted that these negative trends do not reflect evapotranspiration rates in irrigated areas as water supplies are plentiful under normal conditions and as rising temperatures will increase the atmospheric demand correspondingly there.

A MORE COMPLETE ANALYSIS WOULD REQUIRE THE COLLECTION AND ANALYSIS OF ALL AVAILABLE IN-SITU STATION-BASED DATA OVER THE DOMAIN.

3.1.2 Analysis of Gridded Precipitation & Temperature Data

Precipitation

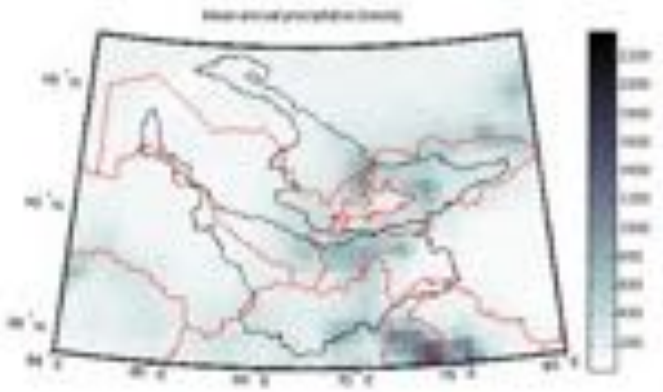

Figure 7: 20th century mean annual precipitation over Central Asia (in mm/a). Data Source: GPCC Precipitation Climatology, 1901 – 2006 (see also Appendix). The influence of the South Asia Monsoon is visible in the lower left corner of the image. River basins outlined in black color, country borders are shown in red.

Analysis of long-term mean annual precipitation in the Central Asian region of the 20th century GPCC precipitation climatology dataset is shown in Figure 7 above. Topography crucially determines the precipitation climate in the mountains. In the Tien Shan in Kyrgyzstan, Kazakhstan and Uzbekistan, the mountain ranges with westerly and north-westerly exposure are the primary orographic features where precipitation is occurring. This holds true for the Kyrgyz and Kazakh Alatau, for the Chatkal, Pskem and Ugam ranges at the western end of the Kyrgyz Alatau and the Fergana range that the eastern end of the Fergana Valley where the highest average precipitation totals are observed in the vicinity of the semi-arid valley.

The Plates in Figure 8 shows long-term mean seasonal precipitation totals. Western and central Pamir regions and the western Tien Shan (including north ridge of Fergana valley, Talas, Susamir and Chu valleys) receive the bulk of precipitation during winter and spring seasons. Conversely, eastern Pamir and northern Tien Shan (including Zailiiskiy Alatau) together with the main runoff formation area of the Syr Darya in central Tien Shan, have spring-summer maximum precipitation (Siegfried et al., 2011).

In the Vaksh River valley along the southern slops of the Alay and Turkestan ranges, one of the main tributaries of the Amu Darya, there is a marked decrease of precipitation from south-west (lower reaches of the Vaksh) to north-east (Surkhob River and Kyzylsu West, the right tributary to the Vaksh).

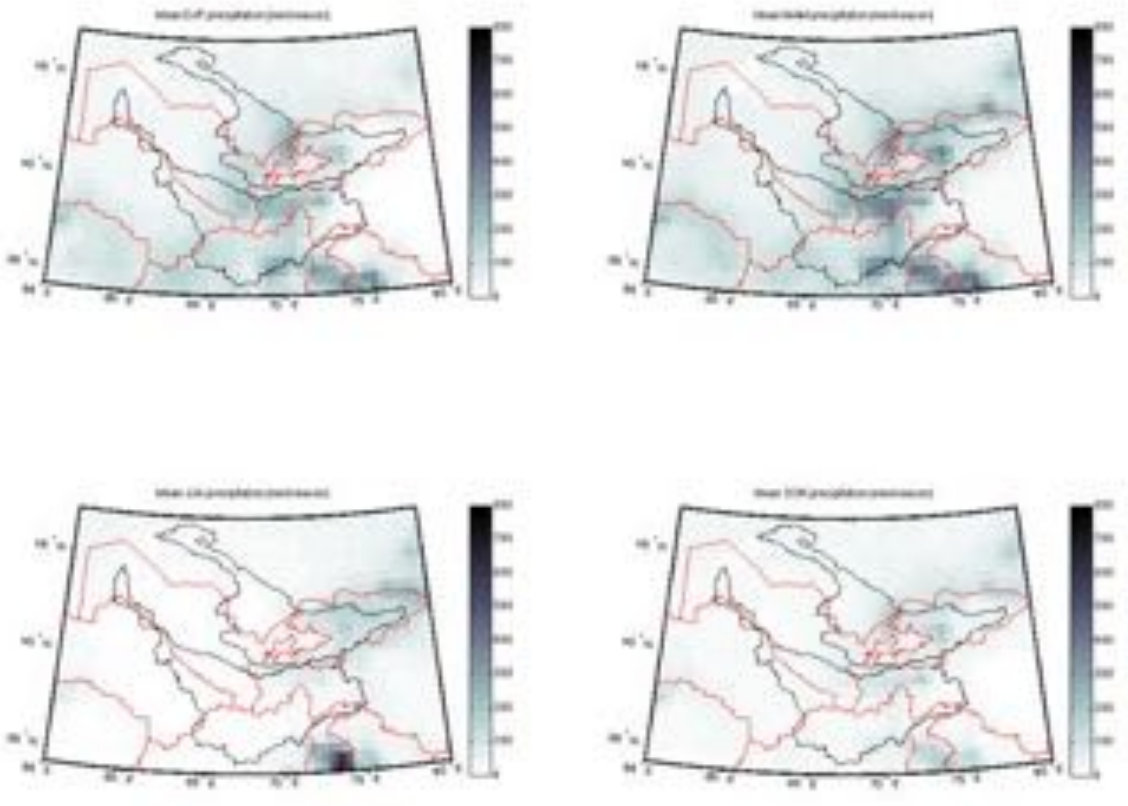

Figure 8: 20th century mean seasonal precipitation over Central Asia. Upper left plate: DJF; upper right plate: MAM, lower left plate: JJA; lower right plate: SON. Data Source: GPCC Precipitation Climatology, 1901 – 2006 (see also Appendix). River basins outlined in black color, country borders are shown in red. River basins outlined in black color, country borders are shown in red.

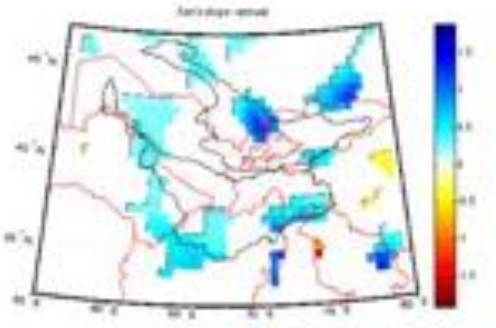

Figure 9: Robust linear regression (Sen's slope) for the GPCC Precipitation Climatology data set. Total precipitation annual data are used (mm/a). The slope values are in mm/a. Blue hued cells indicated a positive trend, yellow to red hues are negative trends. Only cells with statistically significant trends are shown. River basins outlined in black color, country borders are shown in red.

Using the GPCC 20th century precipitation climatology the data for analysis of grid cell annual precipitation totals, robust trends in precipitation are shown in Figure 9. Figure 10 shows a similar type of analysis for seasonal precipitation trends. Two key observations from the analysis of this dataset emerge. First, the precipitation climate has become slightly wetter over the course of the 20th century in selected regions. These include parts of the Kyrgyz and Kazakh Alatau in the vicinity of the Arys, Keles and Talas Rivers and in the Almaty region of Kazakhstan as well as the Wakhan corridor region in the border area of Tajikistan, Afghanistan and Pakistan and in the north-western Afghan provinces of Badghis and Ghor. Second, the signals are mainly from increasing winter precipitation in the Tien Shan and increasing summer precipitation in the vicinity of the Amu Darya catchment to the south.

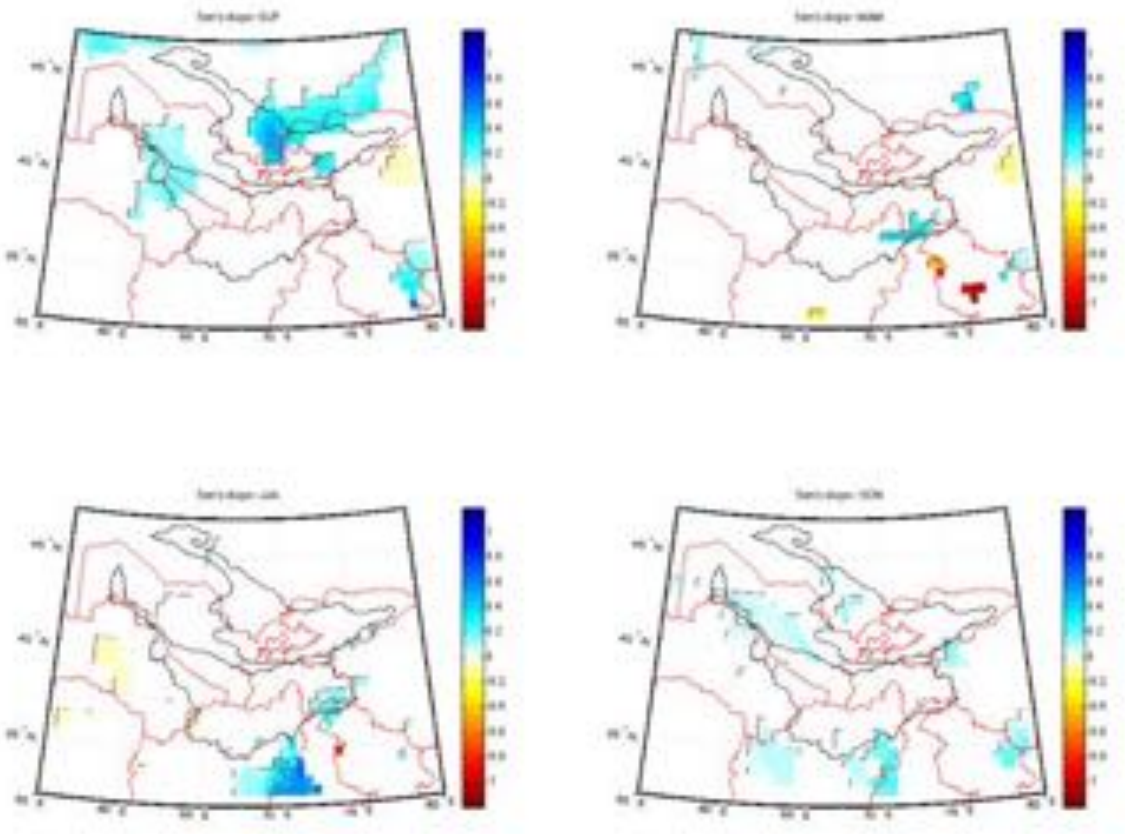

Figure 10: Robust linear regression (Sen's slope) for the GPCC Precipitation Climatology data set. Trends are calculated for every season (total precipitation in mm/season).Slope values are in mm/a. Upper left plate: DJF; upper right plate: MAM; lower left plate: JJA; lower right plate: SON. Blue hued cells indicated a positive trend, yellow to red hues are negative trends. Only cells with statistically significant trends are shown. River basins outlined in black color, country borders are shown in red.

The latter is possibly linked to an increasing moisture spill-over from the Indian Summer Monsoon[2]. Inn most locations of Central Asia, however, no robust precipitation trend signals are discernible.

Figure 11 and Figure 12 show grid cell level coefficients of variations (CV) of annual and seasonal time series for precipitation. The coefficient of variation is a normalized measure of the dispersion of the grid cell level time series (Fatichi, Ivanov, & Caporali, 2012). Data show that the predominantly semi-arid to arid low-lands of the two large river basins feature high CV values which is an indication of high interannual variability of annual and/or seasonal totals. The high CV values are observed in the dry and hot summer and autumn seasons in the region, especially in the Amu Darya basin.

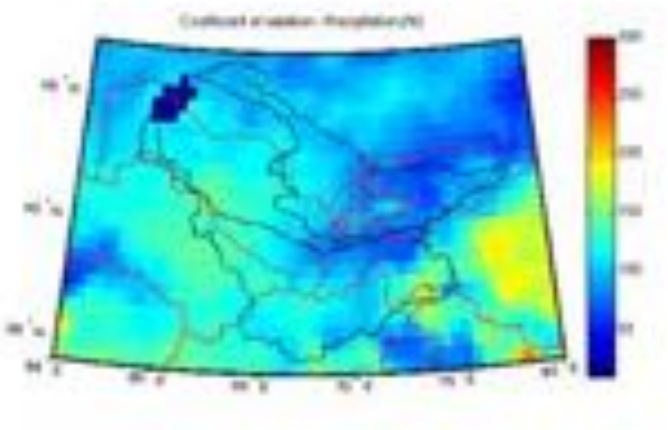

Figure 11: Coefficient of variation of total annual precipitation. Generally, drier areas feature a higher coefficient of variation as compared to wetter regions. River basins outlined in black color, country borders are shown in red.

[2] It should be noted that this analysis could also be carried out with other gridded precipitation datasets so as to further confirm the validity of the signals.

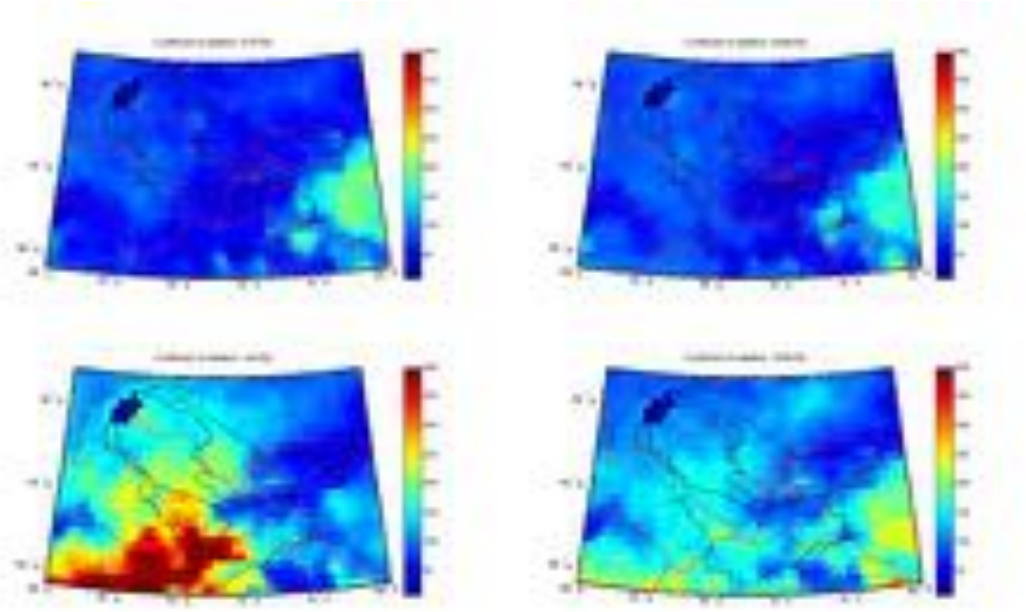

Figure 12: Coefficient of variation of total mean precipitation. Upper left plate: DJF; upper right plate: MAM; lower left plate: JJA; lower right plate: SON. Generally, drier areas feature a higher coefficient of variation as compared to wetter regions. River basins outlined in black color, country borders are shown in red.

Temperature

Analysis of 20th century grid level temperature data in the Central Asian region are shown in Figure 13 and Figure 14. The dataset is described in the Appendix.

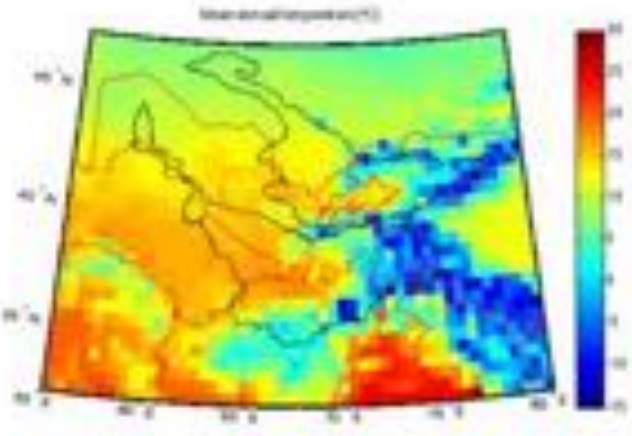

Figure 13: Mean annual temperatures in degrees Celsius. The Western Himalayas, the Hindukush, the Pamis and the Tien Shan mountain ranges are clearly visible. River basins outlined in black color, country borders are shown in red.

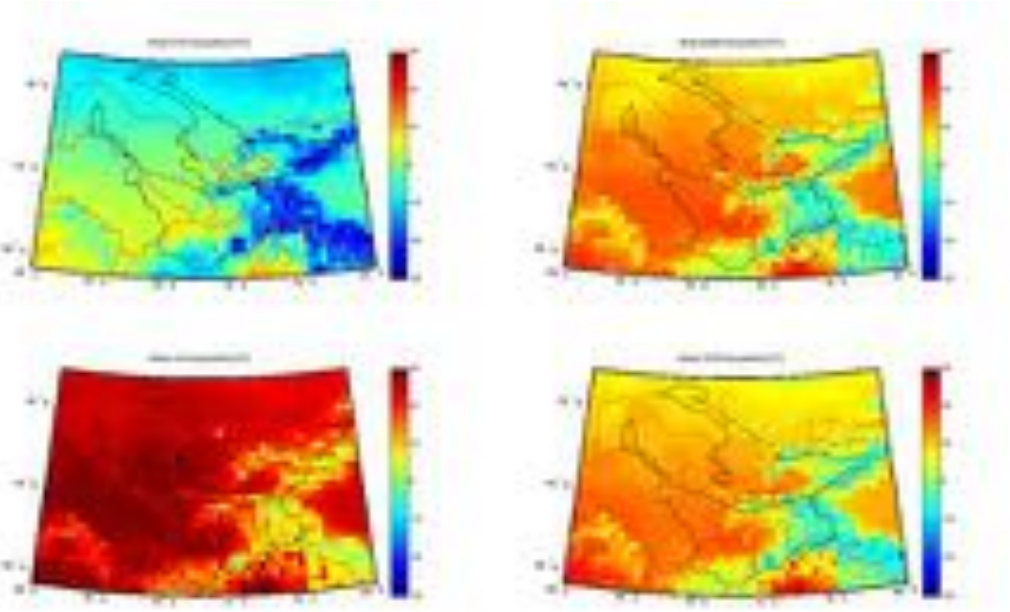

Figure 14: Mean seasonal temperatures (in Deg. C). Upper left plate: DJF; upper right plate: MAM; lower left plate: JJA; lower right plate: SON. Red colors indicate warm temperatures, blue colors are cold temperatures. River basins outlined in black color, country borders are shown in red.

The highland versus low-land distinction in the basins is easily visible from looking at the large-scale temperature distribution in the region.

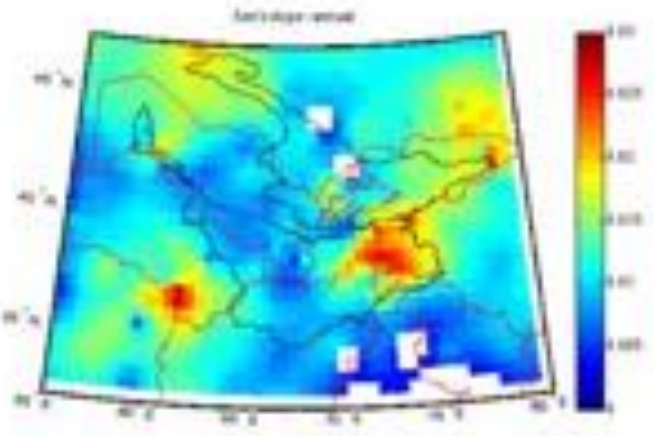

Figure 15: Robust linear regression (Sen's slope) for the University of Delaware air temperature data set. Mean annual data are used (deg. C.). Slope values are in deg. C per year. Blue hued cells indicated a positive trend, yellow to red hues are negative trends. Only cells with statistically significant trends are shown, i.e. white cells are non-significant trend cells. River basins outlined in black color, country borders are shown in red.

The analysis of robust temperature trends reveals interesting large-scale spatial organization of these trends (see Figure 15 and Figure 16). First, most of the Central Asian region experi-

enced a warming over the 20th century. Trends of annual warming are high in the eastern Kazakh Alatau and in the Alay range as well as the Pamirs. Except for the Aral sea region, most of the lowlands in the river basins experienced only moderate warming. The warming in the heavily snow and ice covered upstream zones of runoff formation in the two basins has important repercussion on river flows and their seasonality (see Section 5.2 below for more on that).

Interesting robust high warming trends can be observed in the vicinity of the large cities Tashkent in Uzbekistan and Almaty in Kazakhstan. The signals there might in fact be non-climatic and effectively be related to a heat island effect where a growing population in an expanding urban environment has led to local ambient heating that is picked up by the city-based meteorological stations (see e.g. Karl, Diaz, & Kukla, 1988 for more information on non-climatic heat island effects). This is important to acknowledge as many of the remote meteorological stations in Central Asia fell into disrepair, especially after the demise of the Soviet Union. For example, the temperature trend reported in (Savitskiy & Schlüter, 2008) for the Tashkent station and attributed to climate change by the authors, might entirely be related to a heat island effect.

However, it appears that the trends in the Pamirs and parts of the Kyrgyz Tien Shan are particularly robust. They range between a 1.5 to 4 Degree Celsius warming over the 20th century.

DESPITE THE ROBUSTNESS OF THE REPORTED TRENDS HERE IN THE UNIVERSITY OF DELAWARE AIR TEMPERATURE DATASET, IT IS STRONGLY RECOMMENDED THAT A MORE COMPREHENSIVE ANALYSIS SHOULD BE CARRIED OUT IN THE SENSE TO ALSO CROSSCHECK 20TH CENTURY TEMPERATURE TRENDS WITH AVAILABLE STATION DATA SO AS TO ASSESS THE SIGNALS VALIDITY.

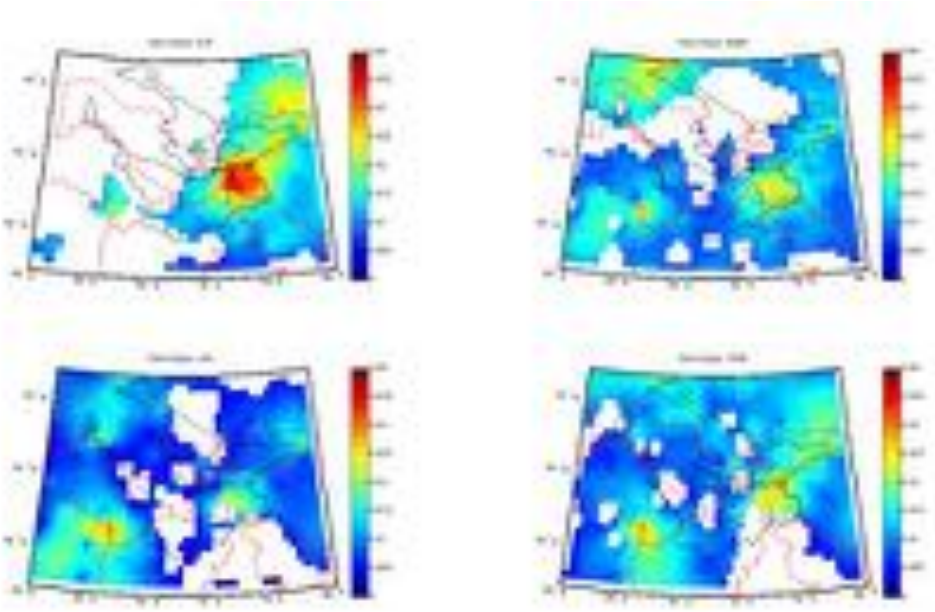

Figure 16: Robust linear regression (Sen's slope) for the University of Delaware air temperature data set. Mean seasonal data are used (deg. C.). Slope values are in deg. C per year. Blue hued cells indicated a positive trend, yellow to red hues are negative trends. Only cells with statistically significant trends are shown, i.e. white cells are non-significant trend cells. Upper left plate: DJF; upper right plate: MAM; lower left plate: JJA; lower right plate: SON. River basins outlined in black color, country borders are shown in red.

Interestingly, robust positive trends are visible for the winter months only in the eastern higher elevation regions of Central Asia.

3.2 Runoff

3.2.1 Analysis of Selected Tributaries to Amu & Syr Darya

Here, long-term time series of selected stations of Syr and Amu Darya tributaries are examined in terms of trends and variability. Care must be taken in selecting appropriate stations in the region that are amendable for long-term, century-scale analysis. Reasons include:

- Hydrological stations located in the lowlands are in a zone of intense water-related activities. Water management in the Syr Darya River began around the 1940ies of the last century (e.g. start of operations of the Great Fergana and Northern Fergana canals). This type activity has increased dramatically since the 60s of the last century (e.g. in 1959, commissioning of Kayrakkum reservoir). For this reason, some of the previous long-term hydrological stations were closed, such as Bekabad (Zaporozhsko) gauge, which started to make runoff observations in 1910.

- In the second half of the last century, an intense period of surface reservoir construction began in the two Daryas. For this reason, some of the long-term hydrological gauging stations were closed while new ones began to make observations of river flow in the downstream reservoirs. For example, the closed Khodzhikent hydrological station on the Chirchik River (after construction and commissioning of the Charvak reservoir in 1978), started measuring runoff in 1901. There are numerous such examples.
- Change in measuring methodology and technology re know to have in some instances affected the quality and homogeneity of long-term runoff time series.
- After 1990, following the collapse of the Soviet Union, the quality of the hydrometric observations deteriorated dramatically. Nowadays, most observations on the hydrological stations are made in violation of the proven procedures. In Soviet times, the National Hydrometeorological services had inspection departments, whose employees which was in charge of checking the gauging stations on a regular basis for compliance with regulations. All this was carried out by very experienced staff so as to ensure highest possible quality and runoff time series measurement homogeneity. This type of quality insurance is in many instances no longer guaranteed.
- Finally, local gauge staff at gauging stations is suffering from adverse economic conditions because of little/no salary payments they receive for their work. As a result, some of them have lost the motivation to ensure the highest quality standards in their works.

For the following time series analysis, we have selected from a sample of stations that cover various types of runoff regimes in different locations over the Central Asian domain and that are known not to have been affected by some of the issues mentioned above. The following Table 4 shows summary characteristics of the individual rivers. Figure 18 - Figure 31 shows the results of the analysis.

River	Tributary	Hydrological station Name	Ridge	Mean watershed elevation [masl]	Catchment area [km^2]	Classification of rivers (by Victor Schultz)
Syr	Chatkal	Khudaydod	Northern slopes of the Chatkal ridge	2'610	7'110	Snow- and Ice
Syr	Pskem	Mullala	Pskem Ridge	2'690	2'830	Snow- and Ice
Syr	Gavasai	Gava	Southern slopes of the Chatkal ridge	2'460	657	Snow- and Ice
Syr	Isfairamsay	Uch-Kurgan	Northern slopes of the Alay ridge	3'240	2'220	Glacier-snow
Syr	Padsha Ata	Tostu	Southern slopes of the Chatkal ridge	2'830	366	Snow- and Ice
Syr	Sokh	Sarkanda	Northern slopes of the Alai ridge	3'480	2'480	Glacier-snow
Amu	Surkhandarya, Tupalang	Tuplang Zarchob	Southern Slopes of Hissar ridge	2'570	2'200	Snow- and Ice
Amu	Vaksh	Darband	Alai, Trans Alai ranges, Peter the First Ridge, Darvaz, Vaksh, Karategin ranges	3'600	29'500	Glacier-snow
Amu	Zerafshan	Rovatkhodja	Turkestan range	NA	12'800	Glacier-snow
Syr	Naryn	Naryn	Central Tien-Shan	3'570	10'500	Glacier-snow

Table 4: Characteristics of rivers investigated for long-term analysis. The list comprises of selected tributaries to the Amu Darya and the Syr Darya.

A map of the selected stations is provided below.

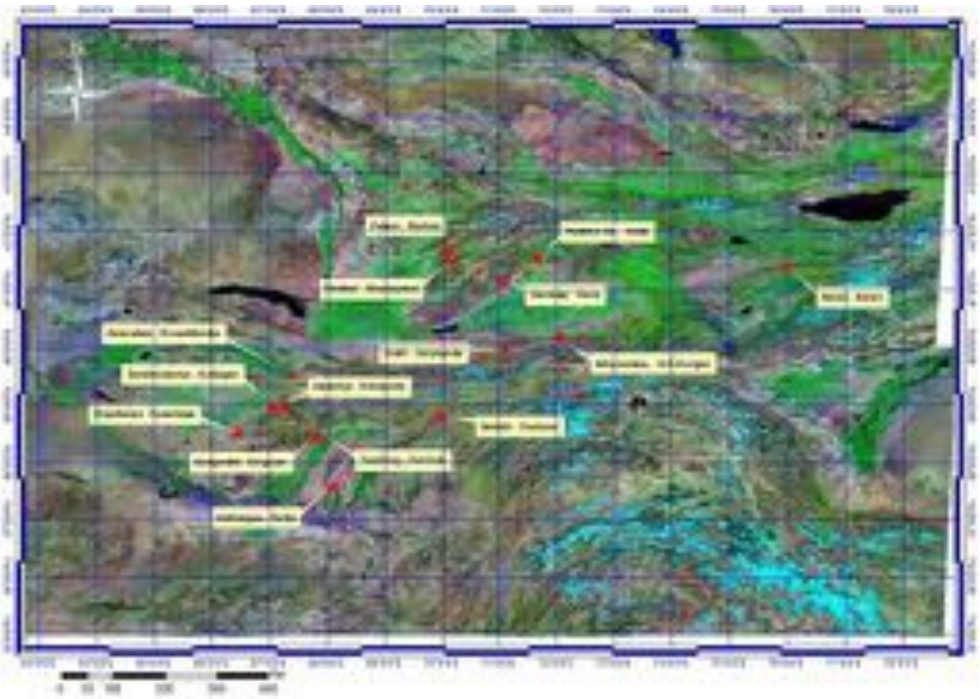

Figure 17: Map of selected gauging stations in the Amu and Syr Darya tributaries utilized for long-term flow analysis.

It should be noted that the analysis carried out below for historic flows should be also viewed in the context of future runoff projections as reported in Chapter 5.2 below.

For the reported Amu Darya stations, the following applies:

- Zerafshan: Inflow into Rovathodzha dam. Until the early 90's of the last century, the water quantity consisted of Zerafshan (Dupuli gauge) and Magiyandarya (Sudjina gauge). After that, the value of water inflow to the Rovathodzha dam was obtained by taking into account the diversions of irrigation water and releases of water from the hydroelectric dams to the lower reach.
- Vaksh: Darband (Komsomolabad): River flow data are provided for several hydrological stations and calculated from them. Up to 1967, on the Tutkaul gauge (catchment area of 31,200 km^3) from 1968 to 1977, the sum of two hydrological stations - Garm on the Vakhsh (catchment area of 20,000 km^3) and Tavildara on Obihingou River (catchment area of 5390 km^3), from 1978 to Komsomolabad (Darband) gauge.
- Tupalang - Zarchob. Since the mid-1980, Tupalang reservoir was built above the gauge. Tupalang reservoir is a reservoir of seasonal regulation and does not significantly influence runoff.

Time Series

Figure 18 shows the time series of runoff at the selected stations. For most rivers, approximately 90 years of monthly are available for analysis. Where necessary for further analysis, gaps were filled with Singular Spectrum Analysis[3]. Visual inspection of minimum and maximum flows reveals low-frequency phenomena (e.g. see minim runoff at Tostu gauge in Padsha-Ata River and how it is modulated over time) and significant levels of interannual variability of the spring-summer runoff peaks.

[3] In time series analysis, singular spectrum analysis (SSA) is a nonparametric spectral estimation method. It combines elements of classical time series analysis, multivariate statistics, multivariate geometry, dynamical systems and signal processing. For analysis the KNMI Climate Explorer (http://climexp.knmi.nl) and the kSpectra tool (http://www.spectraworks.com/web/welcome.html) were utilized.

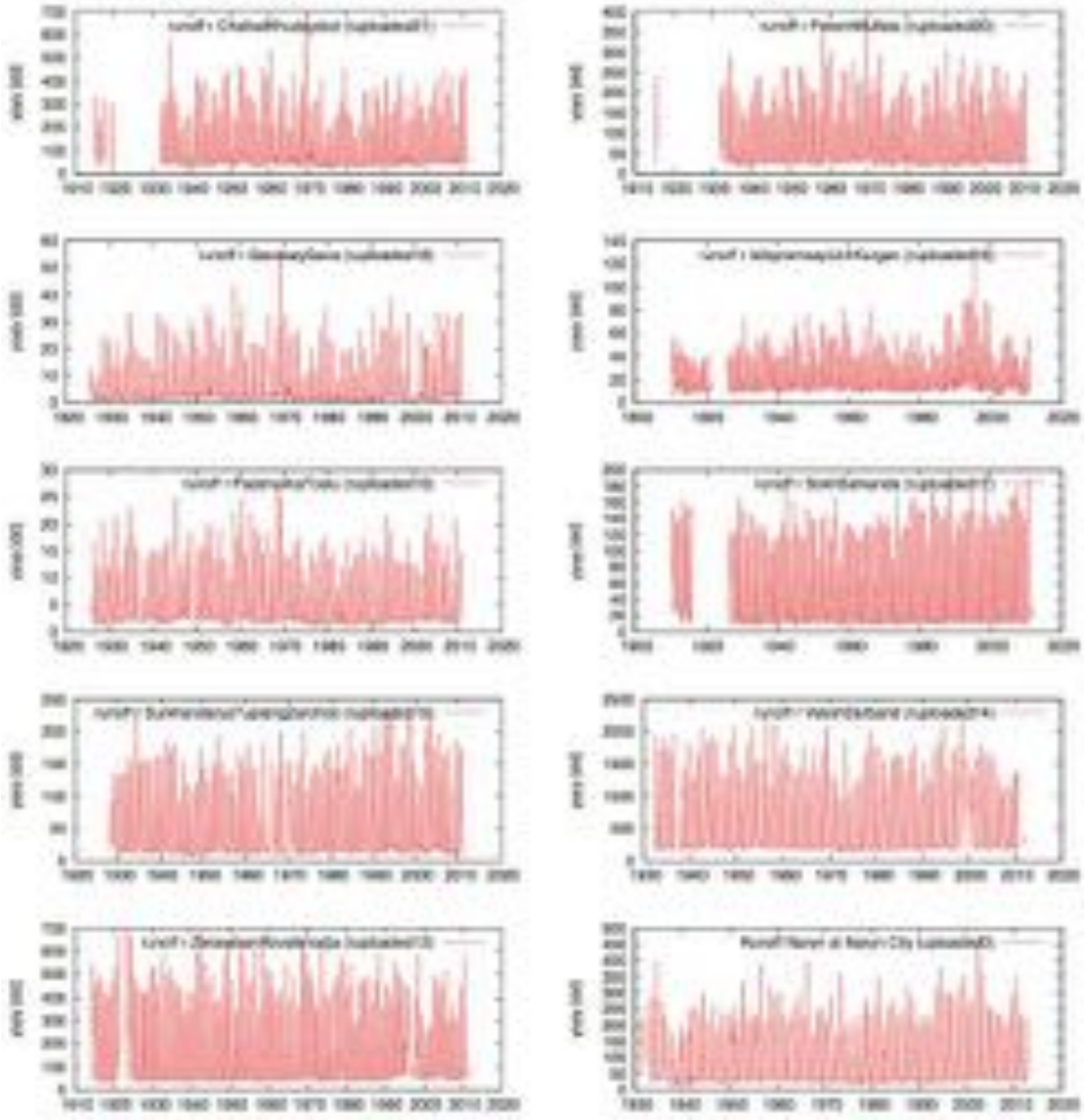

Figure 18: Long-term monthly runoff time series of selected gauging stations in Amu and Syr Darya tributaries. Missing data are indicated by gaps. Units are m^3/s.

In all catchments, the minimum winter runoff features cyclical variability as well as increasing trends in some instances (Sokh and Naryn). Figure 20 below shows corresponding seasonal cycles of the rivers and Figure 21 shows runoff anomalies where interannual scale variability is clearly visible.

Until the seventies of the last century, two gauging stations existed on the Syr Darya that were used to assess low-frequency variability of river flows. These were Hodzhikent on Chirchik River and Uch Kurgan on Naryn. Runoff at the Uch Kurgan gauge, which is located at the foot of the Naryn/Syr Darya cascade shortly after the river enters Uzbekistan from Kyr-

gyzstan is characterized by four distinct periods, i.e. natural runoff and Periods 1-3 as shown in Figure 19 below.

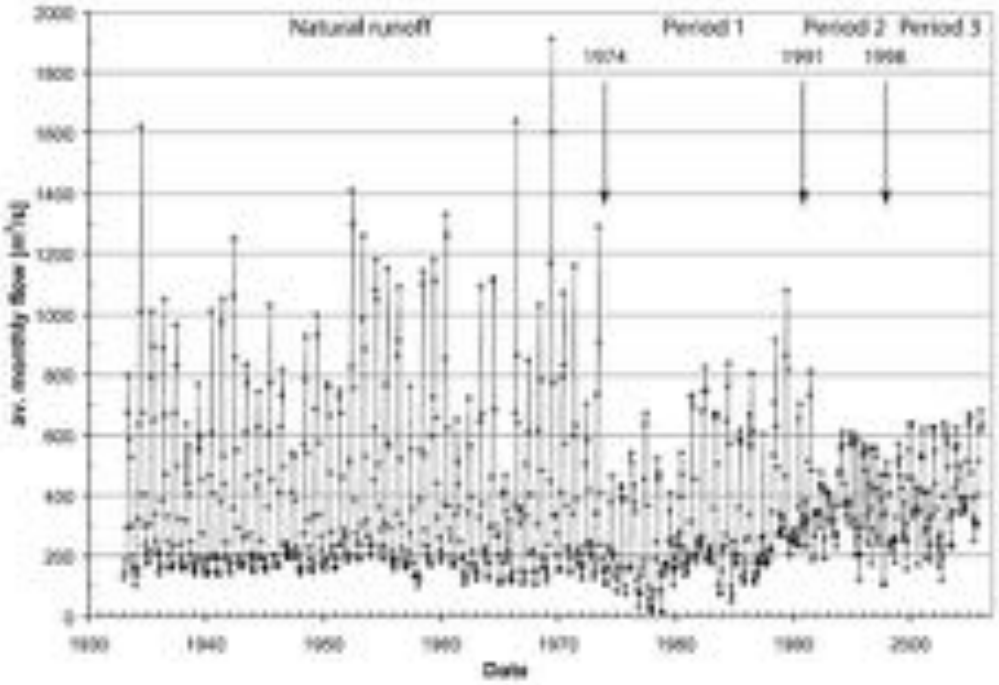

Figure 19: Mean monthly runoff values at Uch Kurgan, below the Toktogul reservoir and the Naryn cascade. The different management periods of the river are indicated. Toktogul dam was close in 1974. The demise of the Soviet Union was in winter 1991. In 1998, a joint framework agreement between the Republics was signed on the joint rational water and energy use in the Syr Darya basin. See (Siegfried & Bernauer, 2007).

When the runoff was largely natural until 1974, that is, determined by seasonal and climatic variability, the mean flow was around 390 m^3/s, with a high interannual variability in summer runoff. At that time it was established that runoff variations due to climate in Chirchik and Naryn are in phase

At Uch Kurgan, a major change in flow patterns set in with the commissioning of the Toktogul reservoir in 1974. This event marks the beginning of what one could label the first river management period (1974–90). This period was characterized by centralized management by the USSR of the Naryn/Syr Darya cascade and the river basin as a whole.

From 1974 to 1990, the management system for the Syr Darya was primarily oriented towards water provision for irrigated agriculture (above all, cotton and wheat production) in Uzbekistan and Kazakhstan. Consequently, the timing of winter and summer flow releases did not change substantially compared to the natural runoff pattern, where peak flows also occur in the agricultural growing season. This water allocation pattern is visible in the hydrograph, where the in- and outflows to and from the Toktogul reservoir are in phase.

After 1991 and until 1998, the management of the river became non-cooperative until 1998 when a new water sharing agreement was established between the upstream and downstream republics (Bernauer & Siegfried, 2012). This agreement states that the allocated quota at transboundary scales should be renegotiated annually.

Seasonality

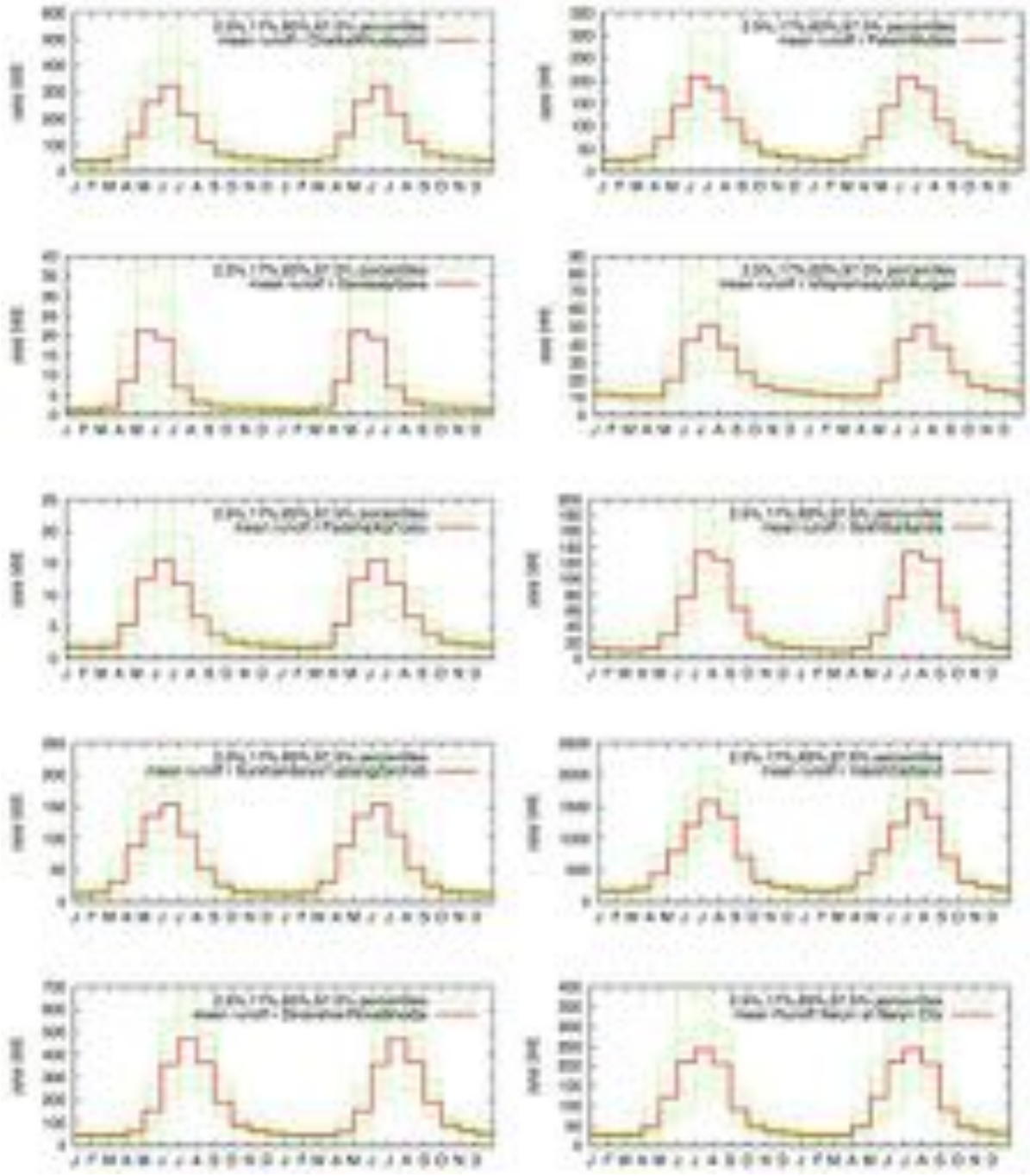

Figure 20: For each gauging station, two annual cycles are shown (computed with all available data). Mean (red color) and 2.5%, 17%, 83% and 97.5% percentiles are shown in green color.

For each of the time series, seasonal cycles were extracted. Figure 20 shows two cycles for each gauging station. Comparing the onset of spring runoff as well as runoff peaks based on long-term flow data and the average catchment elevations reported in Table 4 shows the controlling factor of altitude. All catchments with mean elevation > 3'000 masl peak feature runoff peaks in July as compared to June peaks for catchments where mean elevation is < 3'000 masl.

Anomalies

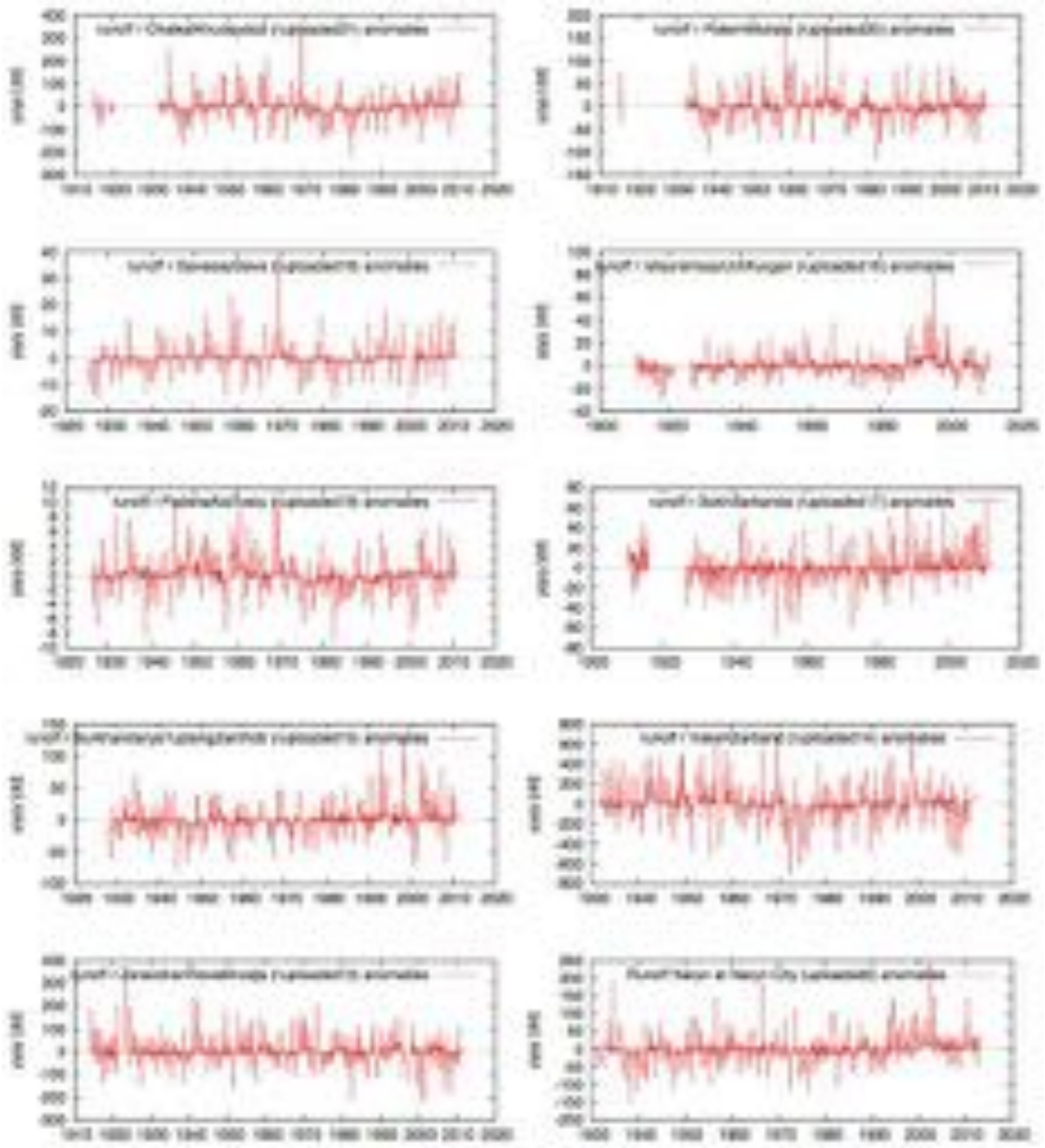

Figure 21: Runoff anomalies (m^3/s) with respected to the corresponding annual cycles shown in Figure 20.

Figure 21 shows runoff anomalies for the selected stations where the seasonal cycles have been subtracted from the original flow series. These time-series will be utilized for spectral analysis and analysis of autocorrelation below.

Running Mean

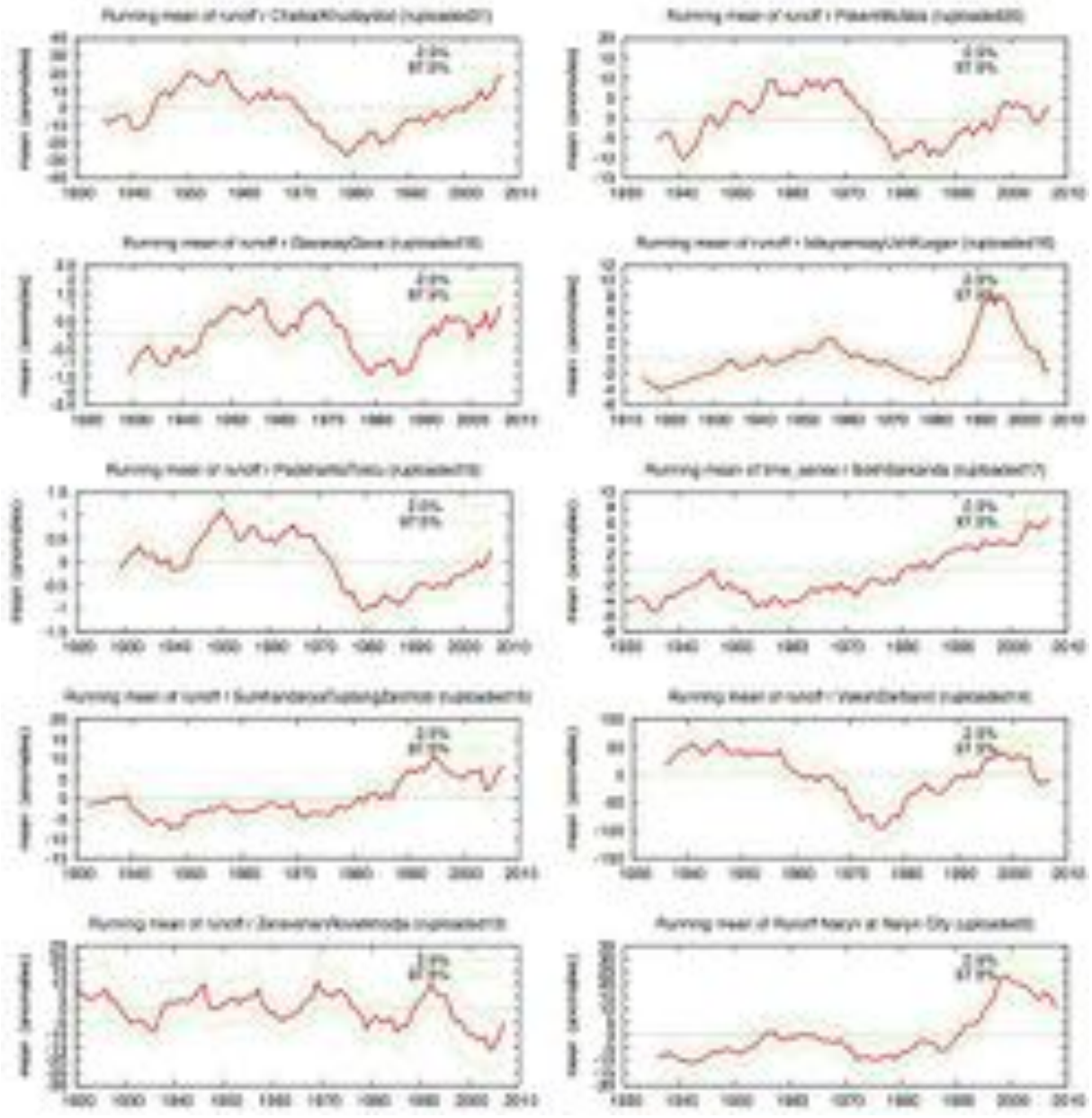

Figure 22: Running mean of long-term time series after subtraction of corresponding annual cycles (see Figure 20). In all instances, a window size of 10 years was used for computation.

Visual inspection of 10 year running mean time series reveals and interesting synchronic modulation in the Syr Darya catchment where after or around 1980, filtered runoff of all tributaries start to increase unanimously after an apparent 40 - 50 year cycle that is visible in much of the Syr Darya tributaries.

The decline of filtered flows in the early 1990ies after the rise in 1980 in Isfayrasamy is hard to explain and regional experts are unsure about its cause (Personal Communication: A. Yakovlev, former Uzbek Hydrometeorological Service, and O. Kalashnikova, former Kyrgyz Hydrometeorological Service). As Figure 26 shows, this hump in the filtered time series is visible in all seasons and might also be related to measurement issues at the gauging station.

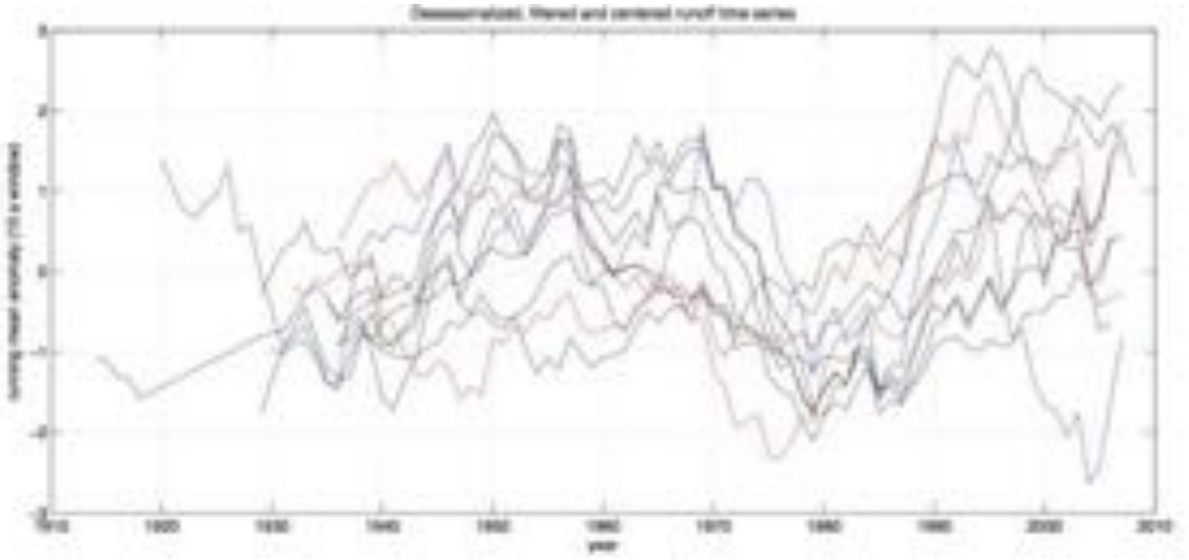

Figure 23: Synchronized low-frequency modulations are apparent in the runoff of selected tributaries to the Amu and Syr Darya. Syr Darya tributaries are shown in black, Amu Darya tributaries are shown in red and Zerafshan running mean runoff data is shown in blue colors.

Sokh River shows interesting behavior too. Since mid-1950, mean runoff has been increasing (Figure 22). This increase was mainly due to increasing MAM and JJA season contributions (see right plate in Figure 27). This might be an indication of increasing contributions to runoff from depletion of glacier storage in the catchment. Interestingly, the neighboring catchments in the Alay and Turkestan ranges that dewater into the South Fergana Valley do not show similar trends (Figure 26).

However, data that analysis the development of glaciation in these river basins has shown that deglaciation rates have declined from 1980 onwards so a more careful analysis is required to further substantiate any claim (see also Section 5.1 for more information on future climate dynamics).

Basin	Area of glaciers, km^2			Mean annual rates of degradation of glaciation [%]	
	1957	1980	2001	1957–1980	1980–2001
Shakhimardan	39.46	30.14	28.19	1.03	0.31
Sokh	246.26	214.63	198.25	0.56	0.36
Isfara	129.74	125.05	120.99	0.16	0.15
Zerafshan glacier	156.57	141.62	135.10	0.42	0.22
Total	572.03	511.44	482.53	0.46	0.27

Table 5: Glacier area in selected catchment in the Alay and Turkestan ranges (Gissar Alay) (see Yakovlev, 2006).

THE RUNOFF TRENDS AS VISIBLE IN THE SOKH AND NARYN RIVER CATCHMENT REQUIRE MORE ATTENTION. ARE THEY FROM INCREASINGLY INADEQUATE RUNOFF MEASUREMENTS WHERE A SYSTEMATIC BIAS IS INTRODUCED OVER TIME DUE TO INSUFFICIENT CALIBRATION OR ARE THEY DUE TO THE INCREASING RUNOFF FROM GLACIER MELTING OR DUE TO CHANGES IN THE PRECIPITATION CLIMATE IN THE REGION OR A JOINT EFFECT?

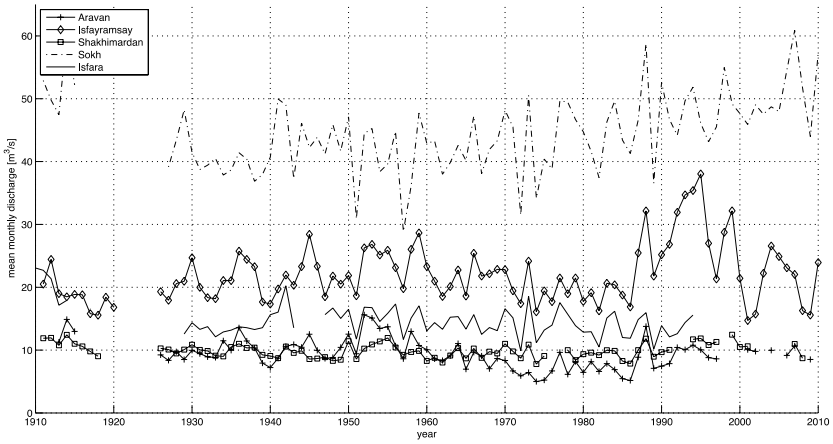

Figure 24: Mean monthly mean discharges of gauged rivers in the southern Fergana Valley. The long-term increasing trend in mean annual runoff in the Sokh river is interesting and might point to increasing contributions from glacier melt due to a net loss of land ice in the upstream of the catchment that is caused by global warming. However, this remains to be investigated more closely.

In the Amu Darya catchment, Vaksh shows a similar low-frequency phase as was visible in the Syr Darya tributaries. Similarly to Sokh, Surkhandarya shows a long-term increasing trend in filtered runoff. Compared to Sokh however, increasing runoff is mostly due to increasing winter flow contributions (see left plate in Figure 28). Mean Zerafshan runoff on the contrary is influenced by decadal-scale variability as is also visible in the spectral analysis (see Fig-

ure 31 below and especially also Figure 31 where the 8-10 year cycle's energy is clearly shown up in the spectrum).

For the Amu Darya, it is important that the synchronistic nature of runoff in the tributaries as is observed in the Syr Darya does not apply do to the extraordinarily complex topography of the basin. However, it is important to mention that Vaksh exhibits the same multi-decadal modulation as most of the Syr Darya tributaries. The main topographic features are a combination of high mountain ranges with deeply incised valleys that cut through them and that extend both in east-west and north-south directions. The basic latitudinal zoning that is apparent from the hydrometeorological perspective in the Syr Darya does therefore not apply to the Amu Darya.

Development of Seasonal Flows

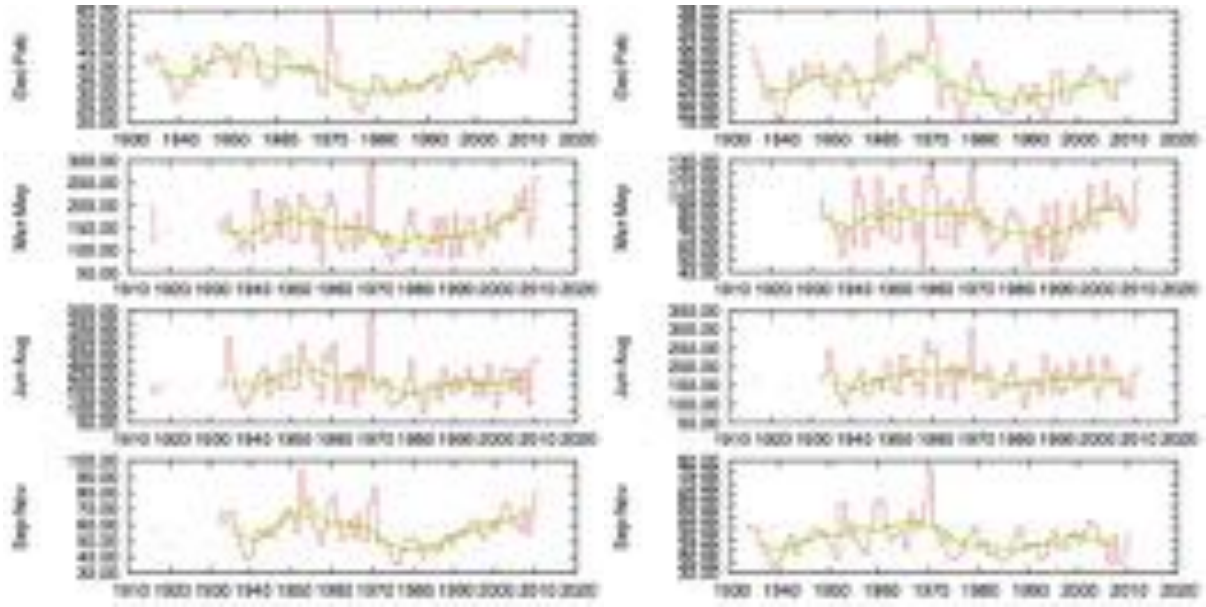

Figure 25: Development of seasonal average flows at Chirchik Chatkal Khudaydod (left plate) and Chirchik Pskem Mullala (right plate).

As expected, the multi-decadal variability at half century scales is clearly visible in most of the catchments' seasonal flows (shown in Figure 25 - Figure 29 below). Zerafshan is an exception here (Figure 29).

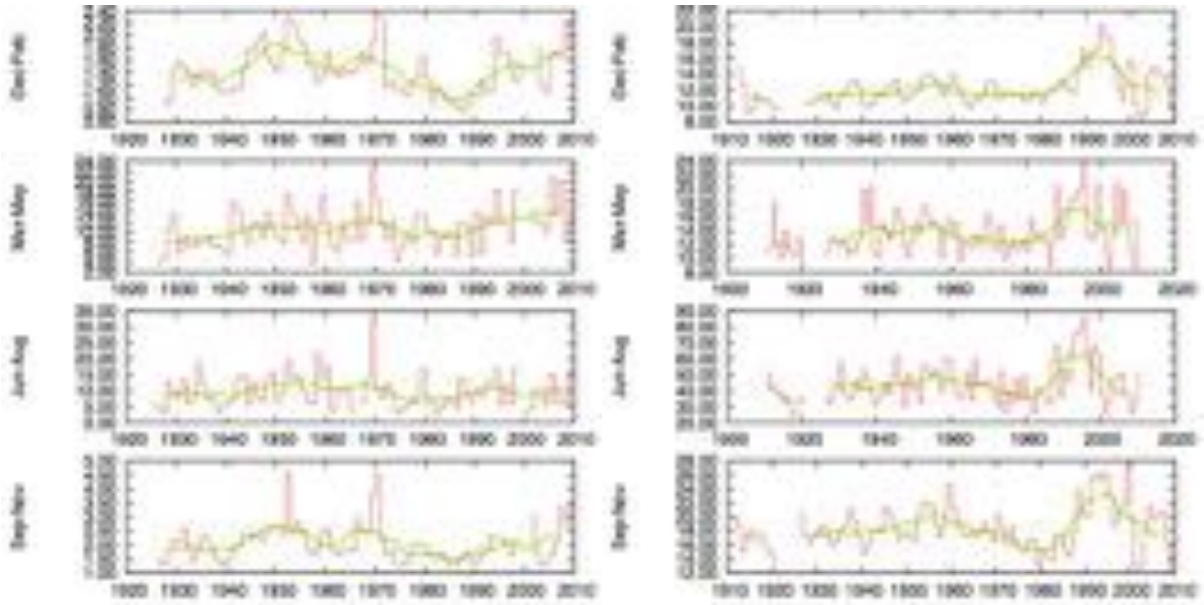

Figure 26: Development of seasonal average flows at Gavasay Gava (left plate) and Isfayramsay Uch Kurgan (right plate).

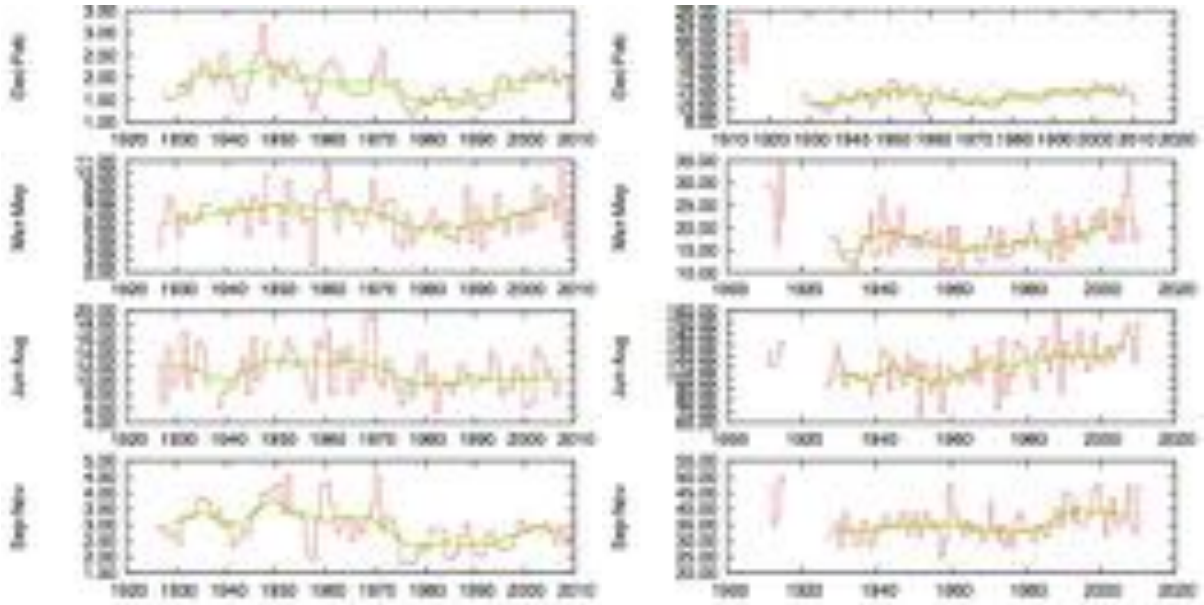

Figure 27: Development of seasonal average flows at Padsha Ata Tostu (left plate) and Sokh Sarkanda (right plate).

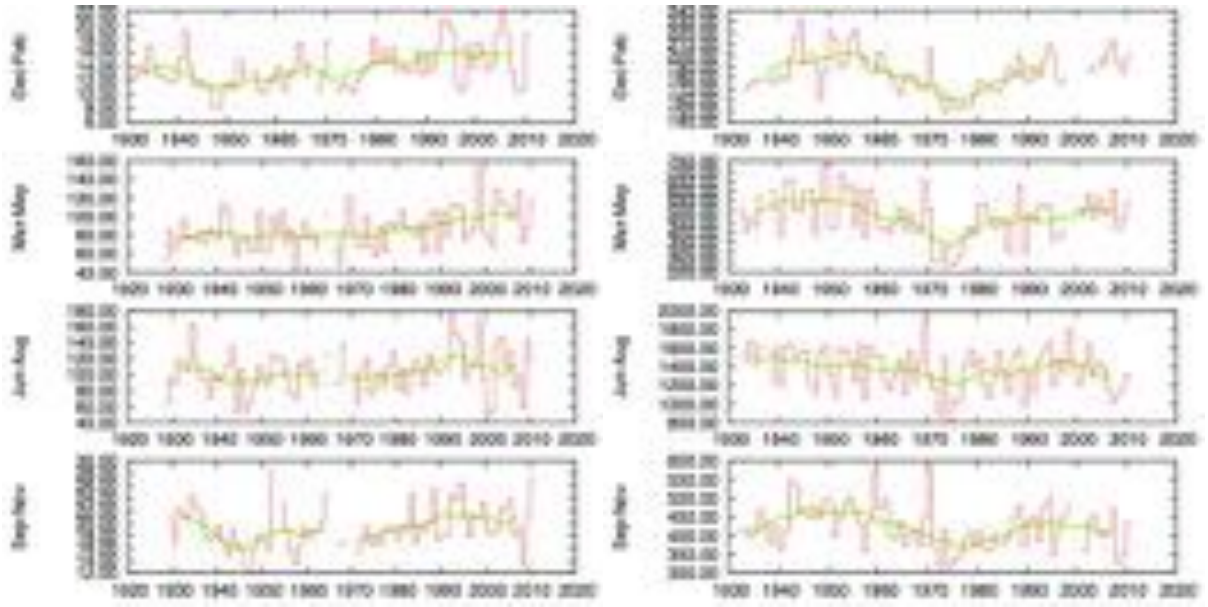

Figure 28: Development of seasonal average flows at Surkhandarya Tuplang Zarchob (left plate) and Vaksh Darband (right plate).

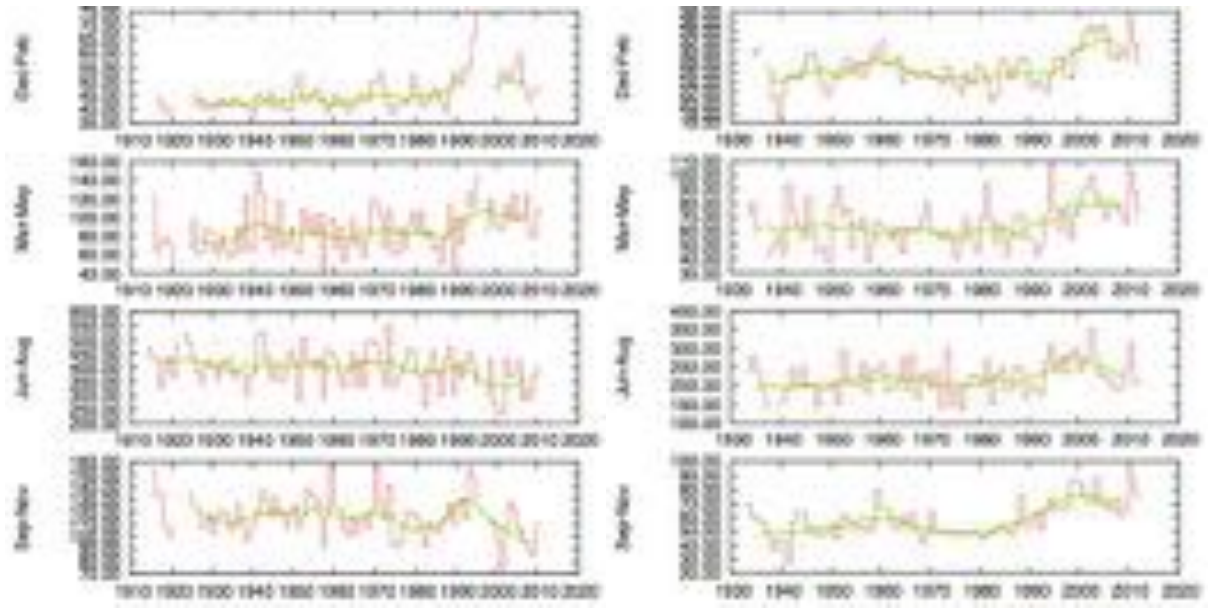

Figure 29: Development of seasonal average flows at Zerafshan Rovatkhodja and Naryn at Naryn city.

Autocorrelation

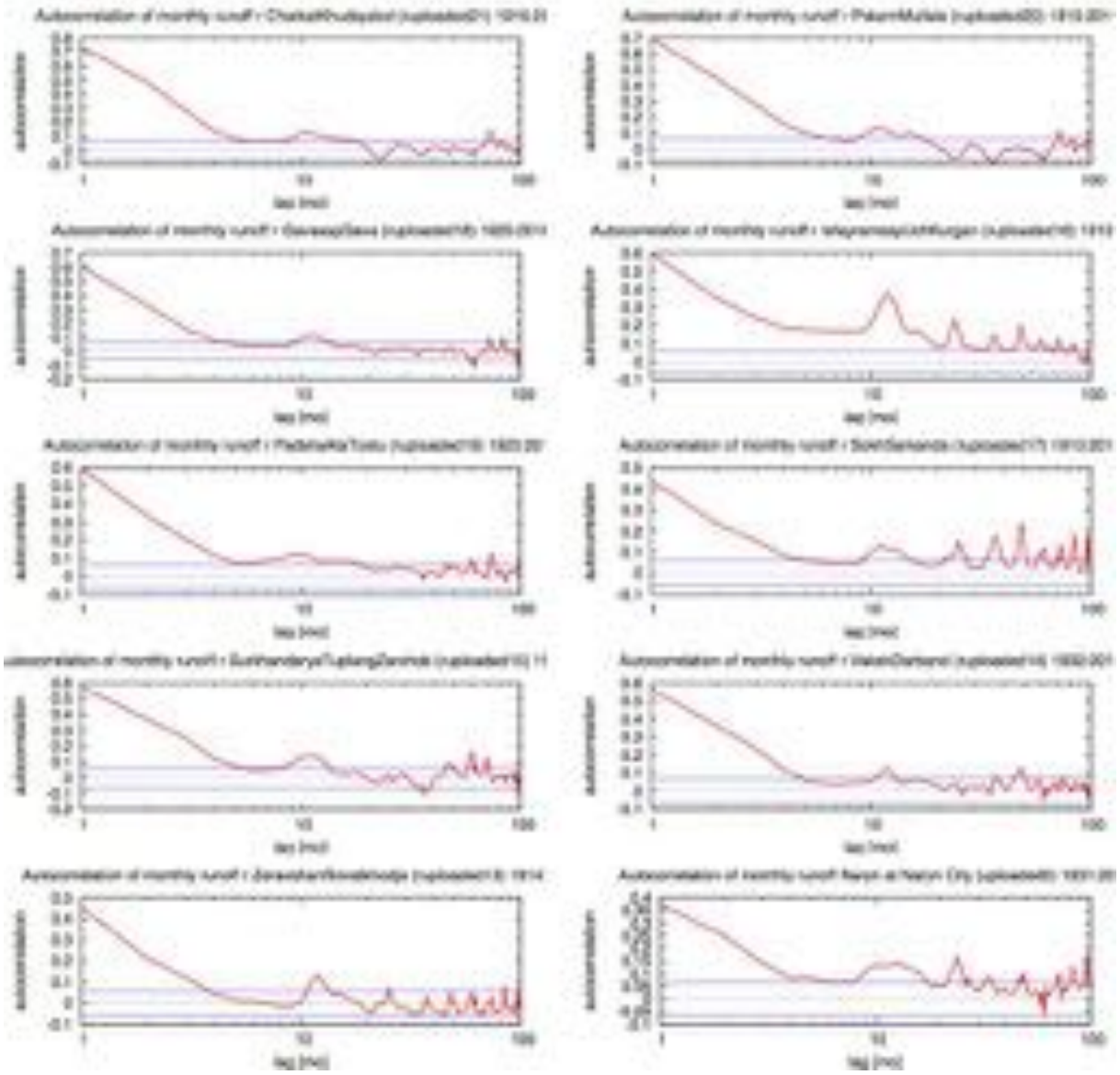

Figure 30: Autocorrelation function for long-term time series (vertical axis shows autocorrelation values). The horizontal lines give the 95% significance for a single point in the case of white noise, assuming all measurements are independent. The seasonal cycle has been subtracted for computation.

It is possible to identify the cyclicity or randomness in a time series by the analysis of auto-correlation and periodogram (see Figure 31 below). Both methods were used here to look for the long-term cycles of runoff decrease and increase in the analyzed runoff time series.

Figure 30 and Figure 31 recover the statistically significant low-frequency variability at half-century or more scales in the case of all tributaries to the Syr Darya (70 years period) as well as for the Vaksh (40 years period). Furthermore, many basins appear subject to an 8-10 year periodic forcing that is most pronounced for the Pskem and the Zerafshan (see also corresponding plates for the spectral analysis shown in Figure 31).

Spectral Analysis

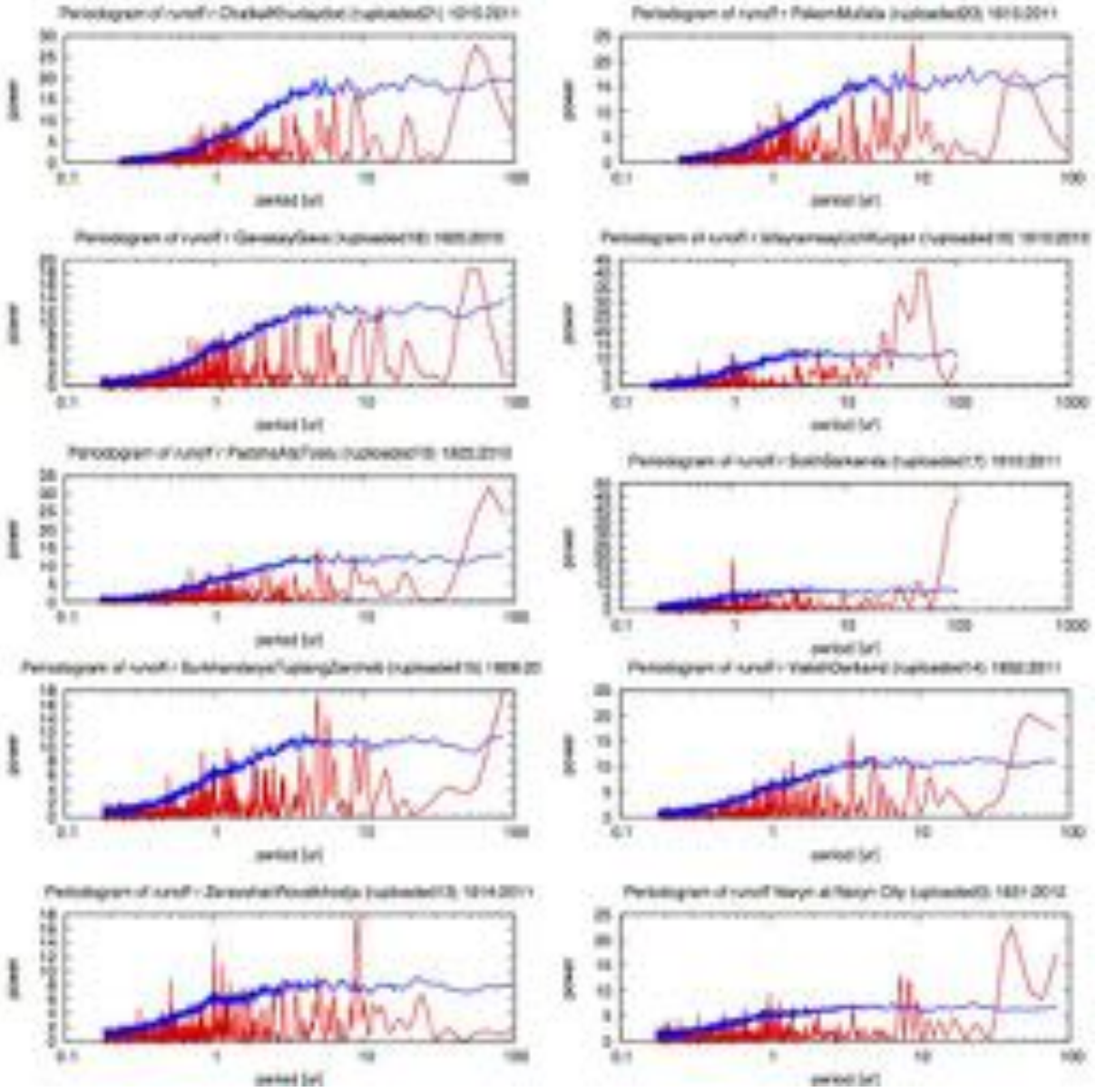

Figure 31: Periodograms of long-term time series of flow anomalies. The blue lines denotes the 95% highest spectrum of n AR(1) processes with the same autocorrelation of the corresponding time series. It is noteworthy to mention that the spectrums of Sokh and Surkhandarya are 'polluted' by their long-term increasing hydrographs. This explains the centennial scale peaks in their spectra.

3.2.2 Analysis of Extremes

For the analysis of extremes in the Amu and Syr Darya basin, we use naturalized flows of the two large rivers[4].

For the Syr Darya, the calculation of annual water consists of the following components:

1. Naryn River - a tributary of the water in the Toktogul reservoir.
2. Kara Darya River - a tributary providing water to the Andijan reservoir.
3. Chirchik - water flow into Lake Charvak and Ugam River flow.
4. Lateral flow of water in the Syr Darya River - the area of the confluence of the Naryn and Kara to Kayrakkum reservoir.
5. Lateral flow of water in the Syr Darya River - the area between the Kayrakkum and Chardara reservoir.
6. Lateral flow of water into the Kara Darya - the area from Andijan reservoir to the mouth of the river.
7. Lateral flow of water into the Chirchik River - the area from the Charvak reservoir to the mouth of the river.

The sum of all these components is called the Naryn-Syr Darya cascade. It describes the river flow under the hypothetical assumption that the total water intake in the Syr Darya basin is zero. This flow is called *conditionally naturalized flow* of the river Syr Darya at the gauging station Chinaz.

For the Amu Darya, we used the modern calculation scheme to arrive at the conditionally naturalized Amu Darya runoff above Kayrakum Canal. The components are

1. Atamyrat (Kerki) gauge runoff
2. Intake to irrigation canals above Atamyrat (Kerki) gauge (Karshi main canal, Karakum canal, Amuzang canal and other smaller canals)
3. Volumetric changes in Nurek reservoir

Experts in the region use back-of-the-envelope approaches on the one hand and quantitative methods for the assessment and quantification of a particular hydrological year in the two big basins. The former approach relies on expert knowledge and long-term experience in the region. For example, the actual flow of the river Chirchik (inflow into Charvak reservoir) for the period April-September 2011 was 78 percent of normal. Experts referred to 2011 in the Chirchik basin as a year of water shortage.

[4] Information on naturalized flows in the large river systems was obtained from the Uzbek Hydrometeorological Service.

Another example is the April – September 2012 period in the Chadak and Gavasay Rivers (see line scheme of the Syr Darya in Figure 41 for the location of these rivers). Experts referred to this period as a 'wet year' for these two rivers (134 percent and 143 percent above normal). These threshold assessments vary from expert group to expert group as they are based on informal back-of-the-envelope approaches.

The quantitative methods utilized in the region for the assessment of the hydrological years rely on two empirical formulas that are going back to Soviet hydrologists. The first one is the Kritskyi-Menkel formula (which is recommended to be used in the regulatory guidelines of the Central Asian Hydrometeorological Services) and the formula of Chegodaev:

$$p = m \ / \ (n + 1)$$ Kritskyi-Menkel Formula

$$p = (m - 0.3) / (n + 0.4)$$ Chegodaev Formula

Here, p is the probability of exceedance of the empirical value, expressed as a decimal or percentage, m is the order (rank) of the runoff value of a particular year and n is the length of observations (i.e. the number of years of data available). Before performing the calculation of the order (rank), all flows should be sorted in descending order.

Table 6 shows results for the Syr Darya and Table 7 for the Amu Darya.

Syr Darya												
	1900										2000	
Year	I	II	III	IV	V	VI	VII	VIII	IX	X	I	II
0							37%	15%	52%	43%	54%	4%
1							89%	41%	57%	67%	65%	
2							94%	61%	76%	35%	9%	
3							72%	30%	83%	19%	6%	
4							48%	96%	81%	7%	26%	
5							85%	98%	70%	59%	13%	
6							46%	93%	87%	33%	28%	
7							80%	91%	22%	63%	39%	
8						50%	69%	56%	17%	11%	78%	
9						44%	2%	24%	74%	20%	31%	

Table 6: Assessment of hydrological years in the Syr Darya (1958 - 2011) . Calculations are based on the Kritkyi-Menkel formula and use a normalized series of average annual flows in m^3/s. Columns are decades, rows are years. The numbers are the p-values in percentages as reported above. Color coding is - extreme dry year, - dry year, - normal year, - wet year, - extremely wet year, - no data. Normalized runoff data was obtained from the Uzbek Hydrometeorological Service.

It should be noted that for the Syr Darya, prior 1958 analysis is not available since canal intake data is not available prior to this from which lateral inflows could be calculated.

How is the above Table 6 read? As an example, the average annual flow rate with an exceedance probability of 1 percent means that this is a 1 in a 100 years event, statistically speaking. A 5 percent exceedance probability for a particular flow means a 1 in 20 years return period and so on. 50 percent is the definition of the normal year. Probability thresholds are: extreme wet < 5%, 5% < wet < 24%, 25% < normal < 75%, 75% < dry < 95%, 95% < extreme dry.

The analysis of the Naryn - Syr Darya naturalized runoff confirms the analysis from above on long-term runoff in selected tributaries to the river (see especially Figure 22 above). Whereas the second half of the 20th century until 1990 was marked by recurring dry and extremely dry years, flows were normal to above normal from there onwards with the exception of the year 2008, a year where there was severe water stress and conflict in the basin, also due to the fact that water deficits could not be compensated by releases from Toktogul since the latter was near to empty at the beginning of the irrigation season (see also Chapter 1 and Chapter 2 above). Thus, in a lucky turn, the conflict-laden years in the last decade of the 20th century until nowadays were marked by good hydrological conditions that certainly helped muting the transboundary water allocation disputes in the region to a certain extent.

Table 7 shows the assessment for the Amu Darya.

Amu Darya												
	1900										2000	
Year	I	II	III	IV	V	VI	VII	VIII	IX	X	I	II
0							36%	43%	47%	39%	90%	15%
1				54%			74%	81%	71%	32%		17%
2		42%		25%			82%	79%	92%	3%	56%	26%
3		49%				10%	85%	11%	60%	19%	22%	
4		6%				7%	51%	96%	38%	8%	61%	
5		24%				67%	86%	76%	33%	63%	13%	
6		64%	65%	46%		29%	21%	57%	94%	40%	69%	
7		89%	72%			83%	50%	78%	44%	68%	88%	
8			18%				53%	28%	14%	4%	99%	
9			31%				1%	58%	93%	35%	75%	

Table 7: Assessment of hydrological years in the Amu Darya (1959 - 2011) . Calculations are based on the Kritkyi-Menkel formula and use a normalized series of average annual flows in m^3/s. Columns are decades, rows are years. The numbers are the p-values in percentages as reported above. Color coding is - extreme dry year, - dry year, - normal year, - wet year, - extremely wet year, - no data. Normalized runoff data was obtained from the Uzbek Hydrometeorological Service.

Similarly to the situation in the Syr Darya, 2008 was a critical extremely dry year in the Amu Darya basin.

4 Future Climate Change

Global climate model output, from the World Climate Research Programme's (WCRP's) Coupled Model Intercomparison Project phase 3 (CMIP3) multi-model dataset (Meehl et al., 2007), were obtained from www.engr.scu.edu/~emaurer/global_data/. Only data from the SRES A2 project is utilized here. These data were downscaled as described by Maurer et al. (2009) using the bias-correction/spatial downscaling method (Wood et al., 2004) to a 0.5 degree grid, based on the 1950-1999 gridded observations of Adam and Lettenmaier (2003). Data from 16 models was used, i.e. BCCR-BCM2.0, CGCM3.1 (T47), CNRM-CM3, CSIRO-Mk3.0, GFDL-CM2.0, GFDL-CM2.1, GISS-ER, INM-CM3.0, IPSL-CM4, MIROC3.2 (medres), ECHO-G, ECHAM5/MPI-OM, MRI-CGCM2.3.2, PCM, CCSM3 and UKMO-HadCM3 (see above cited link for more information).

4.1 Precipitation Trends from 2000 - 2050

Here, we investigate multi-model mean robust trends of the future precipitation climate in Central Asia. The period from 2000-2050 was used for analysis. Figure 32 and Figure 33 show results. When analyzing annual climate projection data, model results suggest that there are no robust trends in the mountainous regions, i.e. in the zones of runoff formation. Robust negative trends can be identified in much of the lower lying parts of the Amu Darya basin and especially on the Afghan side of the catchment.

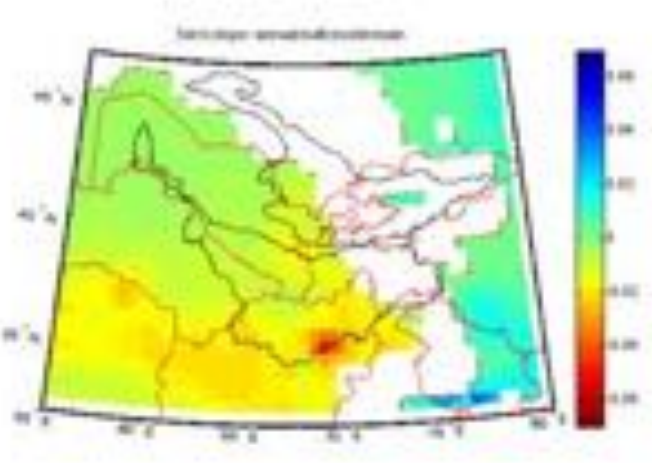

Figure 32: Robust linear regression (Sen's slope) for the climate change SRES A2 multi-model mean precipitation data. Slope values are in mm per year. Only cells with statistically significant trends are shown, i.e. white cells are non-significant trend cells. River basins outlined in black color, country borders are shown in red.

A more nuanced picture emerges when seasonal rainfall trends are looked at (see Figure 33). Here, it appears that over much of the Central Asian Tien Shan and the Pamirs, precipitation trends are small and positive at the 5% significance levels during the winter months (DJF, upper left plate in the Figure). During spring, climate model output suggests that there are slightly negative precipitation trends over much of the Amu Darya region. During summer months, a slightly negative precipitation trend is visible in parts of the Pamirs and over much of the upstream Syr Darya.

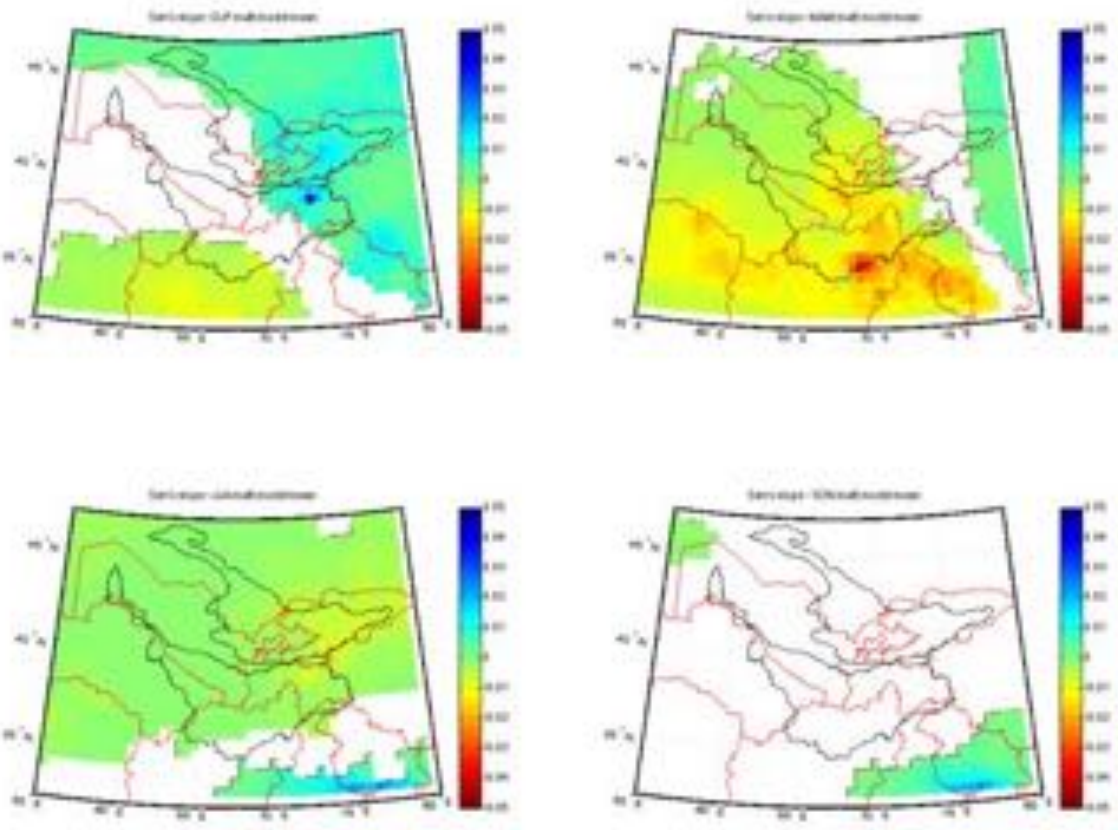

Figure 33: Robust linear regression (Sen's slope) for the climate change SRES A2 multi-model mean seasonal precipitation data. Slope values are in mm per season. Only cells with statistically significant trends are shown, i.e. white cells are non-significant trend cells. River basins outlined in black color, country borders are shown in red.

This analysis has to be viewed in the context of the overall large uncertainty with regard to the development of future precipitation in the region. Figure 34 shows for each gird cell the minimum and maximum significant trends that were derived from each of the 16 multi-model members. Comparing the two Plates in the Figure, it is evident that there are large spreads between the model trends, especially in the Pamirs, over much of the Tien Shan and in the Fergana Valley region, and also between the directions of trends. The latter point is

particularly important as there is apparently no good understanding of the key climate change processes in the future precipitation climate of Central Asia in the mountains there.

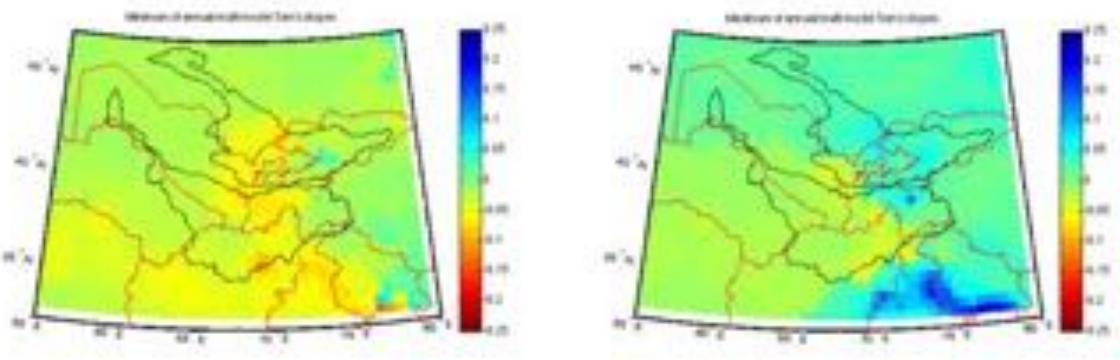

Figure 34: Robust linear regression (Sen's slope) for the climate change SRES A2 multi-model dataset. Slope values are in mm per year. For each cell, the left plate shows the minimal (significant) trend value out of the set of the 16 models. The right plate shows the same information but for the maximum trends. Only cells with statistically significant trends are shown, i.e. white cells are non-significant trend cells. River basins outlined in black color, country borders are shown in red.

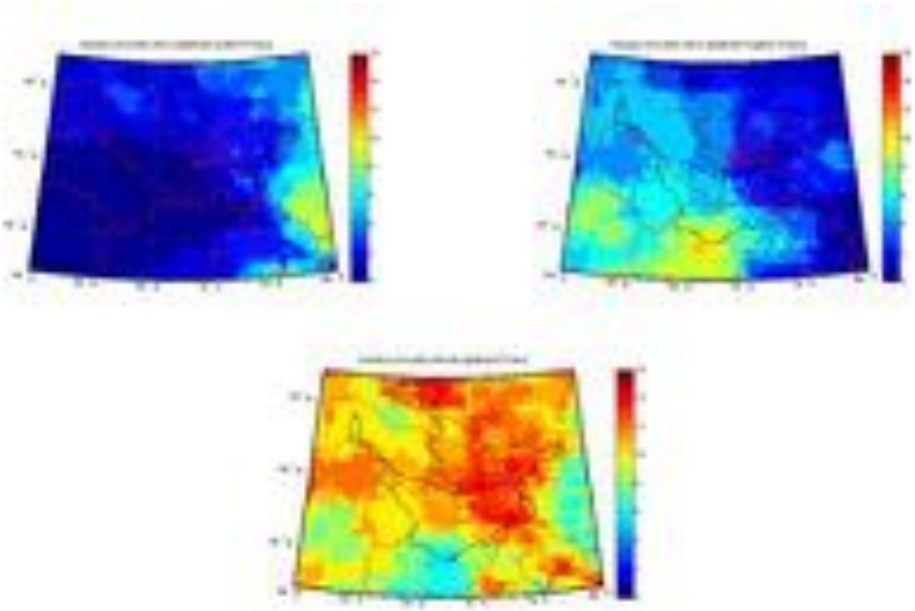

Figure 35: Number of multi-model ensemble members with a significant positive trend (upper left plate). Number of multi-model ensemble members with a significant negative trend (upper right plate) and number of models (out of 16 ensemble members) without significant annual future precipitation trends (lower center plate).

Figure 35 shows model inconsistencies in a more explicit way. Again, the main point is that there is absolutely no consistency across predicted annual trends in the Amu Darya and Syr Darya runoff formation zones and thus no confidence at all with regard to implications on future water availability in the two rivers.

AN INTERESTING FUTURE ANALYSIS WOULD LOOK AT THE NEW CLIMATE SCENARIOS THAT ARE PRODUCED UNDER THE CMIP5 COUPLED MODEL INTERCOMPARISON PROJECT SO AS TO SEE WHETHER OR NOT THESE INCONSISTENCIES PERSIST THERE (SEE HTTP://CMIP-PCMDI.LLNL.GOV/CMIP5/DATA_PORTAL.HTML).

This finding also has important repercussions for any impact and mitigation study with regard to the estimation of future runoff in the two basins. Care should be taken to properly quantify uncertainties in such undertakings as otherwise false conclusions are likely to be drawn. The lack of a good understanding of future water availability in the basins should also guide decision-makers in the region to prepare flexible, yet effective mitigation measures and sound management strategies. The current water sector reforms in the upstream republics Kyrgyzstan and Tajikistan should also be reviewed in light of this (Siegfried, 2012a).

4.2 Temperature Trends from 2000 – 2050

Conversely to precipitation, future temperature trends show consistent and strong positive signals across all multi-model members (see Figure 36, Figure 37 and Figure 38 below). Annual scale robust trends are shown in Figure 36. Over Central Asia, multi-model mean climate model output suggests a warming between 2 – 2.75 Degrees Celsius from 2000 – 2050. For both river catchments, the warming trends are higher in the uplands as compared to the lowlands. The south-western region, including the Pamirs is more strongly affected by global warming than the other regions. An interesting transition zone exists between the two large consistent regions with lower and higher temperature trends.

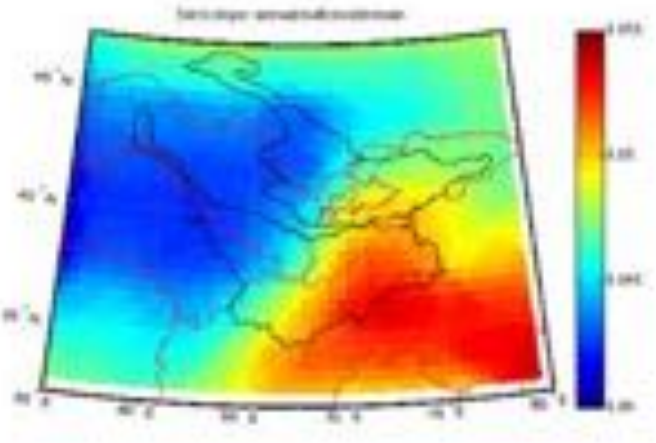

Figure 36: Robust linear regression (Sen's slope) for the climate change SRES A2 multi-model mean data for temperature. Slope values are in deg. C. per year. Only cells with statistically significant trends are shown, i.e. white cells are non-significant trend cells. River basins outlined in black color, country borders are shown in red.

Seasonal robust trends are shown in Figure 37. In all seasons, positive trends persist with the highest trends visible during the winter time over the Western Himalayas, the Pamirs and the Hindu Kush mountains.

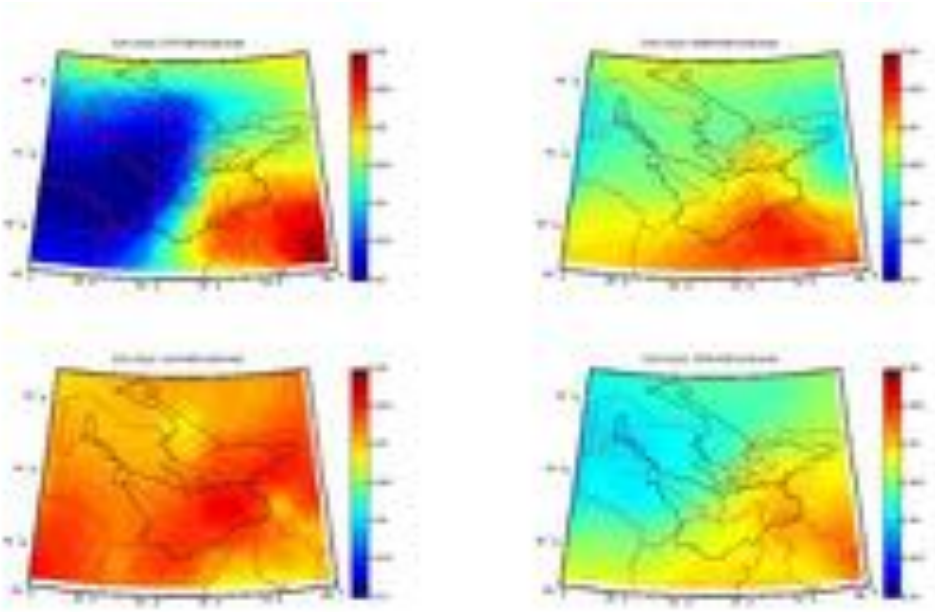

Figure 37: Robust linear regression (Sen's slope) for the climate change SRES A2 multi-model mean seasonal temperature data. Slope values are in deg. C. per season. Only cells with statistically significant trends are shown, i.e. white cells are non-significant trend cells. River basins outlined in black color, country borders are shown in red.

Figure 38 shows that there is consistency across the multi-model ensemble members with regard to the direction of the development of the trends. The range of multi-model trends is from 1 to 3.5 Degrees Celsius over the domain.

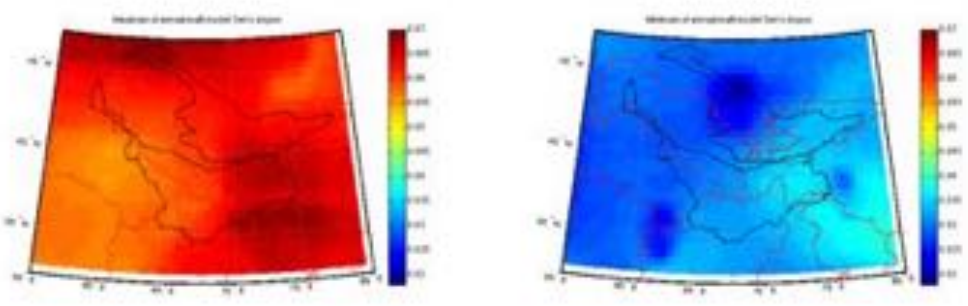

Figure 38: Robust linear regression (Sen's slope) for the climate change SRES A2 multi-model temperature dataset. Slope values are in deg. C. per year. For each cell, the left plate shows the minimal (significant) trend value out of the set of the 16 models. The right plate shows the same information but for the maximum trends. Only cells with statistically significant trends are shown, i.e. white cells are non-significant trend cells. River basins outlined in black color, country borders are shown in red.

5 Climate Impacts

Here, we mainly report findings from climate impact studies in the Syr Darya catchment. We draw on work from (Bernauer & Siegfried, 2012; Pereira-Cardenal et al., 2011; Siegfried, 2012b; Siegfried et al., 2011).

5.1 Glacier Melt & Impacts on Runoff in the two Daryas

(Siegfried et al., 2011) report findings on the future dynamics of glaciers in the Syr Darya catchment in the Tien Shan ranges. Their analysis shows that, depending on the emissions scenario, glacier-melt will continue to contribute to runoff during the first half of the 21st century in the Syr Darya. Under the SRES A2 emissions scenario, approximately one third of present total land-ice volume will melt over this period, with an expected volumetric loss of 31 ± 4 percent (see Figure 39 below). The mean annual runoff contribution from ice is expected to be in the order of 50 m^3/s under this scenario. This corresponds to roughly 2.7 ± 2 ercent of total natural basin runoff, or around one third of present average inflow into the Aral Sea after all upstream consumptive water use has been accounted for. Basin-wide glacier-melt contributions to river flow are and will likely remain small in the Syr Darya when compared with the natural runoff regime.

Relative ice loss in the Syr Darya subcatchments is shown in Figure 40. As is visible, it is mainly the lower lying catchments that will suffer the highest volumetric percentage loss by 2040-2049 over today's situation. Especially glaciers in the north Fergana valley and the western Tien Shan are expected to suffer the greatest losses.

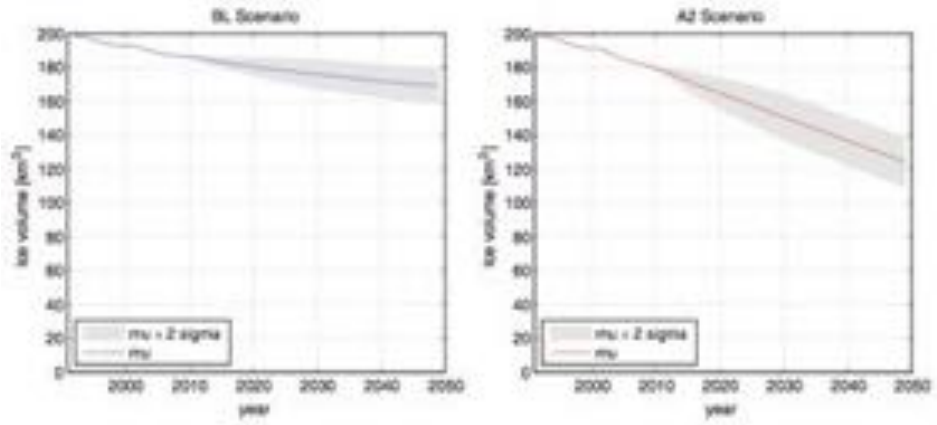

Figure 39: Projected ice loss in the Syr Darya catchment for a baseline climate scenario (left plate) that assumes the continuation of the observed 20th century warming trend in the Tien Shan. Th right plate shows the expected ice loss under the SRES A2 scenario in the catchment and associated uncertainties. Compare with Figure 40 below (Siegfried et al., 2011).

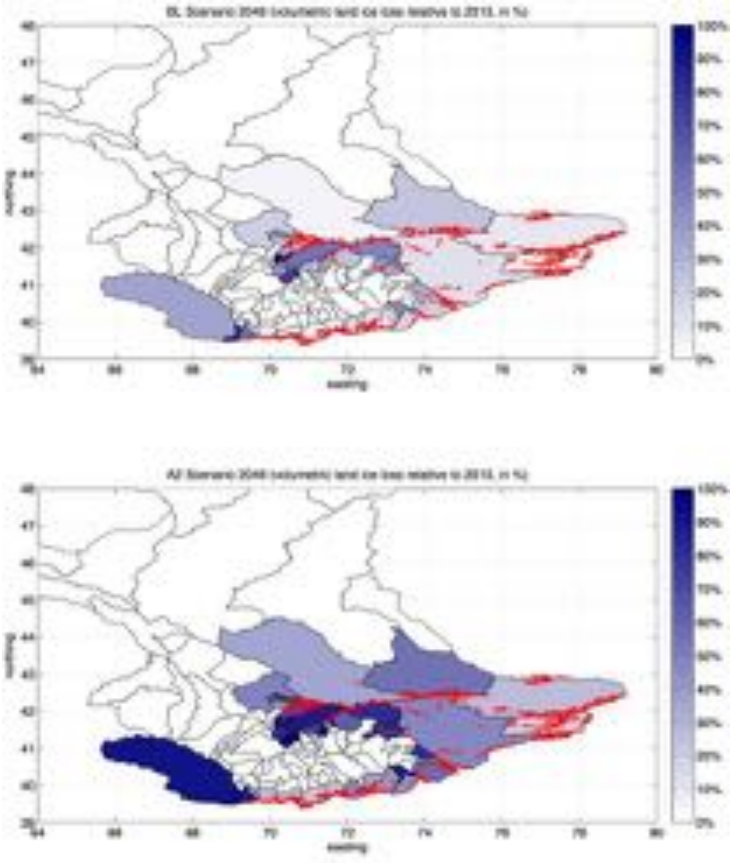

Figure 40: Relative volumetric land ice loss for a baseline scenario (continuation of current temperature trends, upper plate) and for the SRES A2 scenario. Data from the GLIMS (Global Land Ice Measurements from Space) database was used (see Siegfried et al., 2011 for more details).

In the Amu Darya catchment, (Wagner & Hoelzle, 2010) carried out a careful analysis of the development of glaciation in the upstream Pianj and Vaksh catchments. The authors used a simple parameterization scheme assuming quasi steady state conditions to infer the ice volumes for two different time periods in the past and to extrapolate future changes. The calculated volumes for the World Glacier Inventory (WGI) are 170 - 200 km^3 for the Pianj catchment and 200 - 240 km^3 for the Vaksh catchment. This corresponds to an overall ice volume in both catchment areas of around 370 - 440 km^3 or roughly double the one in the entire Syr Darya. The authors emphasize that based on the uncertainties in the calculation of the ice thickness, a general uncertainty range of ± 25 – 30 percent has to be taken into account in these volumetric estimations. Comparing these values to estimations calculated for the European Alps with 126 km^3 or the Southern Alps of New Zealand with 67 km^3, shows the importance of the ice reserves in the Amu Darya within the semi-arid catchment.

From the mid of the 20th century to 2003, an area (volume) decrease of 8.2 percent (10.5 percent) for the Pianj and 7.5 percent (4.1 percent) for the Vakhsh catchment was deter-

mined. A comparison of two digital elevation models (SRTM of the year 2000 and Aster of the year 2008) shows a mean glacier mass change of -0.61 m/a in the Vaksh and -0.81 m/a in the Pianj basins for the eight-year period (Wagner & Hoelzle, 2010).

The authors of the study mention that their analysis of regional climate simulations project a warming of 1.8°C up to 2.9°C until 2050 which compares well with what is reported in Chapter 3. At the same time, they too mention that it remains unclear, if and in what direction precipitation will change. Finally they show that under the assumption of an average temperature increase of 2°C until 2050 and no change in precipitation, the ice reserves in the two catchments will decline at an accelerated rate, compared to the past with total volume reduction of 75.5 percent for the Pianj basin and of 53 percent for the Vakhsh basin (Wagner & Hoelzle, 2010).

Using a simple back of the envelope approach and assuming uniform melting of the total volume from 2003 - 2050, it can be shown that this volumetric loss will translate into annual additional runoff contributions in the order of 4.8 km^3 – 5.8 km^3 or an additional 6.5 percent – 7.8 percent of runoff over the long-term mean (reported in Table 2). The relative contribution of glaciers in the Amu Darya to overall runoff under an A2 scenario is thus roughly three times larger as compared to the Syr Darya.

It should be noted that the figures reported by (Wagner & Hoelzle, 2010) compare well with other assessments, e.g from (Immerzeel, Lutz, Droogers, & Bank, 2012; A F Lutz, Droogers, Immerzeel, & Bank, 2012). However, the authors' results of the two latter studies suggest that due to a compounded effect of glacier melt and climate change, total runoff in the Amu Darya will greatly reduce in the order of 26 percent – 35 percent which is completely at odds with physical reality and any reasonable understanding about what could actually happen in the basin over the course of the next four decades. This is even truer in light of the fact that nobody knows what is happening on the side of the precipitation climate.

Another recent report (prepared for FAO on behalf of the Tajik government) that investigates climate impact on tributaries to the Amu Darya, states that even under a drying precipitation climate, river flows will largely be insensitive (Klemm & Hagg, 2012). The report states that 'precipitation changes seem to be of secondary importance compared to the high temperature sensitivity of the runoff.' It continues to say that 'according to these results, water availability for agricultural use will – at least up to about 2050 - not change significantly: but in those parts of the Amu Darya basin where population already now suffers from water shortage in summer, the situation will be worse in the future.'

Thus, the conclusions in this FAO report are pointing exactly into the opposite direction as compared to the ADB report. While these greatly diverging findings point (as in the case of the ADB report) to underlying intrinsic problems of the approach chosen, it is also an expression of the fact that we do not have a good sense about the direction of change with regard to water availability in the region.

To summarize, we know that seasonality of runoff will change in the Amu Darya, very much like what is expected in the Syr Darya, and that glaciers will continue to shrink in their volumes over the coming decades and that this ice wastage will contribute to additional runoff in the basins.

5.2 Expected Changes in River Hydrographs

5.2.1 Shifts in Runoff Seasonality in the Syr Darya River Tributaries

Here, expected shifts in runoff in the Syr Darya tributaries are discussed. For the investigation, we use the SRES A2 scenario and the time period 2040 – 2050 and compare it with the long-term average runoff situations over the course of the 20th century until the year 2012. The model described in (Siegfried et al., 2011) is utilized for impacts assessment.

As discussed in Chapter 3 above, the development of precipitation is highly uncertain over the Central Asian domain. On the contrary, the temperature forcing signal is pretty consistent and showing in the same increasing direction over all multi-model members that were investigated under the Assessment Report 4 (AR4). Hence, we put emphasis here on investigating changes in runoff seasonality due to this warming trend while assuming in the first place that total annual runoff will not change. Furthermore, we provide a lower (dry year) and upper (wet year) bound scenario for runoff in the main tributaries to the Syr Darya river. The results are shown in Figure 42 - Figure 50 and numbers reported in Table 8 - Table 11.

The methods utilized for the investigation of climate impacts on the Syr Darya consist of coupling a physically-based rainfall runoff modeling to different realization of future climate under the SRES A2 forcing. With the model, a monthly runoff correction factor is calculated. A factor exceeding 1 for a particular month means that runoff is increasing relative to long-term mean runoff 20th century values for the particular catchment under consideration. Conversely, if the climate change correction factor is smaller 1, this suggests that flows will be expected to decrease under the SRES A2 scenario in the corresponding month in the 2040 – 2049 decade.

The rivers for which data is reported are shown in the line scheme of Figure 41. Tributaries for which no mean monthly runoff data is available, e.g. because they were never gauged, a first order assumption would be that monthly climate change correction factors are similar to the ones in neighboring catchments. However, it is clear that this method is potentially a strong oversimplification of reality, esp. due to the different degrees to which snowpack and glaciers can contribute to runoff formation, even in neighboring catchments (see e.g. Pertziger & Asian, 1990 on the topic of how greatly variable the runoff formation processes and their dynamics can be, even in adjacent smaller-scale catchments).

As discussed below, the rainfall-runoff model is not performing well in selected very small catchments in the South Fergana Valley. This is indicated at the corresponding location.

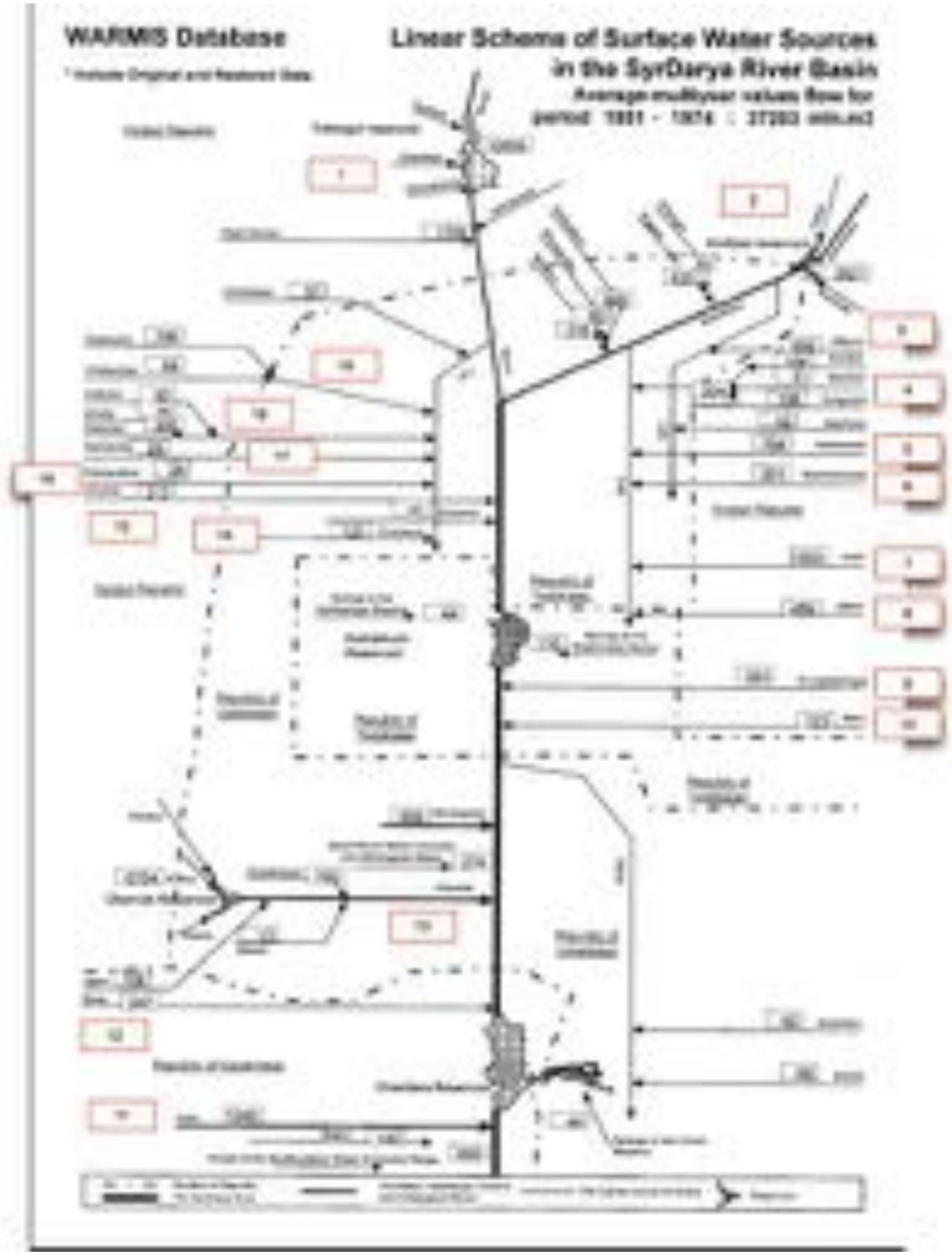

Figure 41: Linear scheme of the Syr Darya River. Provided by COWI, Denmark.

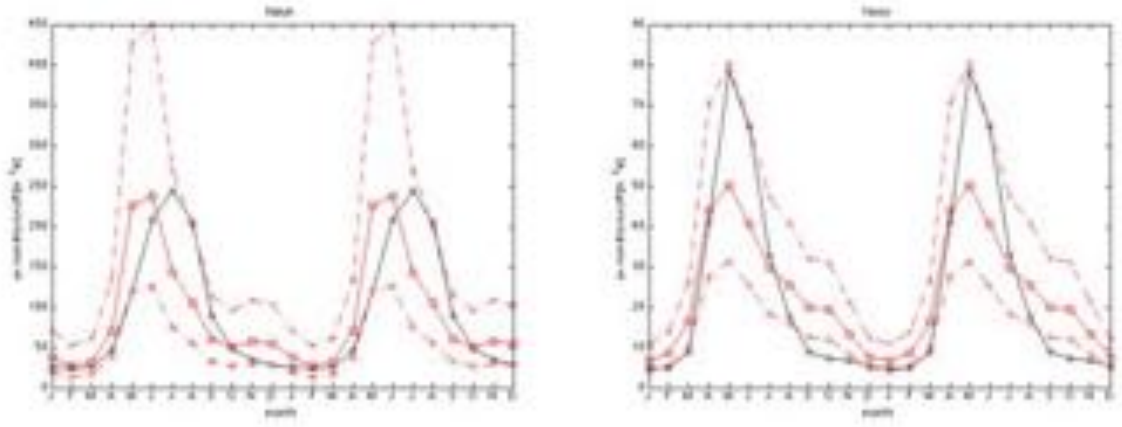

Figure 42: SRES A2 climate scenario impacts on the Naryn River (left plate) and the Yassy River (tributary to Kharadarya, right plate) – see line scheme in Figure 41 for location. Changes in runoff are shown for the period from 2040 – 2050 (red colored lines). Solid red line: mean future runoff (no volumetric change assumption); dashed red line with crosses: wet year runoff, dashed red line with diamonds: dry year runoff. Data from hydro-climatological model by (Siegfried et al., 2011). Table 8 - Table 11 list the data. 2 seasonal cycles are shown.

- Naryn: shift in runoff peak from July towards June and slower runoff decay during autumn as well as steeper rise of peak water onset at the start of April.
- Yassy (tributary to Karadarya): Much reduce runoff peak but higher flow persistence throughout the irrigation season.

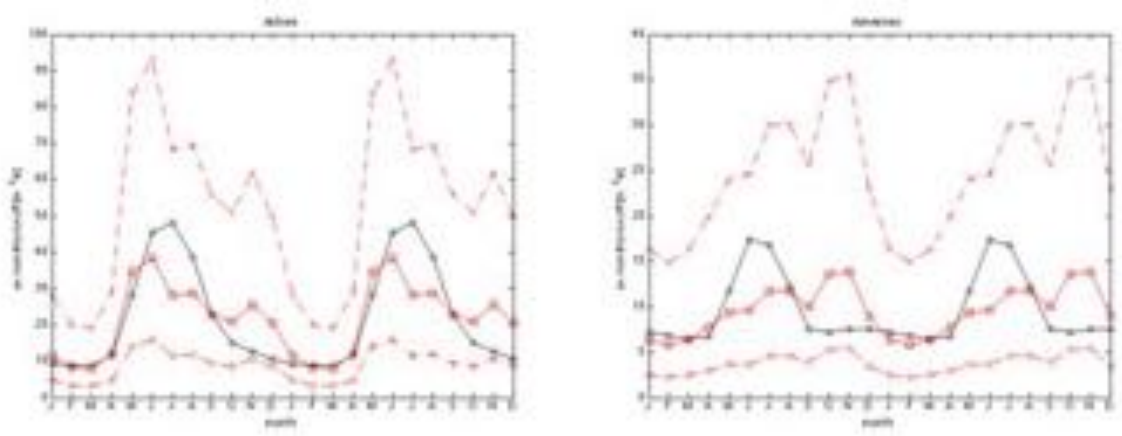

Figure 43: SRES A2 climate scenario impacts on the Akbura River (left plate) and the Aravansay River (right plate) – see line scheme in Figure 41 for location. Changes in runoff are shown for the period from 2040 – 2050 (red colored lines). Solid red line: mean future runoff (no volumetric change assumption); dashed red line with crosses: wet year runoff, dashed red line with diamonds: dry year runoff. Data from hydro-climatological model by (Siegfried et al., 2011). Table 8 – Table 11 list the data. 2 seasonal cycles are shown.

- Akbura: Decrease of peak flow in favor of a broader distribution of runoff throughout the year
- Aravansay: Results from the rainfall-runoff model likely not valid.

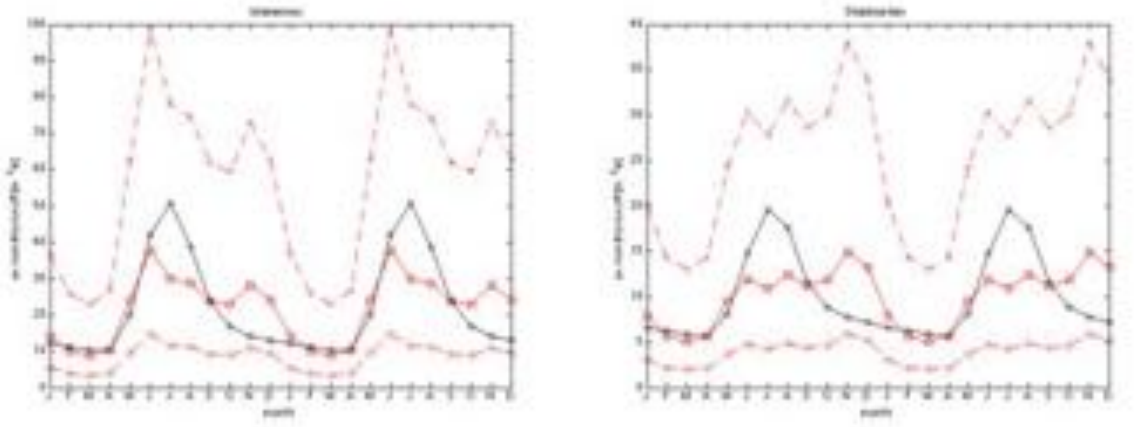

Figure 44: SRES A2 climate scenario impacts on the Isfaramsay River (left plate) and the Shakimardan River (right plate) – see line scheme in Figure 41 for location. Changes in runoff are shown for the period from 2040 – 2050 (red colored lines). Solid red line: mean future runoff (no volumetric change assumption); dashed red line with crosses: wet year runoff, dashed red line with diamonds: dry year runoff. Data from hydro-climatological model by (Siegfried et al., 2011). Table 8 - Table 11 list the data. 2 seasonal cycles are shown.

- Isfaramsay: Reduction in peak flow. Second peak in November/December likely spurious modeling result.
- Shakimardan: Likely inadequate performance of the rainfall-runoff model.

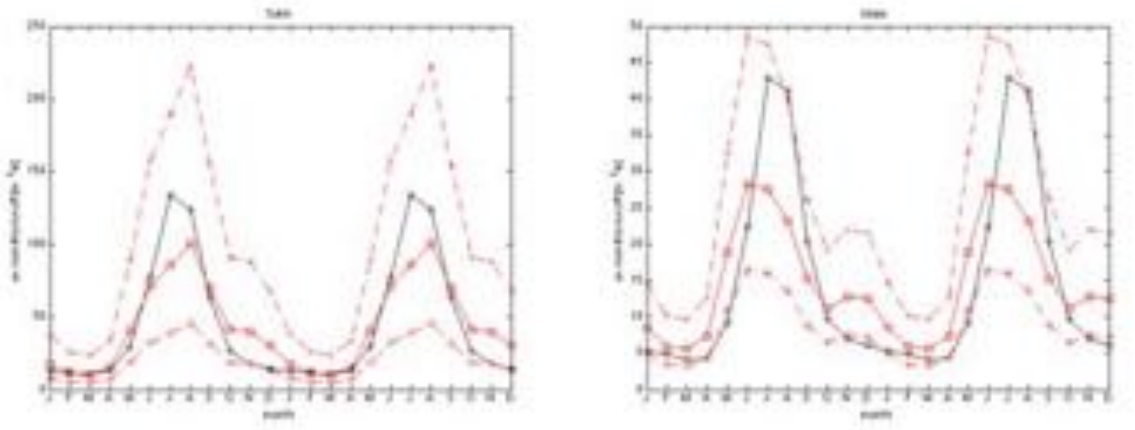

Figure 45: SRES A2 climate scenario impacts on the Sokh River (left plate) and the Isfara River (right plate) – see line scheme in Figure 41 for location. Changes in runoff are shown for the period from 2040 – 2050 (red colored lines). Solid red line: mean future runoff (no volumetric change assumption); dashed red line with crosses: wet year runoff, dashed red line with diamonds: dry year runoff. Data from hydro-climatological model by (Siegfried et al., 2011). Table 8 – Table 11 list the data. 2 seasonal cycles are shown.

- Sokh: Reduction/shift in peak flows and slower decay of runoff throughout the summer season.
- Isfara: Shift and reduction in peak flows.

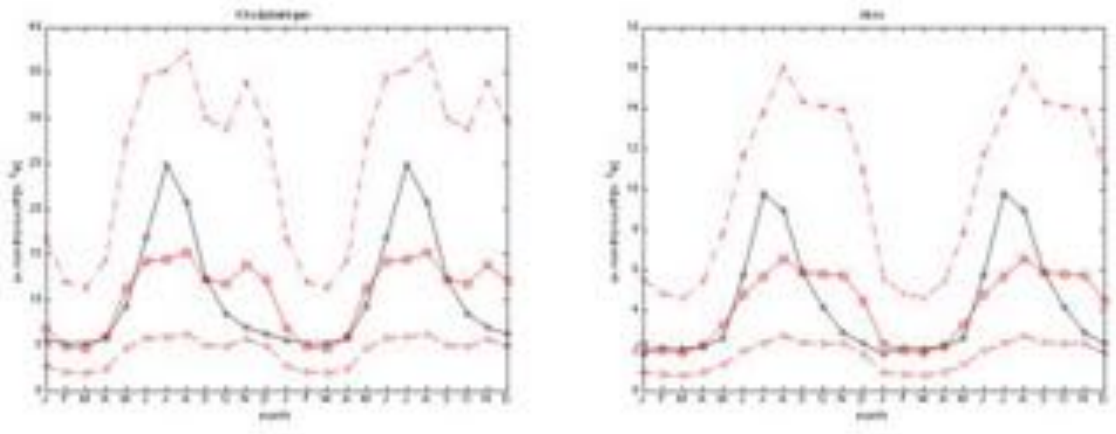

Figure 46: SRES A2 climate scenario impacts on the Khodjabakirgan River (left plate) and the Aksu River (right plate) – see line scheme in Figure 41 for location. Changes in runoff are shown for the period from 2040 – 2050 (red colored lines). Solid red line: mean future runoff (no volumetric change assumption); dashed red line with crosses: wet year runoff, dashed red line with diamonds: dry year runoff. Data from hydro-climatological model by (Siegfried et al., 2011). Table 8 - Table 11 list the data. 2 seasonal cycles are shown.

- Khodjabakirgan: Reduction in peak flows and dispersion of hydrograph.
- Aksu: Ditto.

It should be noted that the climate change impact assessment for the Arys River will follow as soon as long-term average unregulated flows for the 20th century can get hold off.

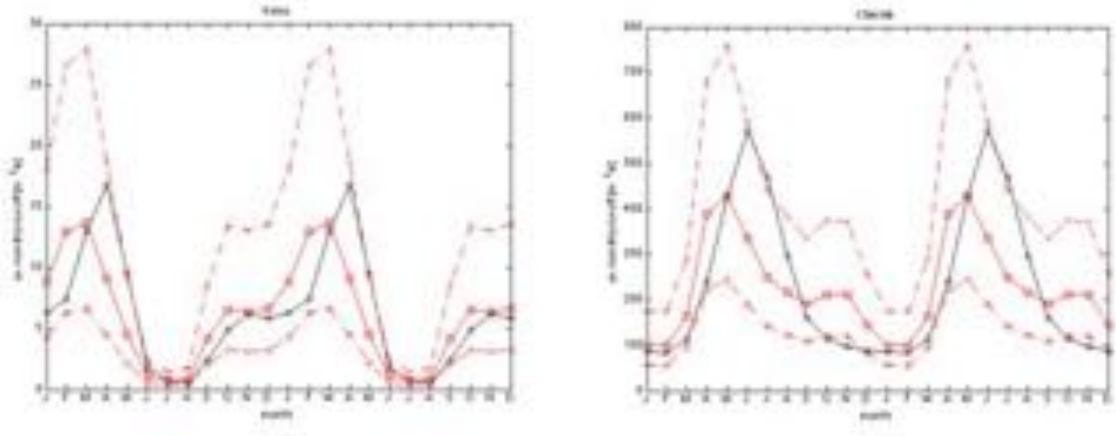

Figure 47: SRES A2 climate scenario impacts on the Keles River (left plate) and the Chirchik River (right plate) – see line scheme in Figure 41 for location. Changes in runoff are shown for the period from 2040 – 2050 (red colored lines). Solid red line: mean future runoff (no volumetric change assumption); dashed red line with crosses: wet year runoff, dashed red line with diamonds: dry year runoff. Data from hydro-climatological model by (Siegfried et al., 2011). Table 8 - Table 11 list the data. 2 seasonal cycles are shown.

- Keles: Shift in peak flows towards late winter from early spring.
- Chirchik: Shift in peak flows towards spring from early summer. Higher early autumn early winter runoff.

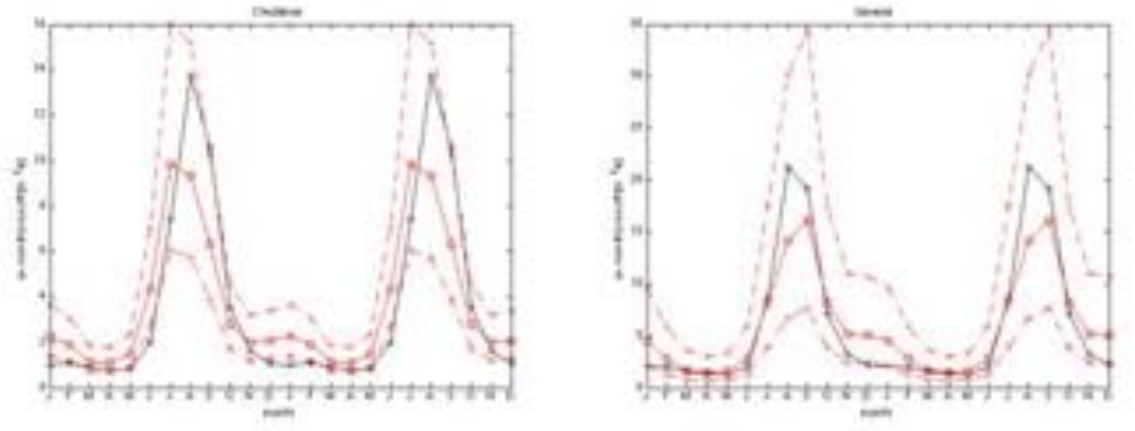

Figure 48: SRES A2 climate scenario impacts on the Chadaksai River (left plate) and the Gavasai River (right plate) – see line scheme in Figure 41 for location. Changes in runoff are shown for the period from 2040 – 2050 (red colored lines). Solid red line: mean future runoff (no volumetric change assumption); dashed red line with crosses: wet year runoff, dashed red line with diamonds: dry year runoff. Data from hydro-climatological model by (Siegfried et al., 2011). Table 8 – Table 11 list the data. 2 seasonal cycles are shown.

- Chadaksai: dispersion of runoff peak and higher winter runoffs.
- Gavasi: dispersion of runoff peak and higher winter runoffs.

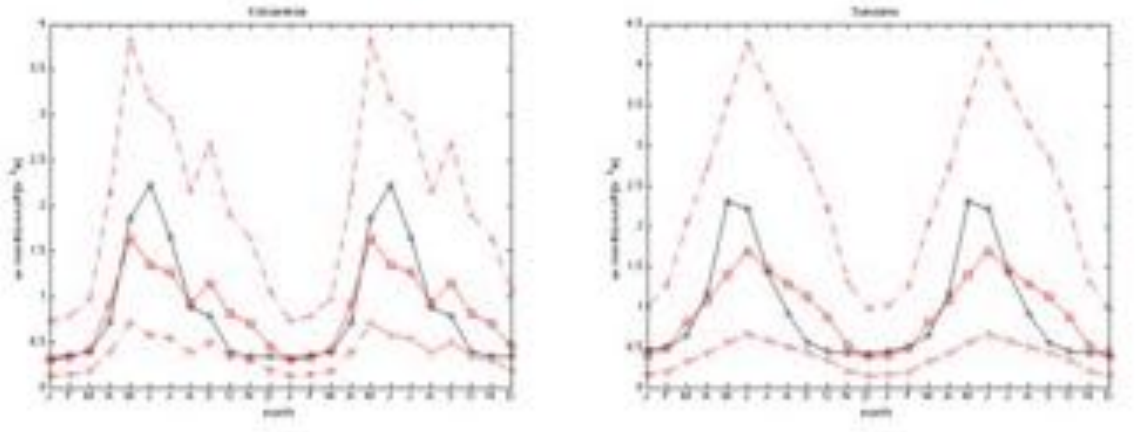

Figure 49: SRES A2 climate scenario impacts on the Koksareksai River (left plate) and the Sumsarsa River (right plate) – see line scheme in Figure 41 for location. Changes in runoff are shown for the period from 2040 – 2050 (red colored lines). Solid red line: mean future runoff (no volumetric change assumption); dashed red line with crosses: wet year runoff, dashed red line with diamonds: dry year runoff. Data from hydro-climatological model by (Siegfried et al., 2011). Table 8 – Table 11 list the data. 2 seasonal cycles are shown.

- Koksareksai: Dispersion of runoff peak, higher late irrigation season and early winter runoff.
- Sumsarsa: Dispersion of runoff peak.

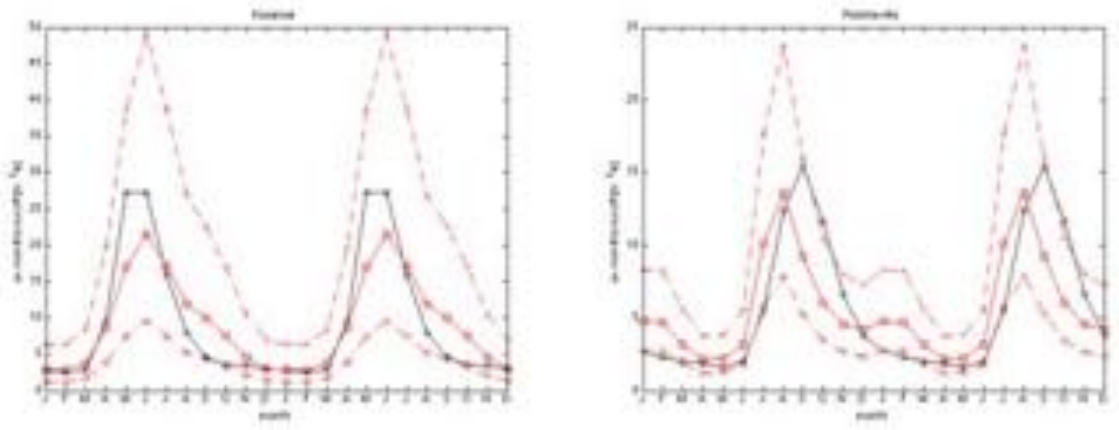

Figure 50: SRES A2 climate scenario impacts on the Kasansai River (left plate) and the Padsha-Ata River (right plate) – see line scheme in Figure 41 for location. Changes in runoff are shown for the period from 2040 – 2050 (red colored lines). Solid red line: mean future runoff (no volumetric change assumption); dashed red line with crosses: wet year runoff, dashed red line with diamonds: dry year runoff. Data from hydro-climatological model by (Siegfried et al., 2011). Table 8 – Table 11 list the data. 2 seasonal cycles are shown.

- Kasansai: Dispersion of runoff peak.
- Padsha-Ata – Shift of runoff peak towards summer months. Increased winter runoff.

Unregulated Mean Monthly Runoff - 20th Century													
	Catchment	Month											
#	Name	J	F	M	A	M	J	J	A	S	O	N	D
1	Naryn	25.8	24.7	26.1	46.4	119.5	207.9	243.8	204.9	88.6	47.9	34.4	28.9
2	Yassy	4.9	4.9	8.8	40.9	78.2	64.7	32.7	17.5	8.9	7.3	6.8	5.5
3	Akbura	9.3	8.8	8.8	11.6	28.1	45.5	48.1	38.8	22.7	15.0	12.7	10.6
4	Aravansay	7.2	6.8	6.5	6.7	11.8	17.4	16.7	12.3	7.6	7.1	7.6	7.6
5	Isfaramsai	12.1	11.2	10.4	10.5	19.9	42.3	50.7	38.7	23.9	16.9	14.3	13.0
6	Shakimardan	6.6	6.3	6.0	5.7	8.1	14.8	19.6	17.6	11.6	8.9	7.8	7.2
7	Sokh	12.5	11.4	10.8	13.4	29.9	76.9	134.1	124.1	63.0	26.7	18.0	14.4
8	Isfara	5.4	4.8	4.2	4.4	9.1	22.5	42.9	41.1	20.4	9.7	7.0	6.0
9	Khodjabakirgan	5.5	5.3	5.2	5.8	9.3	16.9	24.9	20.8	12.2	8.5	7.0	6.3
10	Aksu	1.8	2.1	2.1	2.2	2.6	5.7	9.7	8.9	5.8	4.1	2.9	2.3
11	Arys	23.3	33.8	54.4	57.1	33.8	11.9	4.79	2.57	7.45	11	13.5	18.6
12	Keles	6.2	7.4	12.9	16.8	9.5	1.8	0.8	0.5	2.4	4.9	6.2	5.8
13	Chirchik	84.5	82.1	112.3	239.1	427.3	571.5	469.8	296.0	160.3	113.1	98.0	88.9
14	Chadaksai	1.0	1.1	0.9	0.8	0.8	2.0	7.4	13.7	10.6	3.5	1.6	1.1
15	Gavasi	2.1	2.0	1.6	1.4	1.3	2.0	8.6	21.2	19.2	7.1	3.3	2.2
16	Koksareksai	0.3	0.4	0.4	0.7	1.9	2.2	1.7	0.9	0.8	0.4	0.4	0.4
17	Sumsarsa	0.5	0.5	0.7	1.2	2.3	2.2	1.4	0.9	0.6	0.5	0.4	0.4
18	Kasansai	2.9	2.6	2.8	9.6	27.3	27.3	15.8	7.9	4.7	3.6	3.5	3.0
19	Padshata	2.7	2.3	2.0	1.8	1.7	2.0	5.5	12.4	15.5	11.7	6.6	3.8

Table 8: Unregulated mean monthly runoff of selected tributaries to the Syr Darya.20th century and data from 2000-2013 was used.

Normal Mid-21st Century Mean Monthly Runoff (2040 – 2049)													
	Catchment	Month											
#	Name	J	F	M	A	M	J	J	A	S	O	N	D
1	Naryn	37.4	27.3	32.3	70.7	225.3	237.1	142.1	104.6	59.9	50.1	57.3	54.7
2	Yassy	6.7	8.6	16.4	43.9	50.1	40.4	29.5	25.3	19.9	19.3	13.3	7.6
3	Akbura	11.6	8.3	8.0	12.0	34.6	38.5	28.1	28.7	23.0	21.0	25.6	20.6
4	Aravansay	6.4	5.8	6.4	7.8	9.4	9.6	11.7	11.8	10.0	13.6	13.9	9.0
5	Isfaramsai	14.2	10.1	8.9	10.4	24.2	38.0	30.1	28.8	24.0	23.0	28.2	24.2
6	Shakimardan	7.9	5.6	5.1	5.6	9.5	11.9	10.9	12.4	11.2	11.8	14.9	13.3
7	Sokh	17.1	11.8	10.7	15.2	40.4	71.4	86.1	100.9	70.1	41.2	39.8	30.6
8	Isfara	8.6	5.9	5.7	7.3	19.0	28.3	27.6	23.2	15.2	11.2	12.8	12.5
9	Khodjabakirgan	6.9	4.9	4.6	5.9	11.3	14.2	14.4	15.3	12.3	11.8	13.9	12.1
10	Aksu	2.3	2.0	1.9	2.2	3.2	4.8	5.7	6.6	5.9	5.8	5.7	4.5
11	Arys	NA	NA	NA	NA	NA	NA	NA	NA	NA	NA	NA	NA
12	Keles	8.8	12.9	13.6	9.1	4.5	1.1	0.7	0.8	4.2	6.5	6.3	6.6
13	Chirchik	99.2	98.4	165.6	388.3	430.0	336.3	250.1	216.9	190.4	212.6	210.6	144.7
14	Chadaksai	2.2	1.9	1.1	1.1	1.5	4.3	9.8	9.3	6.3	2.8	2.0	2.1
15	Gavasi	4.5	2.8	1.7	1.4	1.6	2.8	8.3	14.2	16.2	8.2	5.2	5.0
16	Koksareksai	0.3	0.3	0.4	0.9	1.6	1.4	1.3	0.9	1.1	0.8	0.7	0.5
17	Sumsarsa	0.4	0.5	0.8	1.1	1.4	1.7	1.5	1.3	1.1	0.9	0.5	0.4
18	Kasansai	2.8	2.8	3.7	8.7	17.1	21.6	17.1	11.9	10.0	7.5	4.6	3.0
19	Padshata	4.8	4.7	3.2	2.1	2.2	3.2	10.2	13.6	9.2	6.0	4.6	4.2

Table 9: Normal mid-21st century mean monthly runoff values (2040 – 2049). It should be noted that the reported flows here for Arys River (Shaulder Gauge) are influenced by upstream allocation activity. Hence, no reasonable climate change shift scenario can be determined for this minor tributary to the Syr Darya.

Wet Mid-21st Century Mean Monthly Runoff (2040 – 2049)													
	Catchment	Month											
#	Name	J	F	M	A	M	J	J	A	S	O	N	D
1	Naryn	70.8	51.8	61.2	134.0	427.1	449.5	269.5	198.4	113.6	95.0	108.6	103.6
2	Yassy	10.8	13.8	26.3	70.4	80.3	64.8	47.3	40.6	31.9	30.9	21.3	12.2
3	Akbura	28.1	20.0	19.3	29.1	83.7	93.2	68.1	69.6	55.7	50.9	61.9	49.8
4	Aravansay	16.3	14.9	16.3	19.9	24.1	24.6	30.0	30.1	25.7	34.8	35.5	23.0
5	Isfaramsai	36.8	26.0	23.0	26.8	62.6	98.2	77.9	74.4	62.0	59.6	72.9	62.7
6	Shakimardan	20.2	14.3	13.0	14.3	24.3	30.4	27.8	31.6	28.6	30.1	38.0	33.9
7	Sokh	37.8	26.0	23.6	33.5	89.1	157.5	189.9	222.6	154.6	90.8	87.8	67.5
8	Isfara	14.7	10.1	9.8	12.6	32.6	48.6	47.4	39.8	26.1	19.2	22.0	21.5
9	Khodjabakirgan	16.8	12.0	11.2	14.5	27.7	34.6	35.3	37.3	29.9	28.7	34.0	29.6
10	Aksu	5.5	4.8	4.5	5.4	7.8	11.7	13.8	16.0	14.3	14.1	13.9	10.9
11	Arys	NA	NA	NA	NA	NA	NA	NA	NA	NA	NA	NA	NA
12	Keles	18.0	26.5	28.0	18.6	9.2	2.3	1.5	1.7	8.6	13.4	13.0	13.6
13	Chirchik	174.8	173.5	291.9	684.5	758.0	592.8	440.8	382.4	335.5	374.8	371.2	255.0
14	Chadaksai	3.7	3.0	1.9	1.8	2.4	7.0	16.0	15.2	10.3	4.5	3.2	3.4
15	Gavasi	9.6	5.9	3.7	3.1	3.3	6.0	17.6	30.1	34.4	17.4	11.0	10.7
16	Koksareksai	0.7	0.8	1.0	2.1	3.8	3.2	3.0	2.2	2.7	1.9	1.6	1.1
17	Sumsarsa	1.0	1.3	2.0	2.7	3.5	4.3	3.7	3.2	2.9	2.2	1.3	1.0
18	Kasansai	6.4	6.4	8.4	19.6	38.7	49.0	38.8	26.9	22.7	17.1	10.5	6.9
19	Padshata	8.3	8.2	5.6	3.7	3.8	5.5	17.7	23.7	16.0	10.5	8.0	7.3

Table 10: Wet mid-21st century mean monthly runoff (2040-2049).

Dry Mid-21st Century Mean Monthly Runoff - 20th Century (2040 – 2049)													
	Catchment	Month											
#	Name	J	F	M	A	M	J	J	A	S	O	N	D
1	Naryn	19.7	14.4	17.0	37.3	118.9	125.1	75.0	55.2	31.6	26.4	30.2	28.8
2	Yassy	4.2	5.4	10.2	27.4	31.2	25.2	18.4	15.8	12.4	12.0	8.3	4.7
3	Akbura	4.8	3.4	3.3	5.0	14.3	15.9	11.6	11.9	9.5	8.7	10.6	8.5
4	Aravansay	2.5	2.3	2.5	3.0	3.7	3.7	4.6	4.6	3.9	5.3	5.4	3.5
5	Isfaramsai	5.5	3.9	3.4	4.0	9.4	14.7	11.6	11.1	9.3	8.9	10.9	9.4
6	Shakimardan	3.1	2.2	2.0	2.2	3.7	4.7	4.3	4.9	4.4	4.6	5.9	5.2
7	Sokh	7.8	5.3	4.9	6.9	18.3	32.4	39.0	45.7	31.8	18.7	18.0	13.9
8	Isfara	5.0	3.4	3.3	4.3	11.0	16.5	16.1	13.5	8.9	6.5	7.5	7.3
9	Khodjabakirgan	2.8	2.0	1.9	2.4	4.6	5.8	5.9	6.2	5.0	4.8	5.7	5.0
10	Aksu	0.9	0.8	0.8	0.9	1.3	2.0	2.3	2.7	2.4	2.4	2.3	1.8
11	Arys	NA	NA	NA	NA	NA	NA	NA	NA	NA	NA	NA	NA
12	Keles	4.3	6.3	6.7	4.4	2.2	0.6	0.4	0.4	2.0	3.2	3.1	3.2
13	Chirchik	56.3	55.8	93.9	220.3	243.9	190.8	141.9	123.1	108.0	120.6	119.5	82.1
14	Chadaksai	1.4	1.2	0.7	0.7	0.9	2.7	6.1	5.8	3.9	1.7	1.2	1.3
15	Gavasi	2.1	1.3	0.8	0.7	0.7	1.3	3.9	6.7	7.6	3.8	2.4	2.4
16	Koksareksai	0.1	0.1	0.2	0.4	0.7	0.6	0.5	0.4	0.5	0.3	0.3	0.2
17	Sumsarsa	0.2	0.2	0.3	0.4	0.6	0.7	0.6	0.5	0.4	0.3	0.2	0.2
18	Kasansai	1.2	1.2	1.6	3.8	7.5	9.6	7.6	5.2	4.4	3.3	2.0	1.3
19	Padshata	2.7	2.7	1.8	1.2	1.3	1.8	5.8	7.8	5.3	3.5	2.6	2.4

Table 11: Dry mid-21st century mean monthly runoff (2040-2049).

Table 12 shows sample monthly change coefficients for the Syr Darya tributaries. They were computed by taking the ratio of the mid-21st century monthly runoff versus the corresponding mean 20th monthly runoff values. Red colors in the Table indicate a relative decrease and blue colors an increase of mean monthly flows correspondingly. The decrease of summer runoff and increases in the cold season runoffs are clearly visible, especially for the South Fergana Valley tributaries. Similar computations can be carried out for corresponding wet and dry year scenarios by using data from Table 10 and Table 11 above.

If aggregated change signals of different positions along the main stem of the Syr Darya are required, corresponding tributaries can be conveniently aggregated from Table 9 - Table 11 above. Finally, it should be noted that the change coefficients could be adjusted for any period in the first half of the 21st century if we assume linear change trajectories between the points of departure and the period of interest.

#	River Name	J	F	M	A	M	J	J	A	S	O	N	D
1	Naryn	1.45	1.11	1.24	1.52	1.89	1.14	0.58	0.51	0.68	1.05	1.67	1.89
2	Yassy	1.37	1.76	1.86	1.07	0.64	0.62	0.90	1.45	2.24	2.64	1.96	1.38
3	Akbura	1.25	0.94	0.91	1.03	1.23	0.85	0.58	0.74	1.01	1.40	2.02	1.94
4	Aravansay	0.89	0.85	0.98	1.16	0.80	0.55	0.70	0.96	1.32	1.92	1.83	1.18
5	Isfaramsai	1.17	0.90	0.86	0.99	1.22	0.90	0.59	0.74	1.00	1.36	1.97	1.86
6	Shakimardan	1.20	0.89	0.85	0.98	1.17	0.80	0.56	0.70	0.97	1.33	1.91	1.85
7	Sokh	1.37	1.04	0.99	1.13	1.35	0.93	0.64	0.81	1.11	1.54	2.21	2.13
8	Isfara	1.59	1.23	1.36	1.66	2.09	1.26	0.64	0.56	0.75	1.15	1.83	2.08
9	Khodjabakirgan	1.25	0.92	0.88	1.02	1.22	0.84	0.58	0.74	1.01	1.39	1.99	1.92
10	Aksu	1.28	0.95	0.90	1.00	1.23	0.84	0.59	0.74	1.02	1.41	1.97	1.96
11	Arys	NA	NA	NA	NA	NA	NA	NA	NA	NA	NA	NA	NA
12	Keles	1.42	1.74	1.05	0.54	0.47	0.61	0.88	1.60	1.75	1.33	1.02	1.14
13	Chirchik	1.17	1.20	1.47	1.62	1.01	0.59	0.53	0.73	1.19	1.88	2.15	1.63
14	Chadaksai	2.20	1.73	1.22	1.38	1.88	2.15	1.32	0.68	0.59	0.80	1.25	1.91
15	Gavasi	2.14	1.40	1.06	1.00	1.23	1.40	0.97	0.67	0.84	1.15	1.58	2.27
16	Koksareksai	1.00	0.75	1.00	1.29	0.84	0.64	0.76	1.00	1.38	2.00	1.75	1.25
17	Sumsarsa	0.80	1.00	1.14	0.92	0.61	0.77	1.07	1.44	1.83	1.80	1.25	1.00
18	Kasansai	0.97	1.08	1.32	0.91	0.63	0.79	1.08	1.51	2.13	2.08	1.31	1.00
19	Padshata	1.78	2.04	1.60	1.17	1.29	1.60	1.85	1.10	0.59	0.51	0.70	1.11

Table 12: Monthly climate change coefficients for the Syr Darya tributaries. Ratio of normal mid-21st century versus mean 20th century runoff is shown. Colors indicate directions of change with red colors indicating a decrease of monthly average flows and blue colors indicating an increase accordingly. Coefficients for wet and dry years (not shown) can be computed accordingly.

5.2.2 Shifts in Runoff Seasonality in the Amu Darya

The Amu Darya runoff is equal to two-thirds of the total water resources of the Aral basin. On average, 83 percent of the runoff is generated in Tajikistan. Two large right-hand tributaries, the Kafirnigan and Surkhandarya Rivers, and one left-hand tributary, the Kunduz River, enter the main stream in its middle course. Further downstream, the Amu Darya has no tributaries, it crosses the deserts and semi-deserts, separating the Kara Kum and Kyzyl Kum deserts. On its way to the terminal sink, it loses its runoff through evaporation, infiltration into groundwater and through consumptive water utilization, mainly in irrigation (Agal'tseva, Bolgov, Spektorman, Trubetskova, & Chub, 2011).

Similarly to the Syr Darya, the Amu Darya River water regime is a snow and glacier-melt driven River. It is characterized by a high summer runoff and a low winter runoff. Mean long-term monthly runoff values of key Amu Darya tributaries are shown in Figure 51. The bulk of

the runoff is generated by the Vakhsh and Pyandzh tributaries (85 percent approx.). About 15 percent of the runoff stems from the Surkhandarya, Kafirnigan, and Kunduz. The annual runoff variability in the long-term regime is low (CV = 0.15), but the irregularity of the intra-annual distribution is well pronounced: 77 – 80 percent of the annual runoff falls on April–September and only 10 – 13 percent on December– February (Agal'tseva et al., 2011; Borovikova et al., 2003; Steiner & Siegfried, 2013).

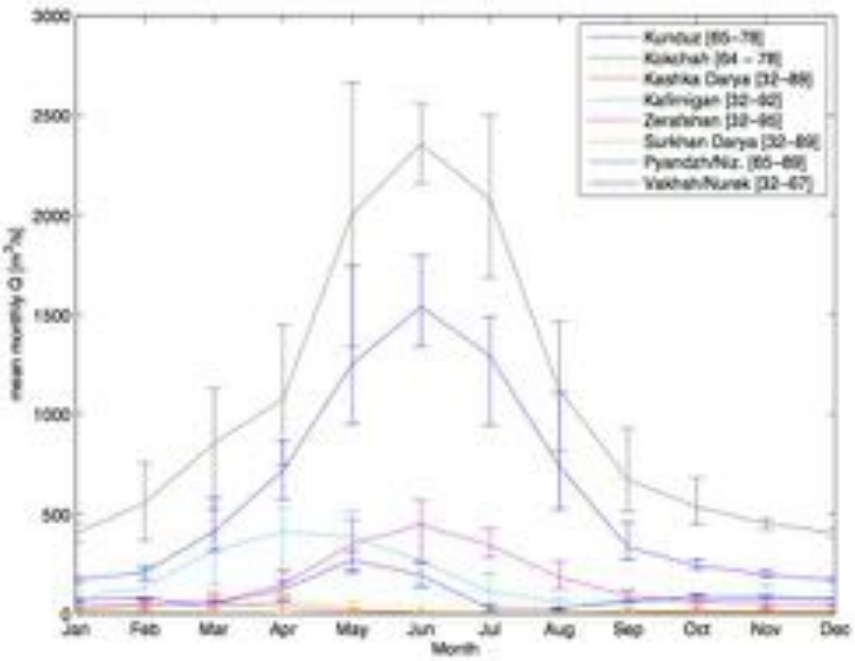

Figure 51: Long-term mean monthly runoff of key Amu Darya tributaries. The bars denote the year to year spread as measured over the corresponding time horizons for which data was available. Source: (Steiner & Siegfried, 2013).

There exist several climate impact studies in the Amu Darya. Here, the following key studies are reviewed:

- Report No. 72495-UZ, Reducing the Vulnerability of Uzbekistan's Agricultural Systems to Climate Change: Impact Assessment and Adaptation Options, Nov. 2012. Report prepared on behalf of the World Bank by a team lead by William Sutton of the Sustainable Dev. Dept., Europe and Central Asia Region, together with J. Srivastava and with the Consulting Firm Industrial Economics Inc (Sutton & Industrial Economics Inc., 2012).
- Report Contribution to ADB Study TA 7532: Climate Change Impacts on the Upstream Water Resources of the Amu and Syr Darya River Basins, March 2012. Report prepared on behalf of ADB by W.W. Immerzeel, A. F. Lutz and P. Droogers from FutureWater, Netherlands (Immerzeel et al., 2012)

- FAO report: Climat[e] Impact on Stream Flow in the Amu Dar[i]ya Basin, 2012. Prepared by FAO Investment Centre through Water Klemm, Senior Water and Land Dev. Engineer and Wilfried Hagg, Climate Scientist and Hydrologist (Klemm & Hagg, 2012).

Report No. 72495-UZ, Reducing the Vulnerability of Uzbekistan's Agricultural Systems to Climate Change: Impact Assessment and Adaptation Options

The report uses climate projections and coupled crop / water models to assess impacts on water supplies in Uzbekistan. The Water Evaluation and Planning System (WEAP) model is then used, using the inputs from CLIRUN to analyze potential basin-level shortages in water available to agriculture. The study then formulates policy requirements and adaptation measures, given these findings. The authors of the study compare three climate scenarios (multi-model means) for the region with a base assumption of no change. Based on their CLIRUN rainfall-runoff model, Figure 52 below shows their assessment for the Amu Darya flows and climate impacts thereon. The monthly climate change coefficients can easily be derived by dividing the corresponding monthly values of a particular scenario run (High, Med, Low) with base runoff values (see Figure 52 below).

CLIRUN is a two-layer, one-dimensional infiltration and runoff estimation tool that uses historic runoff as a means to estimate soil characteristics. A quick assessment reveals that model results are dubious at best.

First, a quick glance at Figure 52 suggests that the glacier-snowmelt fed Amu Darya River has boreal spring-time peak runoffs. This would also suggest that it is actually not river that originates in high mountains but rather a low-land river. This can for obvious reasons not be true.

Second, the authors mention that no in-country data for calibration was available but that they use historical gridded runoff data from the Global Runoff Data Center (GRDC) to make up for this problem. This is problematic as can easily be seen by looking at Figure 53. Here, we overlay actual (naturalized) runoff of Amu Darya with the CLIRUN model results (already shown in Figure 52). The actual naturalized Amu Darya runoff data is the best available past estimate of water availability in Uzbekistan in the basin.

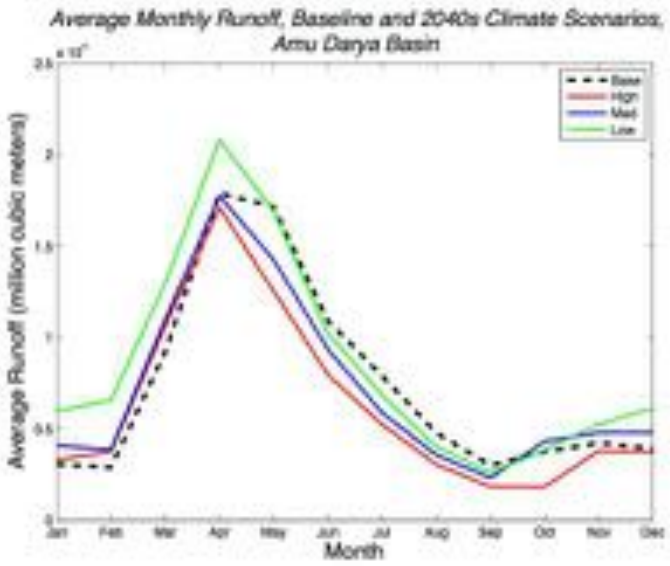

Figure 52: Climate change impact on Amu Darya flows. The base scenario assumes no change over mean historical runoff values and thus allows comparing the individual climate scenarios' impacts. It is unclear for which gauging station these values apply. Figure provided by authors, not shown in actual report.

Now, what should be compared is the black dashed line together with the staircase plot red line of actual mean monthly runoff values. It is obvious that

- the model cannot reproduce the timing of the current runoff seasonality as it suggests peak runoff in April as compared to actual peak runoffs in July (3 months offset).
- The model cannot reproduce actual runoff volumes as the models peak April mean flows are approximately 1.5 higher than actual mean peak flows in July.

For these obvious reasons, the basic underlying supply model utilized in this study is flawed – even without climate change, which adds a lot of additional uncertainty due to the reasons explained.

In summary, it is not recommended to consider the results of this study to be trustworthy and it is certainly not advisable to use any of the author's climate change correction factors for monthly runoff values in any future assessment whatsoever. Doing so would certainly not add credibility to any study which draws on these results and would risk to be discredited by Central Asian stakeholders for obvious and rightful reasons.

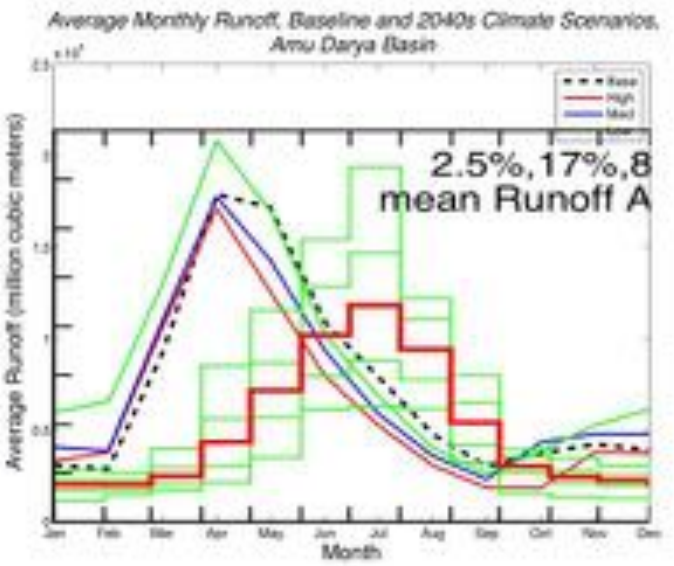

Figure 53: Comparing the reported CLIRUN monthly runoff base data (black dashed line) with actual data on naturalized flows of the Amu Darya above Karakum and Karshi Canal intakes (thick red step-wise line). The obvious mismatch between timing and amounts of runoff is apparent. Compare with Figure 52 above.

Report: Contribution to ADB Study TA 7532: Climate Change Impacts on the Upstream Water Resources of the Amu and Syr Darya River Basins

The study uses a state of the art mathematical modeling approach (PCRaster env. modeling framework) to study impacts of climate change on Syr and Amu Darya river runoff. The authors also study impacts on land ice in the upstream of the two rivers. The study is relevant in our context since it reports detailed climate change impacts for many major tributaries of the Amu Darya from which climate correction factors can easily be derived.

Data for model *calibration* was obtained from www.cawater-info.net. Calibration period was 2001 – 2010. It is unknown which period was taken for model *validation*. Data from 5 Global Circulation Models (GCMs) were used and the delta change method applied for simulating 5 different future climates as suggest by the GCMs. That is, temperature and precipitation series for the reference period 2001-2010 were repeated four times (2011-2050) and the daily projected change (increase or decrease) in temperature and precipitation was added/subtracted to the corresponding day in the reference period (see Figure 58 where the resulting range of future climate uncertainty is shown). As such, no 'real' downscaling of climate was performed.

The latter, in fact, is where the study's main problems lie, among other things. Here, we are reporting some of the key issues that are worthwhile drawing attention to.

First, let us look at model calibration of an important sample tributary catchment to the Amu Darya, i.e. the Vaksh River (see Figure 54). As is easily visible the calibrated model underestimates runoff in the catchment, especially during the summer peaks and has a peak shift by one month or so. These are important issues that warrant further attention. Furthermore, the authors did not distinguish between a calibration period and a validation period, which is normal for any serious modeling study as the real model performance needs to be quantified with an out-of-sample validation period.

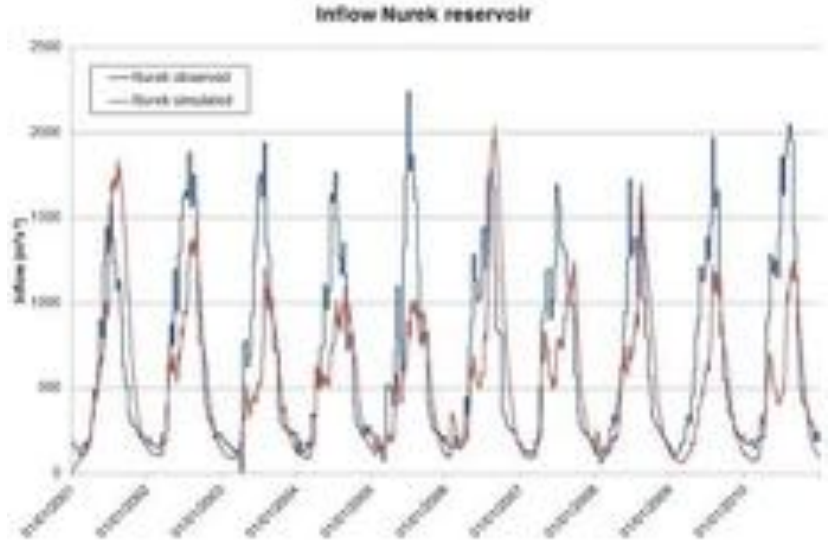

Figure 54: Unsatisfactory model calibration for Vaksh River. The modeled runoff underestimates peak flows almost consistently over the calibration period and suffers from a peak shift. See Figure 5-4 in corresponding report.

Figure 55 below shows that there are issues with the model's initial condition, maybe due to inadequate pre-wetting. If one looks at the baseflow component of the simulated Vaksh River runoff, it can be easily seen that this contribution to total flows is nil at the start. After an initial steep rise of the baseflow component up to approximately 100 m^3/s, the baseflow then inexplicably declines over the calibration period (10 years) to approximately half of that initial peak value. In Figure 57, we see that this decline continues over the 40 year forecast period.

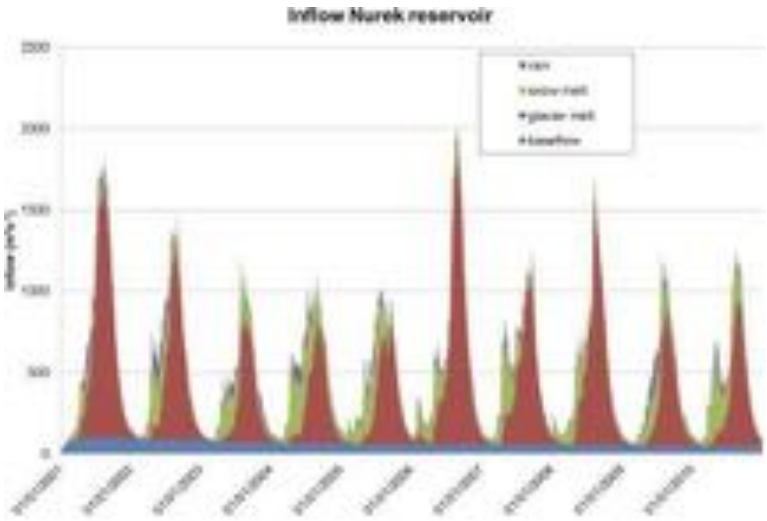

Figure 55: Sample baseflow-related issues in the modeled Vaksh that could, among other things point to the lack of appropriate pre-wetting of the model to arrive at valid initial conditions. See Figure 5-15 in the corresponding report.

Figure 56 shows that the calibrated model des not perform well in reproducing first decade (21st century) flows and their seasonality. In the case of Tupalang reservoir inflows, the peak flows occur 2 months earlier than suggested by the model and in the case of the Vaksh river, as already stated above, the model heavily underestimates actual mean runoff.

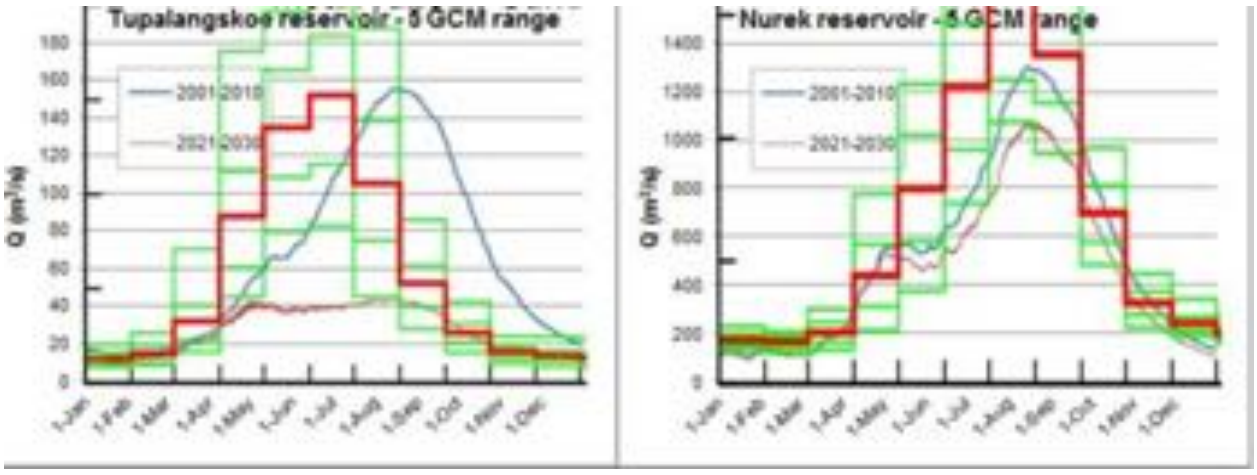

Figure 56: Unsatisfactory calibration results result in bad model performance, even under no climate change scenarios. 2 sample tributaries to Amu Darya are shown and compared with actual gauge values (mean runoff is shown by thick red lines, compare with blue calculated model hydrographs). See plates in Figure 6-43 in corresponding report.

Figure 57 shows results for the development of inflows to Nurek (Vaksh River) over the first decade of the 21st century. As explained above, flows of the first decade are already underestimated (Figure 56). According to model results, the contribution from melting land ice will have entirely vanished around 2040. Over the same period of time, runoff will become predominately from snow melt. The latter point is unintuitive as we would *not* expect to see

more area becoming available under a warming scenario above a mean snow line (which is retreating higher up into the mountains under warming).

The loss of runoff from land ice contributions does not necessarily mean that all land ice will have melted over the period of assessment but rather that the lower lying glaciers will have wasted away entirely over the next 40 years. Rather, the authors report that glacier extent in the Tien Shan and Pamir ranges will by 45 - 60 over present values (not clear if they are speaking about volumetric losses).

For the moment, let us assume that these are volumetric losses and that the total volume of land ice in the Amu Darya is roughly double the one in the Syr Darya (400 km^3 versus 200 km^3). Now let's further assume for the sake of the argument that we are looking at an average volumetric ice loss of 50 % until 2050. Just doing back of the envelope, this would mean that 200 km^3 of ice are melting away in the Amu Darya which would then also mean that (assuming uniform melting per annum) that we are looking at something like 5 km3/a of additional water in the Amu Darya due to the destorage of ice in the upstream.

Using long-term average figures for flows, this corresponds to roughly 7 % additional flow (all back of the envelope). Now, in their conclusions of the report, the authors mention that the

- runoff generation decreases most significantly in upstream areas of glacier retreat; and that
- total annual runoff into the downstream areas is expected to decrease 26-35% for the Amu Darya by 2050.

It is absolutely unclear how the authors of the study arrive at these numbers when there is complete uncertainty regarding the future precipitation climate of Central Asia and when glaciers will actually start to provide more water as they melt under increasing warming. The study's results and our comments here should also be viewed in light of the findings of the FAO Study on climate impacts on selected Amu Darya tributaries (discussed below).

Finally, one should look at their assessment of uncertainty in their projections. However, their accounting of uncertainty is incomplete at best. Normally, one has to distinguish between

- model uncertainty due to incomplete information about process in GCMs;
- scenario uncertainty due to incomplete information about the climate's variability at different time-scales, including decadal and multi-decadal; and
- aleatoric internal variability.

The authors of the study really only look at model uncertainty over the spread of 5 GCMs whereas, in fact Siegfried et al., 2012 showed that 11 GCM and their individual runs perform well in the region and thus are available for analysis. The uncertainty values in future projections are overly narrow and incomplete in light of the best available knowledge (Figure 58).

To summarize, all these issues point to the fact that the study's results have to be reviewed carefully and that they are not necessarily robust in terms of the conclusions reached. Most likely, this is also the reason that the authors of the study, when turning some of their results into an academic paper, were backtracking from the above stark conclusions when they say that 'The wide range in the projections implies an uncertain future, both in terms of Central Asian glacier extent as well as in terms of downstream water availability' – see (A. F. Lutz, Immerzeel, Gobiet, Pellicciotti, & Bierkens, 2012).

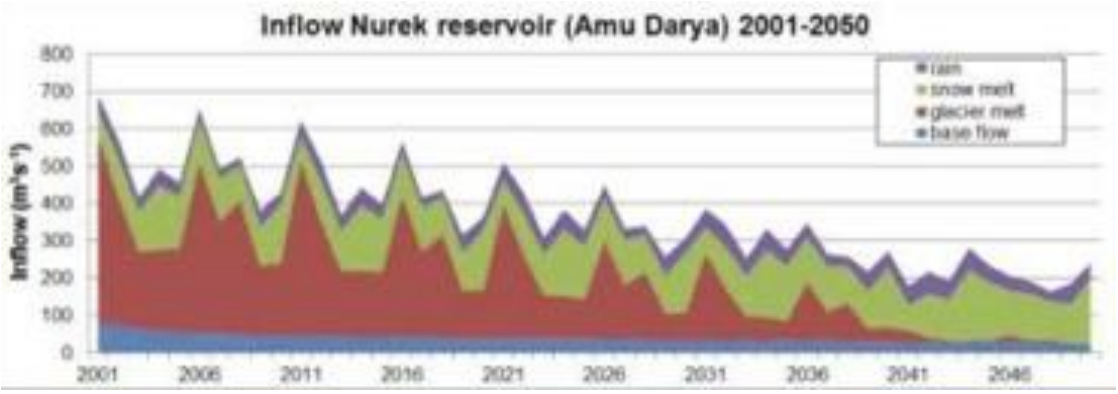

Figure 57: Projections of inflow to Nurek reservoir (Vaksh River catchment). The baseflow issues shown in Figure 55 above carry over into projections. Model results are unintuitive as it is not clear why runoff contributions from glaciers will entirely vanish by 2040 and in return contributions from snow melt almost double as compared to today. See Figure 6-41 in corresponding report.

Again, if the results of the ADB study are taken at face value, there exists are real danger that any study that draws on them risks being simply dismissed as results from the underlying mathematical models are unrealistic and incomplete best and thus climate impacts on the supply-side over the first half of the 21st century likely not quantified in a satisfactory way.

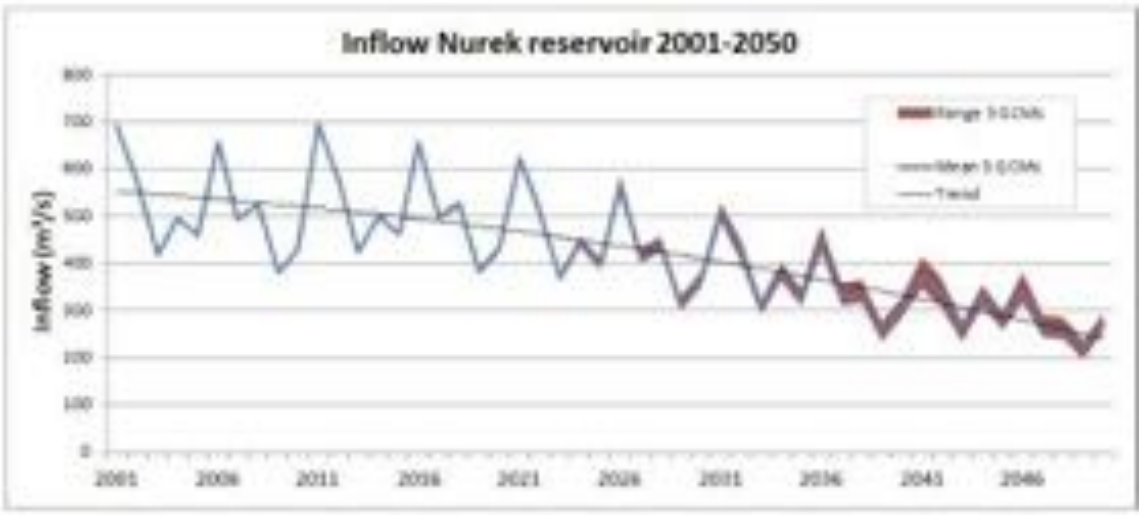

Figure 58: Projected average annual runoff in Vaksh River and associated uncertainty range over 5 GCMs. Model results suggest that despite the great uncertainty on the side of the future precipitation climate, runoff will significantly decline with only little uncertainty in the projections. See Figure 6-39 in the corresponding report.

FAO report: Climat[e] Impact on Stream Flow in the Amu Dar[i]ya Basin

For the study of climate impacts in the Amu Darya basin, a conceptual hydrological model was setup in two smaller tributaries in the upper, high elevation basin. The two subcatchments are Abramov (55.5 km^2) and Kudara (1'575 km^2). The HBV-ETH model was utilized and extended to accommodate snow and ice.

The authors have an extensive set of measured runoff data available from gauging stations for model calibration. They take care to represent all relevant storage compartments and processes at the scale of the two small catchments. They also clearly distinguish between a model calibration and validation period.

For both subcatchments, the authors achieve and excellent goodness of fit, even over validation periods which confirms the validity of their model approach (see Figure 59). Encouraged by their results, the authors used the same approach to model the complete Pianj and Vaksh sub-basins. However, as the results show (see Figure 60 below) and as the authors themselves acknowledge, their approach was overly simplistic using data from a single meteorological station only to drive the rainfall-runoff model. *They mention that modeling adequately the hydrology of larger Amu Darya catchment remains an exciting topic for future research.* This is in line with our understanding of the current work and our recommendations.

The authors then use climate scenarios from a regional climate modeling study to drive their hydrological models of the two small subcatchments.

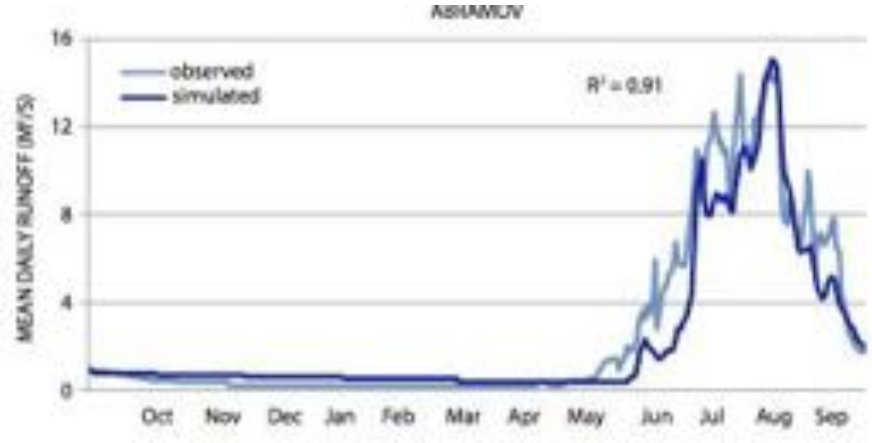

Figure 59: Comparison of observed and simulated hydrographs at the outlet of the Abramov catchment. The R^2 is the goodness of fit (model efficiency criterion after Nash and Sutcliffe, 1970). Calibration period was from 1968/69 – 1977/78. The R2 is excellent which points to a satisfactory model performance for the small catchment.

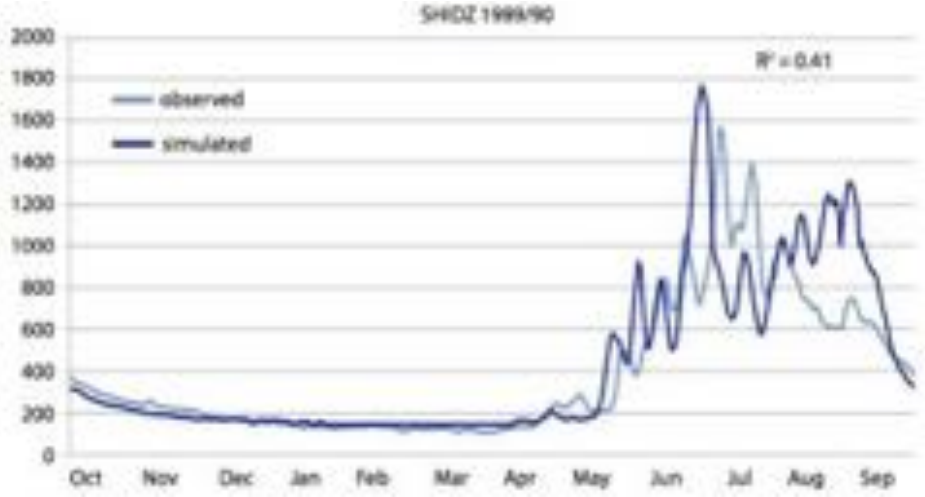

Figure 60: Comparison of observed and simulated hydrographs at Shidz in the downstream. The R2=0.41 indicates a completely unsatisfactory HBV-ETH model performance in the lower reaches of the big tributaries.

For assessing climate impacts in the two subcatchments, the authors generate runoff scenarios by modifying an average hydrological year with corresponding climate change assumptions while also accounting for how these impact basin glaciation. Regional downscaled climate scenarios from the study by (Makhmadaliev, Novikov, Kayumov, Karimov, & Perdomo, 2003) were used. According to the latter, 2050 temperature scenarios for the upper Amu Darya catchment range between +1.8 - +2.9 degree Celsius. For precipitation, the downscaled climate predictions are not consistent. Therefore, the FAO study studies model sensitivities to the following scenarios: a) no precipitation changes, b) precipitation increase of 30 percent and c) precipitation decrease of 30 percent relative to today's numbers. From this 6 bounding scenarios are defined and with which the rainfall-runoff model is then driven. Results for the Abramov catchment are shown in Figure 61 and Figure 62 below.

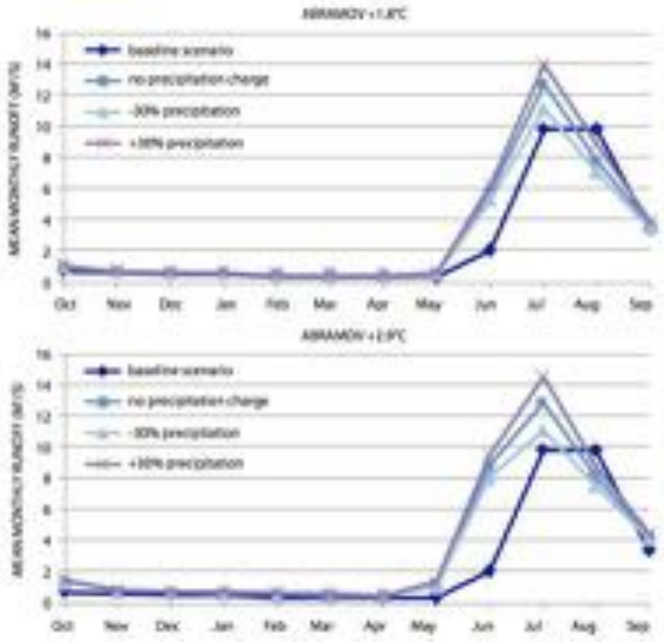

Figure 61: Comparison of baseline and future climate change scenarios in the Abramov catchment. Key model results are a high temperature sensitivity and low sensitivity to changes in precipitation.

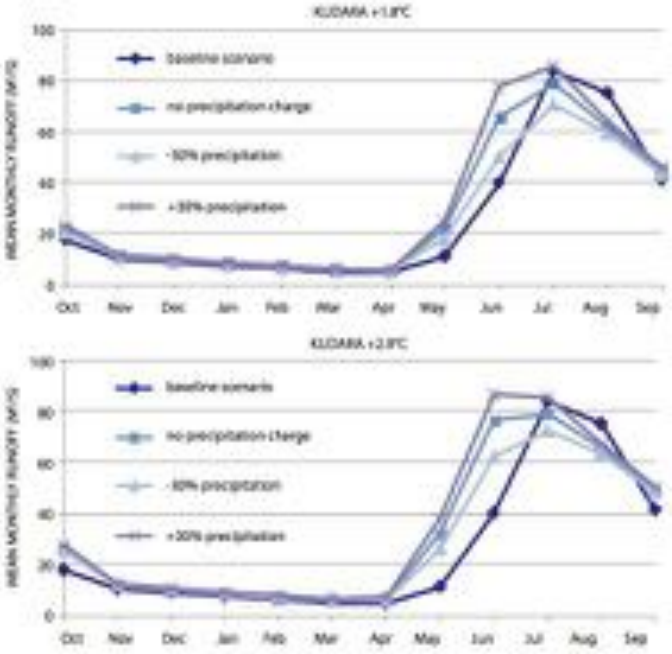

Figure 62: Comparison of baseline and future climate change scenarios in the Kudara catchment. Key model results are a high temperature sensitivity and low sensitivity to changes in precipitation.

Key results are high temperature sensitivities of hydrographs were increasing temperatures lead to earlier melting of snow and land ice and thus runoff in a hydrological year. The authors also find that in both catchments, changes in precipitation (even negative ones) have only a minimal impact on runoffs and their patterns and cannot reverse the temperature-induced trend of earlier in-season runoff (see Table 13 and Table 14 below).

ABRAMOV														
ΔT	ΔP	Oct	Nov	Dec	Jan	Feb	Mar	Apr	May	Jun	Jul	Aug	Sep	Year
Baseline scenario		1.0	1.0	1.0	1.0	1.0	1.0	1.0	1.0	1.0	1.0	1.0	1.0	1.0
	±0%	1.4	1.1	1.1	1.1	1.1	1.1	1.1	1.5	2.8	1.3	0.8	1.1	1.2
	-50%	1.3	1.1	1.1	1.1	1.1	1.1	1.1	1.5	2.6	1.1	0.7	1.0	1.1
+1.8°C	+50%	1.6	1.1	1.1	1.1	1.1	1.1	1.1	1.6	3.1	1.4	0.9	1.1	1.3
	±0%	1.9	1.3	1.3	1.3	1.3	1.3	1.3	2.1	4.3	1.3	0.8	1.2	1.4
	-50%	1.8	1.2	1.2	1.2	1.2	1.2	1.2	2.0	3.9	1.1	0.8	1.2	1.3
+2.9°C	+50%	2.0	1.3	1.3	1.3	1.3	1.3	1.3	2.1	4.7	1.5	0.9	1.3	1.5

The value of the baseline scenario was set to 1.0.
The strongest changes are indicated by colors:
marks changes > 50%
marks changes > 100%
marks changes > 200%

Table 13: Scenario-dependent monthly climate change coefficients for the runoff in Abramov catchment.

KUDARA														
ΔT	ΔP	Oct	Nov	Dec	Jan	Feb	Mar	Apr	May	Jun	Jul	Aug	Sep	Year
Baseline scenario		1.0	1.0	1.0	1.0	1.0	1.0	1.0	1.0	1.0	1.0	1.0	1.0	1.0
	±0%	1.2	1.1	1.1	1.1	1.1	1.1	1.2	2.0	1.6	0.9	0.8	1.1	1.1
	-30%	1.2	1.0	1.0	1.0	1.0	1.0	1.1	1.6	1.2	0.8	0.8	1.0	1.0
+1.8°C	+30%	1.3	1.1	1.1	1.1	1.1	1.1	1.2	2.2	1.9	1.0	0.8	1.1	1.2
	±0%	1.3	1.1	1.1	1.1	1.1	1.1	1.4	2.9	1.9	0.9	0.8	1.2	1.2
	-30%	1.4	1.1	1.1	1.1	1.1	1.1	1.3	2.3	1.8	0.9	0.8	1.2	1.1
+2.9°C	+30%	1.6	1.2	1.1	1.1	1.1	1.1	1.5	3.4	2.1	1.0	0.9	1.2	1.3

The value of the baseline scenario was set to 1.0.
The strongest changes are indicated by colors:
marks changes > 50%
marks changes > 100%
marks changes > 200%

Table 14: Scenario-dependent monthly climate change coefficients for the runoff in Kudara catchment.

The authors of the study show that for all scenarios, annual runoff is increasing with the most significant changes in May and June. One of their key finding is that throughout a typical hydrological year, glaciers melt *stronger* and *longer*.

In summary, the FAO study concludes that the main runoff changes by 2050 in the two subcatchments are:

- a 10 – 50 percent increase in annual runoff
- a significant increase of runoff in May and June due to earlier and more intense snow melt
- a 10 – 30 percent reduction of runoff in August.

The authors mention that these *average changes* in runoff are highly certain for the heavily glaciated high alpine catchments. Since the main tributaries of the Amu Darya, i.e. the Vaksh and Pianj, maintain their characteristics of the nival-glacial runoff regimes as the drain the mountain ranges, it is highly likely that the findings of the small subcatchments reported above will be relevant for the larger catchment too and that there will be a runoff increase of up to 20 percent in the spring and a slight decrease of runoff in August.

Recommendations

In light of the above findings, the critical issues found in the World Bank and ADB reports and due to the lack of otherwise credible scientific work on climate change impacts on the Amu Darya water supplies, it is recommended that the average change coefficients from the FAO study are considered and incorporated into the BEAM modeling study. This will provide a sound, scientifically robust way to incorporate changes from climate into the BEAM model. It will also be compatible with the approach utilized for the Syr Darya and in line of the findings there.

IT IS PROPOSED TO LAUNCH A SCIENTIFICALLY SOUND AND ROBUST ASSESSMENT OF THE QUANTITATIVE IMPACTS ON THE TRIBUTARIES TO THE AMU DARYA RIVER. FOR THIS, RECENT INTERNATIONAL EFFORTS OF STATE-OF-THE-ART IN REGIONAL CLIMATE DOWNSCALING, SUCH AS THE COORDINATED REGIONAL CLIMATE DOWNSCALING EXPERIMENT (CORDEX), SHOULD BE UTILIZED. THIS PROJECT IS ALREADY PRODUCING HIGH-RESOLUTION REGIONAL CLIMATE MODEL (RCM) SCENARIOS FOR PRIORITY REGIONS, INCLUDING CENTRAL ASIA. A KEY ADVANTAGE OF THIS WOULD BE TO USE THE MULTIPLE RCM EXPERIMENTS SO AS TO EVALUATE THE LARGE UNCERTAINTY THAT STEMS FROM DIFFERENT REPRESENTATIONS AND PARAMETERIZATIONS OF THE PHYSICAL PROCESSES OF THE ATMOSPHERE AND HOW THESE TRANSLATE INTO OUR ABILITY TO PRODUCE ESTIMATES OF FUTURE RUNOFF IN THE BASIN.

5.3 Impacts on Downstream Supply-Demand Gaps

The development of future supply versus demand ratios will be determined by combined effects of supply-side variability, i.e. at intra-annual, seasonal, interannual and longer time-scales as well as the development of the water demand where agriculture will continue to be the main driver with highest probability in the region.

The growing population numbers will certainly allocate more water for domestic demand but it is very unlikely that irrigated agriculture will be expanded proportionally to population growth. First, the arable land available for irrigation is limited and large scale development of new desert irrigation oasis is likely not happening, also due to the fact that the use of water resources is already stretched to the limit, at least under the current inefficient systems operation where significant amounts of total runoff are annually lost unproductively, i.e. in Aydar Kul or in Turkmenistan (Bucknall et al., 2003).

Increasing minimum, mean and maximum daily temperatures increases will be the main driver of increasing evapotranspiration over irrigated lands via increases in crop water requirements. (Siegfried et al., 2011) has shown that under the SRES A2 climate scenario, maximum demand coverage deficits are expected to occur in the early growing stages which are the most sensitive periods for plant growth regarding water stress. Careful management interventions, most likely coupled with additional manmade storage in unregulated catchments together with corresponding conveyance will be required to cover this deficit (see Figure 63 below). This estimate assumes that a) irrigated area remains constant, b) the crop mix remains unchanged over the first half of the 21st century and c) that increases in downstream evapotranspirative requirements (+12 percent ±1.7 percent relative to 2000–2009 levels in 2040-2049) are determined by increases in temperature.

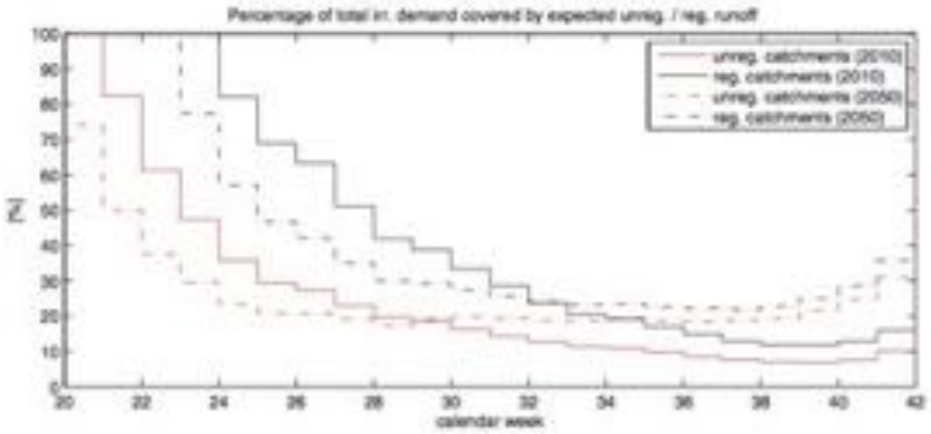

Figure 63: Development of irrigation water demand coverage in the Fergana Valley due to changes in runoff seasonality and increases in evapotranspirative requirements. Source: (Siegfried et al., 2011).

It should further be noted that the analysis above also assumes that the crop calendars will not shift over the time of analysis. Clearly, this is a valid assumption but likely oversimplifying actual future dynamics as crop schedules will necessarily be shifted in line with an earlier onset of seasons. This copying strategy might alleviate some of the eventual water stress that can arise from increasing crop water requirements due to higher evapotranspiration.

For further information on the global shift of growing season, see (Linderholm, 2006) for a comprehensive global overview paper.

THE REPORTED FIGURES OF INCREASES IN EVAPOTRANSPIRATION ARE INDICATIVE OF THE GENERAL TRENDS IN THE LOWLAND REGIONS IN THE SYR DARYA AND AMU DARYA. A MORE DETAILED ANALYSIS WOULD INVESTIGATE TRENDS ALSO IN THE AMU DARYA BASIN BY USING A COMPUTATIONAL RAINFALL-RUNOFF APPROACH.

5.4 Risks & Hazards

Glaciers' lengths will experience significant declines across all size categories as land ice continues to melt in the 21st century. As these glaciers retreat they leave behind unstable terminal moraines behind which significant volumes of melt water can get trapped. If these moraines collapse, glacier lake outbursts (GLOF) can occur that can potentially cause catastrophic flooding in the downstream (see also Nayar, 2009 for a related discussion in the Himalayas). It is highly likely that the Fergana Valley region will become particularly exposed to these geohazards because glaciers surround the valley floor in the south, the east and the north (Siegfried et al., 2011).

The same holds true for Tajikistan which is a hotspot country in the context of risks, threats and hazards, especially when viewed from the fact that the country has insufficient means at her disposition to effectively provide disaster response and mitigation. Clearly, if the loss of land ice is in the projected range as proposed by the SRES A2 climate scenario, GLOF will increasingly threaten the Tajik Amu Darya basin.

Even nowadays, Tajikistan experiences significant natural hazards annually. These include floods, mudflows, landslides, epidemics, droughts, earthquakes, avalanches, insect infestation on cropped land and impacts from storm damage (Asian Disaster Reduction Center, 2006).

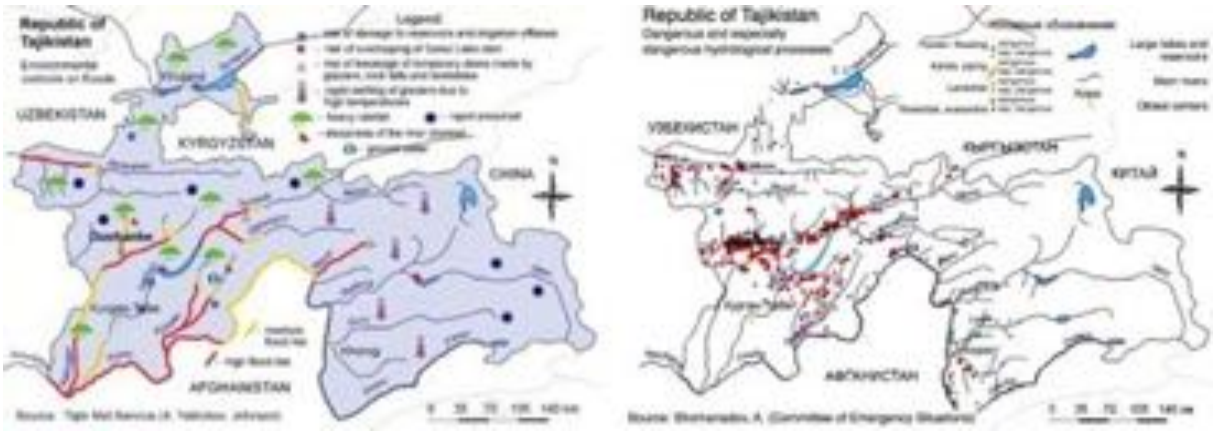

Figure 64: Left plate: Flood mechanisms are depicted along the main rivers. Right plate: Mapping of past hazards related to hydrologically processes. Modified from (Asian Disaster Reduction Center, 2006).

Floods occur mainly during heavy precipitation events in spring or during peak runoff from snow- and glacier-melt in summer. The south-eastern slopes of the Gissar range, the northern slopes of Turkestan range and southern slopes of the Kuramin range are the areas with greatest flood threats. The basins regularly affected are the Yakhsu, Varzob, Vakhsh, Zeravshan and Obihingou Rivers (Figure 64). Thus, it is important to assess the developments of precipitation extremes in the country in a coherent way.

An estimated 85 percent of the total area of the country is threatened by storm triggered mudflows. Seismic and non-seismic landslides regularly threaten settlements and major transportation routes throughout the country. Heavy snowfall in the winter and early spring season can trigger major avalanches in February and March which can cause significant damage to infrastructure. All of these events cause recurring fatalities. Albeit rare, severe droughts can affect the country. Through their adverse effects on crops and livestock, they can have devastating consequences on the poor rural population and their livelihoods (Figure 64).

Earthquakes present a substantial risk for the country and its fragile infrastructure. Direct risk to life, e.g. from collapsing houses and other infrastructure, is amplified by secondary effects such as landslides, rockslides, mudflows that result from the destabilization of mountain slopes during earthquakes and avalanches. Land- and rockslides can be hazardous not only for the larger economy but also a whole river basin catchment if large-volume displacement of material blocks runoff in crucial locations. Prime examples are the landslide which buried the village of Usoy in 1911 and blocked the Murghab River in the Pamir range. The resulting 60 km long Sarez Lake nowadays contains over 17 km^3 of water that is dammed by the so-called Usoy natural dam, the highest dam in the world. The unstable dam poses significant risk to the downstream population that is living in the Bartang and Pyanj river valleys and for the larger Amu Darya as well (Droz & Spasic-Gril, 2006).

New landslides into Lake Sarez could cause a Tsunami that overtops the natural dam and erodes it way with the result of its complete failure. Under the current global warming, these landslide hazards are increasing due to the thawing of the permafrost that is a crucial factor in slope stability in high mountain areas. This is an important and worrisome development to acknowledge that needs further analysis. The March 3 2002 collapse of a mountain flank downstream of the Baipaza hydropower station in the Vaksh catchment and the subsequent formation of an unstable water reservoir is another, more recent example of risk resulting from this hazard (see Siegfried, 2012b and citations therein).

IN LIGHT OF THE THREATS AND DANGERS FROM CLIMATE CHANGE DISCUSSED HERE, IT IS PROPOSED THAT A COHERENT ANALYSIS OF THE DEVELOPMENT OF EXTREMES AND HOW THESE CAN IMPACT LOCAL ECONOMIES SHOULD BE CARRIED OUT. FOCUS SHOULD BE THE UPSTREAM REPUBLICS OF KYRGYZSTAN AND TAJIKISTAN.

6 Conclusions

The observed warming due to anthropogenic climate change will further continue in the 21st century in Central Asia. As land ice is retreating and less precipitation is falling as snow, significant changes in the runoff patterns of the rivers are expected to occur (shift from nival-glacial to pluvial-nival runoff regimes). This means that runoff peaks will occur earlier in the spring time as compared to today. As a result, irrigation season runoff would be greatly reduced in unregulated catchments where runoff cannot be stored intermittently to bring it in phase with irrigation season demands. This brings additional challenges, including greater food insecurity, especially in the smaller unregulated basins in the Amu Darya and the Syr Darya. Due to the gradual addition of tributaries with slightly different flow regimes, the effect will vanish the further away one moves from the glaciers along the streams. It is noteworthy to mention that the potential of aquifers to offset the loss of glacier water storage over the very long-term when glaciers no longer contribute to runoff has not been explored in the region so far.

The loss of land ice due to glacier shrinkage will increase available runoff temporarily as a function of the levels of glaciation in the individual tributary catchments of the large rivers. As glaciers retreat, large volumes of melt water can get trapped behind unstable terminal moraines. If these moraines collapse, glacier lake outbursts can occur. Such outbursts can potentially cause catastrophic flooding downstream. The Fergana Valley region and parts of Tajikistan are particularly exposed to these geohazards. Furthermore, the tributaries of the two larger rivers frequently experience mudflow events. These threaten population and infrastructure, esp. in the spring and summer seasons. Due to global warming, mudflow frequency might be rising under increasing precipitation extremes and decreasing slope stability due to the loss of permafrost. The management of those risks is a major challenge as there are no effective early warning systems in place.

In summary, climate change will affect the Central Asian region mainly through temperature effects on the snow and ice cover in the mountain ranges where runoff is formed. Drastic changes in annual water availability in absolute terms, relative to current conditions, are unlikely as impacts from climate change are likely to unfold gradually over the next 40 years. Neo-Malthusian scenarios of acute water scarcity and conflict over the water resources of the two Daryas are unrealistic. However, the expected impacts from environmental change call for preparedness through adaptation and for mitigation so as to reduce the threats for human wellbeing most effectively.

7 Bibliography

Agal'tseva, N. a., Bolgov, M. V., Spektorman, T. Y., Trubetskova, M. D., & Chub, V. E. (2011). Estimating hydrological characteristics in the Amu Darya River basin under climate change conditions. *Russian Meteorology and Hydrology*, *36*(10), 681–689. doi:10.3103/S1068373911100062

Asian Disaster Reduction Center. (2006). *Tajikistan - Country Report for Asian Disaster Reduction Center*.

Barlow, M. a., & Tippett, M. K. (2008). Variability and Predictability of Central Asia River Flows: Antecedent Winter Precipitation and Large-Scale Teleconnections. *Journal of Hydrometeorology*, *9*(6), 1334–1349. doi:10.1175/2008JHM976.1

Barlow, M., Cullen, H., & Lyon, B. (2002). Drought in central and southwest Asia: La Niña, the warm pool, and Indian Ocean precipitation. *Journal of Climate*, 697–700. Retrieved from http://journals.ametsoc.org/doi/abs/10.1175/1520-0442(2002)015%3C0697%3ADICASA%3E2.0.CO%3B2

Bernauer, T., & Siegfried, T. (2012). Climate change and international water conflict in Central Asia. *Journal of Peace Research*, *49*(1), 227–239. doi:10.1177/0022343311425843

Borovikova, L., Agaltseva, N., Ivanov, Y., Novikov, V., & Borovikova, L. (2003). Estimate of Volume and Flow Regime of the Left Bank Tributaries of the River Pyanj.

Bucknall, J., Klytchnikova, I., Lampietti, J., Lundell, M., Scatasta, M., Thurman, M., & Bank, T. W. (2003). *Irrigation in Central Asia*.

Clark, M. P., Serreze, M. C., & Robinson, D. a. (1999). Atmospheric controls on Eurasian snow extent. *International Journal of Climatology*, *19*(1), 27–40. doi:10.1002/(SICI)1097-0088(199901)19:1<27::AID-JOC346>3.0.CO;2-N

Droz, P., & Spasic-Gril, L. (2006). LAKE SAREZ RISK MITIGATION PROJECT: A GLOBAL RISK ANALYSIS, 1–17.

Fatichi, S., Ivanov, V. Y., & Caporali, E. (2012). Investigating Interannual Variability of Precipitation at the Global Scale: Is There a Connection with Seasonality? *Journal of Climate*, *25*(16), 5512–5523. doi:10.1175/JCLI-D-11-00356.1

Immerzeel, W. W., Lutz, A. F., Droogers, P., & Bank, A. D. (2012). Climate Change Impacts on the Upstream Water Resources of the Amu and Syr Darya River Basins, *31*(March).

Jung, M., Reichstein, M., Ciais, P., Seneviratne, S. I., Sheffield, J., Goulden, M. L., Bonan, G., et al. (2010). Recent decline in the global land evapotranspiration trend due to limited moisture supply. *Nature*, *467*(7318), 951–4. doi:10.1038/nature09396

Karl, T., Diaz, H., & Kukla, G. (1988). Urbanization: Its detection and effect in the United States climate record. *Journal of Climate*. Retrieved from http://journals.ametsoc.org/doi/abs/10.1175/1520-0442(1988)001%3C1099%3AUIDAEI%3E2.0.CO%3B2

Khromova, T. E., Osipova, G. B., Tsvetkov, D. G., Dyurgerov, M. B., & Barry, R. G. (2006). Changes in glacier extent in the eastern Pamir, Central Asia, determined from historical data and ASTER imagery. *Remote Sensing of Environment*, *102*(1-2), 24–32. doi:10.1016/j.rse.2006.01.019

Klemm, W., & Hagg, W. (2012). *CLIMATE IMPACT ON STREAM FLOW IN THE AMU DARIA BASIN*. Rome.

Linderholm, H. W. (2006). Growing season changes in the last century. *Agricultural and Forest Meteorology*, *137*(1-2), 1–14. doi:10.1016/j.agrformet.2006.03.006

Lutz, A F, Droogers, P., Immerzeel, W. W., & Bank, A. D. (2012). Climate Change Impact and Adaptation on the Water Resources in the Amu Darya and Syr Darya River Basins, *31*(May).

Lutz, A. F., Immerzeel, W. W., Gobiet, A., Pellicciotti, F., & Bierkens, M. F. P. (2012). New climate change scenarios reveal uncertain future for Central Asian glaciers. *Hydrology and Earth System Sciences Discussions*, *9*(11), 12691–12727. doi:10.5194/hessd-9-12691-2012

Makhmadaliev, B., Novikov, V., Kayumov, A., Karimov, U., & Perdomo, M. (2003). *National Action Plan of the republic Tajikistan for Climate Change Mitigation*. Dushanbe.

Mariotti, A. (2007). How ENSO impacts precipitation in southwest central Asia. *Geophysical Research Letters*, *34*(16), L16706. doi:10.1029/2007GL030078

Mavromatis, T., & Stathis, D. (2010). Response of the water balance in Greece to temperature and precipitation trends. *Theoretical and Applied Climatology*, *104*(1-2), 13–24. doi:10.1007/s00704-010-0320-9

Nayar, A. (2009). When the ice melts. *Nature*, *V*(October). Retrieved from http://cat.inist.fr/?aModele=afficheN&cpsidt=22021209

Oberhänsli, H., Novotná, K., Píšková, A., Chabrillat, S., Nourgaliev, D. K., Kurbaniyazov, A. K., & Matys Grygar, T. (2011). Variability in precipitation, temperature and river runoff in W Central Asia during the past ~2000yrs. *Global and Planetary Change*, *76*(1-2), 95–104. doi:10.1016/j.gloplacha.2010.12.008

Pereira-Cardenal, S. J., Riegels, N. D., Berry, P. a. M., Smith, R. G., Yakovlev, a., Siegfried, T. U., & Bauer-Gottwein, P. (2011). Real-time remote sensing driven river basin modeling using radar altimetry. *Hydrology and Earth System Sciences*, *15*(1), 241–254. doi:10.5194/hess-15-241-2011

Pertziger, F. I., & Asian, C. (1990). Role of glacier and snow cover melting in runoff variations from the small basins in Pamir and the Alps, (193), 189–196.

Savitskiy, A., & Schlüter, M. (2008). Current and future impacts of climate change on river runoff in the Central Asian river basins. *Adaptive and Integrated …*. Retrieved from http://link.springer.com/chapter/10.1007/978-3-540-75941-6_17

Schiemann, R., & Lüthi, D. (2008). The precipitation climate of Central Asia—intercomparison of observational and numerical data sources in a remote semiarid region. *International Journal of …*, *314*(June 2007), 295–314. doi:10.1002/joc

Schneider, U., Becker, A., Finger, P., Meyer-Christoffer, A., Ziese, M., & Rudolf, B. (2013). GPCC's new land surface precipitation climatology based on quality-controlled in situ data and its role in quantifying the global water cycle. *Theoretical and Applied Climatology*. doi:10.1007/s00704-013-0860-x

Siegfried, T. (2012a). *Development of a Mathematical Model of the Syr Darya Basin for Effective Water Re-sources Management in Kazakhstan*.

Siegfried, T. (2012b). *Scoping Study for the Development of a Mathematical Model for Integrated Water Resources Management in Tajikistan*.

Siegfried, T., & Bernauer, T. (2007). Estimating the performance of international regulatory regimes: Methodology and empirical application to international water management in the Naryn/Syr Darya basin. *Water Resources Research*, *43*(11), n/a–n/a. doi:10.1029/2006WR005738

Siegfried, T., Bernauer, T., Guiennet, R., Sellars, S., Robertson, A. W., Mankin, J., Bauer-Gottwein, P., et al. (2011). Will climate change exacerbate water stress in Central Asia? *Climatic Change*, *112*(3-4), 881–899. doi:10.1007/s10584-011-0253-z

Steiner, J., & Siegfried, T. (2013). *Management of the Vaksh Cascade*. Zurich, Switzerland.

Sutton, W., & Industrial Economics Inc. (2012). *Reducing the Vulnerability of Uzbekistan ' s Agricultural Systems to Climate Change :* Washington D.C.

United Nations. (2010). *Environment and Security in the Amu Darya Basin*.

Wagner, S., & Hoelzle, M. (2010). Glacier Volume Changes in the Panj and Vakhsh Basins future glacier change in the Panj and Vakhsh river basins, (February).

Wood, a. W., Leung, L. R., Sridhar, V., & Lettenmaier, D. P. (2004). Hydrologic Implications of Dynamical and Statistical Approaches to Downscaling Climate Model Outputs. *Climatic Change*, *62*(1-3), 189–216. doi:10.1023/B:CLIM.0000013685.99609.9e

Yakovlev, A. (2006). Monitoring of mountain glaciers selected regions of Gissar–Alay with use of ASTER space images. *ALUMNI association in Uzbekistan. ALUMNI publications*, *1*, 55–60.

Yue, S., & Wang, C. (2004). The Mann-Kendall Test Modified by Effective Sample Size to Detect Trend in Serially Correlated Hydrological Series. *Water Resources Management*, *18*(3), 201–218. doi:10.1023/B:WARM.0000043140.61082.60

8 Appendices

8.1 Data Sources

8.1.1 In-Situ Station Data

Extensive station data for analysis is available in the Syr Darya catchment. The complete record main gauging stations along the Syr Darya and its tributaries cover most of the years from 1920 – 1930 onwards on a monthly basis. Plate a) in Figure 65 shows the locations of the stations.

Plate b) in Figure 65 shows the locations of available meteorological station data in the Syr Darya catchment. The stations are mainly located in the Tien Shan, i.e. the Kuramin, Chatkal, Fergana, Alay and Turkestan ranges.

Another great source of station data is http://gis.ncdc.noaa.gov/map/viewer/#app=cdo (temperature only).

8.1.2 Gridded Data

20th Century Data

In 1989, the need for reliable gridded land surface precipitation data sets, in view of the large uncertainties in the assessment of the global energy and water cycle, has led to the establishment of the Global Precipitation Climatology Centre (GPCC) at Deutscher Wetterdienst on invitation of the WMO. The GPCC has calculated a precipitation climatology for the global land areas for the target period 1901– 2000 by objective analysis of climatological normals of about 67,200 rain gauge stations from its data base. GPCC's new precipitation climatology V6 is used for analysis of gidded precipitation. For more information, see e.g. (Schneider et al., 2013).

University of Delaware Air Temperature data. For more information, see http://www.esrl.noaa.gov/psd/data/gridded/data.UDel_AirT_Precip.html#detail. Data is used from product V3.01 from 1901/01 until 2010/12.

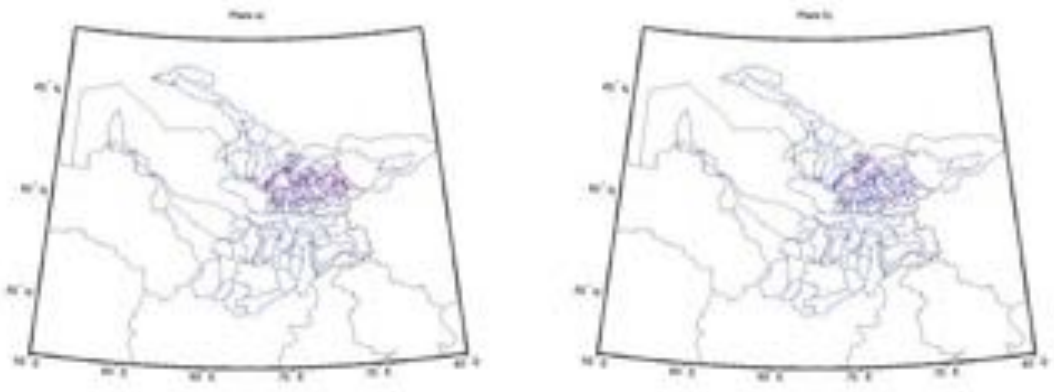

Figure 65: Locations of Syr Darya gauging stations are shown in Plate a) on the left, locations of Syr Darya meteo stations are shown in Plate b) on the right. Note that this is only a subset of available meteorological data

21st Century Climate Data

For climate projections we used globally downscaled climate data for the SRES A2 scenario. Multi-model data from 16 climate models was obtained and analyzed. The data and further information are available at http://www.engr.scu.edu/~emaurer/global_data/ (see e.g. Wood, Leung, Sridhar, & Lettenmaier, 2004).